NBSIR 85-3127

Products of Wood Gasification

T.J. Ohlemiller
T. Kashiwagi
K. Werner

U.S. DEPARTMENT OF COMMERCE
National Bureau of Standards
National Engineering Laboratory
Center for Fire Research
Gaithersburg, MD 20899

April 1985

Sponsored by:
U.S. Department of Energy
Washington, DC 20585

NBSIR 85-3127

PRODUCTS OF WOOD GASIFICATION

T.J. Ohlemiller
T. Kashiwagi
K. Werner

U.S. DEPARTMENT OF COMMERCE
National Bureau of Standards
National Engineering Laboratory
Center for Fire Research
Gaithersburg, MD 20899

April 1985

Sponsored by:
U.S. Department of Energy
Washington, DC 20585

U.S. DEPARTMENT OF COMMERCE, Malcolm Baldrige, *Secretary*
NATIONAL BUREAU OF STANDARDS, Ernest Ambler, *Director*

TABLE OF CONTENTS

LIST OF FIGURES

LIST OF FIGURES (continued)

LIST OF FIGURES (continued)

LIST OF FIGURES (continued)

PRODUCTS OF WOOD GASIFICATION

T.J. Ohlemiller, T. Kashiwagi, and K. Werner

Abstract

The increasing problem of pollution from wood-burning stoves has prompted this examination of the basic gasification process of wood under conditions encompassing those in stoves. The emphasis is on the products generated when wood is heated, without flaming, in atmospheres of varying oxygen concentration (0 to 21% O_2 in N_2). Small wood samples (typically 4 x 4 cm face, 2-4 cm thick; white pine, red oak, plus two tests with yellow pine) were subjected to uniform radiative heat fluxes (2 to 7.8 W/cm^2) on one face. Other variables were sample grain orientation, thickness, exposure time and moisture content. Sample weight was followed in some tests; sample temperature (5 thermocouples) was followed in others. In all tests, all evolved products were either monitored (H_2O, CO, CO_2, total hydrocarbons not condensible at -40°C) or trapped and analyzed (condensible organic species) by gas chromatography and mass spectroscopy. Many of the trends of the major products (CO, CO_2, H_2O, THC, total organic condensible or tar) are qualitatively intelligible in terms of the expected impact of varying temperature or oxygen level, for example. The extent of change in these major products is rather limited (factor of two to four) over the range of variables explored here. The organic condensate was difficult to analyze; it is estimated that only 20% of it was chromatographable. More than forty species in this chromatographable portion were positively or tentatively identified and quantified. Chromatographic fingerprints of the organic condensate indicated that its composition does not vary a great deal for the conditions examined here. The fingerprints from the radiative heating tests bear a strong resemblance to those of the smoke condensate from a wood stove.

1. INTRODUCTION

Wood burning stoves have become a common means for homeowners to lessen their heating bills. However, the popularity of these devices has brought with it an air pollution threat [1]. There are numerous facets to this problem of pollution from wood burning stoves [2]; that addressed here

concerns basic aspects of how the wood gasifies in a stove and what it is converted to in this process. This is part of a larger study under DOE Project No. 133A, DE-A01-76PR06010 aimed at clarifying the generation and fate of pollutants in wood burning devices.

In the first stage of the overall study, the fate of the combustion products in the stack of a wood burning stove was investigated [3]. Permanent gases (CO, CO_2, O_2) and condensibles (phenolic fraction) were monitored at the bottom and top of a 3 meter stack during an "overnight burn" condition. This type of burn condition, also used (as well as simulated) in the present work, represents a severe case with regard to pollution. The air supply to the stove is choked down to the point where a single load of wood will burn for a period of the order of eight hours. As a result of the severely limited air supply, flaming is largely or totally absent and the wood combustion process is basically one of smoldering (surface oxidation of the wood char). A further consequence of this low rate, oxygen-starved burning is a low stack temperature (80-150°C). Consequently one might expect little chemical alteration of the smoke in passing up the stack; this is in fact the case [3]. The only changes found were consistent with the physical process of material exchange to and from the walls of the stack (condensation/evaporation).

Keeping in mind the severe "overnight burn" condition that is the focus here, one sees that the place of origin of the pollutants that emerge from the stack is shifted by the above result to the firebox itself or to the wood. In the present study we focus on the products emerging from the wood. In addition, some comparisons of these products are made with those emerging from the firebox of a stove; we are seeking an indication of the extent of product alteration between the wood surface and the firebox exit. A further goal is the identification of typical major species emerging from the wood so that, in the next stage of this work, we can quantify the necessary conditions (time, temperature, O_2 concentration) required to convert such species to CO_2 and H_2O.

The environment in a wood stove (temperature, heat flux, local oxygen concentration) is variable both from point to point and with time [4]. This makes the wood stove a poor device with which to do detailed studies of the

wood gasification process. In the present work, the wood was instead placed in a precisely-controlled environment where the variables affecting the gasification process could be individually controlled and their effects examined. The wood was subjected to a purely radiative heat source and the effects of heat flux level, exposure time, ambient oxygen, wood type, grain orientation, sample thickness and sample moisture content were examined. All products evolved from the wood were collected with permanent gases being monitored in a time-dependent fashion. The organic condensibles are exceedingly complex. They have been fingerprinted by capillary gas chromatography and to a limited extent, identified.

2. EXPERIMENTAL APPARATUS AND PROCEDURE

2.1 Radiant Heating Apparatus

Figures 1 and 2 illustrate the nature of the radiative heating apparatus and the associated flow system. The radiation source is an electrically-heated graphite plate contained in an argon-purged box. The plate is heated to about 1250°C, thus it is essentially a gray body with an emission peak near two micrometers in the infrared. Radiation emitted from the front of the plate is collected and transferred out of the box by a square light pipe. Essentially all of the spectral content of the radiation is transmitted through the two infrared windows in the system. Until the start of an experiment, the radiation is intercepted by a water-cooled shutter; its removal marks the beginning of the constant flux irradiation process used throughout this work. The flux level is varied from test to test by simply moving the sample chamber relative to the end of the light pipe. The apparatus can generate fluxes up to about 8 W/cm^2; the flux is uniform to within about 5% over the 4 cm x 4 cm face of a typical sample.

The wood samples (2 to 4 cm thick in this study) are placed on top of an electronic balance for continuous weight recording (1 mg sensitivity). Thermocouples can be placed on the sample surface or within holes drilled into the sample but when this is done the thermocouple lead wires preclude useful weight measurements so thermocouple measurements were made in separate experiments. This assembly is placed inside of the sample chamber in which the

gaseous environment can be controlled. The chamber walls are water cooled to prevent their temperature from rising during a test. The atmosphere in the chamber is continually replenished by a slow upward flow (< 1 cm/s) coming through the porous plate in the base. In the present test series, this atmosphere was varied from pure nitrogen to 10-1/2% O_2/89-1/2% N_2 to 21% O_2/79% N_2 in separate tests.

The pressure in the sample chamber during a test was monitored largely for safety reasons; the CaF_2 window in the front of the chamber was not designed to withstand much stress. The pressure normally started at about 1/2 psig (relative to atmospheric pressure) due to the flow resistance of the aerosol filter and the various gas flow lines. During a few of the tests the pressure in the chamber rose as high as 2-1/2 psig at which point the test was stopped. The increased flow resistance was usually due to accumulation of products on the aerosol filter but was also caused by ice build-up in the cold trap in tests with high moisture content samples. The increased pressure is believed to have only a small affect on the wood gasification process.

2.2 Product Collection

The ambient purge gas plus all products (gas and aerosol) emitted by the irradiated wood sample were collected by the funnel above the sample. In some tests that involved an exceptionally rapid product emission in the first few minutes, there was some spillover of products from the funnel into the bulk of the sample chamber volume. This spillover was subsequently swept out of the chamber as the test continued. The net result is some (generally small) distortion of the product time histories (e.g., CO, CO_2). Even though spillover introduced aerosol into the radiation path (between the front window and the sample surface), the attenuation was found to be negligible (a water-cooled flux gage next to the sample monitored the level during each test).

All parts of the sample product collection system likely to be in contact with condensible portions of the products were cleaned and weighed before each test. No attempt was made to keep material from condensing in the lines downstream of the sample chamber. (The water line in Fig. 2 was an exception; it was heated to 60°C to prevent water condensation prior to the hygrometer

sensor. This line diverted only 5% of the flow.) Some small amounts of the condensible organics deposited in the funnel, more condensed in the glass line leading to the cold trap. Water and most of the condensible organics ended up in the cold trap (cooled by a $CaCl_2/H_2O$ slush at -35 to -45°C). The cold trap was designed to be more than adequate in length to assure that the gases passing through it were cooled to the trap temperature. However, aerosol particles formed in various parts of the system were not efficiently caught in the cold trap; this prompted the placing of a glass fiber filter immediately downstream of the cold trap (Gelman* type A/E, > 99.9% retention for particles greater than 0.3 μm). This system for trapping condensibles is not perfect since it lets some semi-volatile components of the aerosol caught in the filter escape downstream; however, the gas (plus particles) impinging on the filter was near -40°C so this effect should be quite small. The trap, filter, lines and funnel were weighed to the nearest 0.01 g after each test and the weight gain was recorded as condensible products. Methanol was used to remove all condensate in the trap, filter, lines and funnel for subsequent analysis.

The flow of permanent gases (plus the chamber purge gas) left by the trap system was split into a series of parallel lines for analysis. Note that the flow in all of the lines was measured by calibrated rotameters or, in the case of the bypass line, by an electronic mass flowmeter. The latter device indicated relative flow variations during a test, assumed valid for all of the lines. This information plus the initial flows and the measured gas concentrations integrated over time give the total mass of CO, CO_2 and gaseous hydrocarbons. The time-dependent CO and CO_2 concentrations in the present tests were measured by an Infrared Industries* non-dispersive infrared analyzer; the time-dependent gaseous hydrocarbons were measured by a Beckman flame-ionization instrument. Both instruments were calibrated routinely as per the manufacturer's instructions. Hydrogen was not measured since no suitable instrument was available. Some hydrogen was very likely present [5] but its low molecular weight means that it would account for a small fraction of the mass of the permanent gases.

---

*In order to adequately describe equipment, it is occasionally necessary to identify commercial products by manufacturer's name. In no instance does such identification imply endorsement by the National Bureau of Standards nor does it imply that the particular equipment is necessarily the best available for that purpose.

Measuring the time-dependent water evolution from the wood samples proved to be quite problematical. Even though the manufacturer's literature emphasizes the insensitivity of the hygrometer probe to chemical interferences, it ultimately became apparent that the probe was changing its calibration with each exposure to the numerous organic components of the wood smoke. Repeated re-calibrations were ultimately fruitless. The data obtained on the time-dependent evolution of water are qualitatively valid but quantitatively inaccurate. The total water (integral over time) evolved from each sample was obtained separately by chromatographic analysis of the condensate in the cold trap.

2.3 Test Procedure

Samples (usually from a single large piece of kiln-dried lumber) were cut to size and conditioned for at least two months at 50 ± 5% relative humidity and 21-24°C. If thermocouples were to be used in a given test, holes 0.5 to 0.6 mm diameter were drilled halfway through the wood blocks at carefully spaced distances back from the face to be irradiated (e.g., 5, 10, 15 mm). Chromel/alumel thermocouples with a 0.025 cm diameter stainless steel sheath were inserted to the bottoms of these holes and glued in place (glue at the outer edge of the hole only). Surface thermocouples (0.005 cm diameter chromel/alumel wire on front surface; 0.0075 cm diameter on rear surface) on pine samples were mounted by the technique developed by Attreya [6]; the junction was held near the center of the surface by a very small amount of general purpose glue (Elmer's Glue-All). For red oak samples the lead wires were fed through the pores of the wood and the junction itself was again glued in place. These mounting techniques generally succeeded in keeping the thermocouple junction in contact with the surface (despite shrinkage) until rather late in a test exposure.

The sample was placed on top of the electronic balance and its top surface was covered with aluminum foil (omitted in a few tests) to prevent excessive heating of the top by radiation reflected from the collector cone. After the sample and balance assembly were sealed in the chamber, it was purged for several minutes to assure complete replacement of air by the environmental test gas. This was done before connecting the cold trap into

the exhaust line so that no moisture originally in the chamber would deposit in the cold trap. The radiant source was run for a few minutes to stabilize its temperature. At time zero, the shutter was dropped to begin the irradiation of the front surface of the wood sample; at the same time data recording from the various instruments was initiated by a computer. Data were recorded at intervals of the order of 2-4 seconds. One operator monitored the radiant flux level during a test and adjusted the source power input to hold it constant; the other operator monitored the behavior of the sample.

Because of problems with thermal shock breakage of the infrared window on the chamber, the irradiation was ended not by closing the shutter (except in some of the earlier tests) but rather by turning off the source power. As a result, the radiation on the sample decayed over one to two minutes. The computer, however, stopped taking data as the source power was cut and the cold trap was pulled from the exhaust line at this point as well. One consequence of the slow radiation decay was that the sample continued to lose some weight so that its weight after the test was not a precise measure of the weight loss during the constant flux exposure. In tests where thermocouples were used, and the electronic balance could therefore not be used, the sample weight loss reported here includes the additional loss during the radiation decay.

The cold trap, aerosol filter and glass lines with condensate were weighed immediately after the test and then extracted with methanol. The methanol contained 0.2% of triphenyl methane as a free radical trap; this was an attempt to inhibit apparent long term changes in early condensate samples. The methanol solutions were kept refrigerated (0°C) until analyzed.

2.4 Chromatographic Analyses

Gas chromatography was used for three purposes: to analyze the water content of the cold trap, to analyze the mixture of hydrocarbon gases going to the total hydrocarbon (THC) analyzer and to separate and fingerprint the organic condensate collected from the cold trap, lines and aerosol filter.

The water content of the cold trap condensate was analyzed on a Carle Model 311 using a Porapak QS packed column at 120°C and a thermal conductivity detector. It proved necessary to homogenize the trap condensate/methanol solution in an ultrasonic bath prior to sampling because two phases were present in many of the samples. Quantitation was done against a calibration curve with known concentration of water and anhydrous methanol. The hydrocarbon analyses were done on a Hewlett-Packard Model 5710 using a Carbosieve-B packed column at 275°C and a flame ionization detector. The gas samples for this purpose were obtained by grab sampling with a syringe downstream of the aerosol filter. Identification was done by retention time comparison with a known mixture of C_1 to C_4 hydrocarbons. The principal purpose here was to obtain an estimate of the mean molecular weight of the gases going to the Beckman hydrocarbon analyzer; that estimate ($\overline{MW} \simeq 20$ g/mole) was used in deducing the overall mass of permanent gas hydrocarbons.

The organic condensate separations and fingerprints were done on a Hewlett-Packard Model 5793, primarily using a J&W DB-1701 capillary column (30 m) programmed at 2°C/min from 27°C to 280°C and a flame ionization detector. A J&W inlet splitter with a split ratio of about 75:1 was used. The injection port was normally at 280°C; a few runs at 230°C did not yield qualitatively different results.

Not all of the organic condensate was able to be chromatographed. Some of it never left the injection port and some stayed on the GC column after injection. The quantity remaining in the injection port was estimated by making 50 successive injections into the GC injection port after placing a clean, pre-weighed glass liner in it; the results showed that one third of the injected material was non-volatile and remained in the injection port. The fraction of injected material which actually reached the detector was estimated as follows. Flame ionization response factors were computed for the forty or so species identified and an effective overall response factor was calculated from a mass-weighted average of these. This result (0.65) was applied to the total peak area reported by the chromatograph integrator to estimate the total mass emerging from the column. The use of an average response factor is, of course, crude but there was no realistic alternative. The result was a rough estimate that only 20% of the organic condensate

injected into the chromatograph is actually coming through the chromatograph. This, coupled with the previous result, implies that about 50% is staying permanently on the capillary column. Gradual discoloration of the front end of the column confirmed that some material was indeed retained there. It should be borne in mind, then, that the organic condensate fingerprints and analyses discussed below do not represent the total amount of material produced and the loss is selective, i.e., the lost material represents some set of species different than those that are seen. This situation is not really satisfactory but it is, in fact, similar to that in previous studies on wood combustion products that have used more elaborate analysis schemes [7].

An attempt has been made to identify the major peaks in the chromatographable portion of the organic condensate. Selected samples were sent to the Mass Spectroscopy Center at West Virginia University. These samples were chromatographed under essentially identical conditions to those used for the fingerprinting and the output peaks subjected to mass spectral analysis. Pattern searches were done against a library of 31,000 compounds. The output of this search (comparing the mass spectrum obtained at the apex of each GC peak with the library) is a listing of the five most probable compounds from the library based on statistical measures of the closeness of fit. Nearly all of these reported fits were ambiguous with two or three compounds (usually completely different chemically) being suggested as equally good fits. In the case of several other major peaks, the library search produced no good statistical fit with a known compound. Biller-Bieman enhancement of the resolution between successively eluting chromatograph peaks failed to improve the mass spectral identification process [8]. The cause of these difficulties is almost certainly the co-elution of two or more chemical species from the capillary column even for "clean" looking peaks; in spite of the very high resolution of such columns, it is inadequate for the present purpose. Some sort of pre-separation (solvent partitioning, liquid chromatography) would be needed to improve the effective final separation capability of the capillary GC column. Such resources were not available in this study and, indeed, it was not the goal here to identify the majority of the species in the organic condensate.

Some sixty-two pure compounds suggested by the mass spectral analysis have been compared with the unknown peaks on both the DB-1701 column and on a Supelco-wax 10 column (30 m capillary, programmed from 50°C to 270°C at 2°C/min). Retention time agreement between known and unknown on both columns established the identity of twenty-nine compounds in the organic condensate; about fifteen others were less-certainly identified.

3. RESULTS AND DISCUSSION

As noted previously, the wood gasification process may depend on heat flux level, ambient oxygen level, exposure time, wood type, grain orientation, sample thickness and sample moisture content. In view of this large number of parameters, it was necessary to restrict the experimental plan to individual parametric variations on a base case. The case about which each of the parameters was singly perturbed was as follows: heat flux of 4 W/cm^2, ambient oxygen level of 10-1/2% (balance N_2), exposure time of 12-15 min., grain (longitudinal wood pores) perpendicular to exposed surface, sample thickness of 3.9 cm (2.9 cm in the case of red oak), and sample moisture content dictated by equilibration with 50% relative humidity at 24°C. This base case and perturbations about it were run for both white pine and red oak; the base case condition was also done with yellow pine.

The choice of the base case conditions was a result of several considerations. The flux level of 4 W/cm^2 was estimated to be a mid-level value to be expected as a result of blackbody radiation from smoldering wood surfaces in the 600-700°C range; the results from Batelle [4] confirmed this. The oxygen level of 10-1/2% was suggested by our previous wood stove stack measurements [3]; again the Batelle results confirmed this [4]. The exposure time of 12-15 min. was considered to be long enough to reveal the range of wood behavior. Sample thickness was largely limited by the 50 gram upper limit on the electronic balance that followed the sample weight. The perpendicular grain orientation was chosen so that the high wood permeability in the direction perpendicular to the exposed surface would facilitate product evolution and minimize irregular splitting which could cause data scatter.

3.1 Time-Dependent Behavior

Consider first the behavior of a wood sample in an inert environment, nitrogen. While the incoming radiation is the ultimate forcing function in the wood gasification, it is the temperature within the sample which directly dictates its degradation behavior. Figure 3(a) shows a typical set of temperature versus time plots for the five thermocouples at various depths in a sample of white pine.* Inspection of Fig. 3(a) prior to 60 seconds indicates a minor problem in the tests: some of the radiation going into the sample chamber was finding its way to the back surface of the sample (even though the chamber walls were painted black and were water cooled). This is a deviation from ideal behavior but it is not likely to have any significant effect on the results.

The slowing in the rate of temperature rise near 100°C apparent in all but the front surface thermocouple record is due to water evaporation. This effect is much more pronounced in the high water content cases, as will be seen.

It is apparent that after about five minutes or so the surface temperature is nearly constant (due to re-radiation) and the major change is continuing inward movement of the thermal wave. This inward movement is more easily seen in Fig. 3(b) which is a crossplot of the data from Fig. 3(a). The reversal in curvature evident in Fig. 3(b) for long times is most likely an artifact. The surface is actually regressing (with the thermocouple attached) and has moved backward about 1-1/2 - 2 mm by the end of the test. If the last "zero" point is moved to the right this distance, the reversal in curvature disappears. Lee, et al [9] made a similar point.

---

* It should be noted that in the first minute or so (up to ~ 400°C), the front surface thermocouple record in all tests is not necessarily an exact depiction of the behavior of the entire front of the sample; the small film of glue in the area of the thermocouple junction always darkened faster than the wood surface itself (initial reflectance ≈ 30-35% for radiation used here) so that it doubtless heated somewhat faster. By ~ 400°C the wood was equally dark and this discrepancy disappears.

Under thermogravimetric (TG) conditions (constant heating rate ≈ 5°C/min = 0.08°C/s), white pine begins to gasify rapidly at about 300°C. At the higher heating rates (see Fig. 3(a)) in the wood sample, this could be pushed up to perhaps 350°C. With a possible band of 300-350°C for the initiation of rapid gasification, it is apparent from Fig. 3(b) that by the end of the test, the wood gasification process has penetrated about 10 mm into the 37 mm depth of the sample. On the other hand, the drying process (up to 100-110°C) appears to have penetrated the full depth of the sample.*

Although the thermal wave appears in Fig. 3(b) to make rather steady progress inward, the resultant mass efflux (Fig. 4(a)) varies considerably with time. The mass flux is deduced from the recorded weight-time history by numerical differentiation and subsequent smoothing. When the irradiation starts, the sample begins to lose mass virtually immediately. The rate of mass loss accelerates rapidly as the front surface temperature climbs; successive portions of the wood inward from the surface are first dried and then raised to the 300-350°C range where rapid pyrolysis begins. Since the principal components of wood (cellulose, hemi-celluloses, lignin) have differing thermal stabilities, there will, in the first few tens of seconds of degradation, be a tendency for selective product generation. That is, hemicelluloses with their lesser thermal stability will dominate the first instant of gaseous product production, then cellulose products will begin evolving followed finally by lignin degradation products [10]. This varying stability of the wood components could be an important consideration in the piloted ignition of wood but here it is quickly overridden by the continuing rise in temperature. This causes all three components to degrade (at their own rates) first at the sample surface and then in increasing depth; the evolved products at the surface are a summation over this distributed pyrolysis zone.

---

* Since water can move both forward and backward as the thermal wave penetrates from the front, some water probably came out the back of the samples near the end of a test such as that in Fig. 3. In a thicker sample this backward moving water would not have escaped. Similarly, volatile pyrolysis products can presumably move forward and backward [10], but since the pyrolysis wave penetrates only about one quarter of the sample depth, no escape of such products from the back is expected. The sample collection system used here captures all products regardless of what surface they emerge from.

A product of the degradation of all three components (especially lignin) is a carbon-enriched solid or char. This solid comprises about 35% of the original mass of the wood under TG conditions. In the present situation, this char accumulates progressively from the front surface of the sample; during this process it tends to shrink slightly and crack to a limited extent. In this experiment, as in a wood stove, the heat flux from the outside is absorbed on the front surface of the char. The char is not completely inert but, in the absence of oxygen, it is much more resistant to pyrolysis than is the original wood. A major role of the char then is that it forms a rather poorly conductive barrier between the incoming heat flux and the inward propagating pyrolysis zone (and water vaporization zone). Some of the incoming radiation is re-emitted from the char surface while a progressively decreasing portion penetrates the thickening char by conduction and radiative transfer. The rate of gasification must therefore decrease; Fig. 4(a) shows that the rate decreases by more than a factor of three over a 12 minute exposure. This type of behavior was previously observed by Lee, et al [9] and Attreya [6]; it is predicted by the wood gasification models of Kung [11] and Kansa, et al [12], both of which use only a single step reaction to represent the complex pyrolysis.

In the present work, we have resolved the composition of the evolved products underlying the mass efflux pattern of Fig. 4(a); the result is shown in Fig. 4(b). The tar (organic condensibles) evolution pattern was not directly measured but was inferred from the other measured curves by difference (the summation of CO, CO_2, H_2O, THC and tar should equal 100% of the products in pure pyrolysis). The tar curve is not quantitatively accurate for three reasons. First, the mass balance for this run showed only 92% recovery, not 100%. Second, the THC curve as shown does not include the small (~ 25%) upward correction to its mass percentage due to the non-methane components (see below). Third, as previously noted, the hygrometer used to follow water evolution frequently exhibited a shifted sensitivity (generally downward) due to interferences from some of the volatile organic constituents of the smoke; in Fig. 4(b) the hygrometer output looks much more credible with regard to absolute water percentage than it did for many other tests. The net result, however, is that the indicated tar percentages as a function of time are high. Nevertheless, the basic shape should be correct.

Figure 4(b) indicates, as one would expect, that the initial mass evolution from the sample is essentially pure water. However, the water is quickly followed by a large efflux of organic condensibles (tar) which dilute the water. In Fig. 3(a) this is seen to correspond approximately to the surface region passing upward through the 300-400°C range. The permanent gases (CO, CO_2, THC) rise somewhat more slowly at about the same time.

The more interesting feature of Fig. 4(b) is the downward turn in the tar evolution. Comparing the flux of tar at 120 s to that at 600 s for example, one gets (using Fig. 4(a) and Fig. 4(b)) 0.35 mg/cm^2s for the former and 0.04 mg/cm^2s for the latter. Thus the tar flux drops off more than twice as much as does the mass flux over this interval. This is consistent with, but not proof of, the idea that the pyrolytic tars are altered as they pass through the accumulating char on the front of the sample. It has been suggested that these tars may undergo cracking to small hydrocarbons and/or polymerization to a char [13, 14]. Figure 4 does not give clear evidence as to the fate of the tars as they pass through the char. It does not appear consistent with the idea that they are converted largely to hydrocarbons since THC does not rise nearly as much as tar falls. Figure 4 seems to suggest that the tars are converted to water. This cannot literally be true but water could be a product of a char formation process.

In the presence of ambient oxygen, the only new qualitative feature is oxidation of the surface char. Under TG conditions (5°C/min in air), the char oxidation process occurs between 400 and 500°C; at the higher heating rates here this could shift upward somewhat. In the present configuration, the only clear-cut indication of the onset of char oxidation is the appearance on the front surface of gray ash left when the local char is fully consumed. (There is also some increase in the rate of surface temperature rise between 400 and 450°C possibly indicating the outset of the char oxidation exotherm; see Fig. 5(a).) Typically the gray ash appears along the lower edge of the sample (and sometimes along one of the vertical side edges). Even though the heating process on the face of the sample is essentially uniform, the oxygen supply is inherently two-dimensional; thus oxidation progresses most rapidly along the lower portions of the sample face where the buoyant boundary layer is thinnest.

Inspection of Figures 5 and 6 confirms the qualitative similarity when ambient oxygen is present; all conditions are the same as in Fig. 3 and 4 except that air is the environmental gas. Quantitative comparisons reveal some significant differences, however. The peak surface temperature is 100-150°C hotter in the presence of air due to the char oxidation process. (The surface temperature indicated in Fig. 5(a) drops suddenly at about 600 s because the thermocouple broke away from the surface.) Comparison of Fig. 6(a) with Fig. 4(a) shows that the peak mass flux is nearly twice as high in air as in nitrogen and this ratio persists throughout the exposure. This is a consequence of char oxidation which has two effects: (1) it directly increases the rate of mass loss since the char is also being gasified, (2) it indirectly raises the heat flux into the pyrolysis zone since the char oxidation heat supplements the external radiation.

Note that in Fig. 6(b) the tar percentage curve is not shown. Unlike the inert atmosphere case, here we cannot assume that the summation of the five gasification "products" adds up to 100%. Some of the oxygen in the CO, CO_2 and H_2O has come from the atmosphere in this case and our analytical approach cannot distinguish how much. Note that by 600 s the summation of the four products shown approaches 150%. It appears from the low height of the early water peak that the hygrometer was probably reading 30-50% low during this test; thus the water curve should be higher and the other curves lower. Nevertheless, it is apparent that there is much more CO and CO_2 in this case than in nitrogen; again this is an expected consequence of char oxidation. The hydrocarbon gases (THC) appear essentially unchanged by the presence of oxygen. Although we cannot infer any semi-quantitative tar percentage history, it appears probable that it would qualitatively resemble that in Fig. 4(b).

3.2 Time-Integrated Behavior

Although time-dependent data of the above type were obtained in all of the radiative heating tests, it is much easier to compare parameter effects using the time-integrated data on product evolution. All of the time-dependent data were qualitatively similar so the previous discussion suffices to clarify the major trends; time-dependent data will be referred to below only when they support some point to be made with the time-integrated data.

Inspection of Fig. 4(b) and 6(b) indicates that the product compositions evolving from the wood are still changing at 12 minutes, though relatively slowly compared to the first five minutes or so of the heat exposure. Thus the time-integrated numbers discussed below are not completely unique; they would change somewhat if longer exposures were used. This should be borne in mind. It is most pertinent to comparisons in which the parameter varied might, in some part of its range, substantially prolong the early, stronger transient phase of gasification (e.g., very low heat fluxes or very high water content in the wood).

Consider first the reproducibility of the product compositions integrated over the constant flux exposure time. Figure 7(a) shows the results of four tests on white pine at the same conditions; Fig. 7(b) shows the results of two tests on red oak at the same conditions. Reproducibility of the permanent gases and the total weight loss appears good. (The weight values shown dashed are expected to be higher because the shutter was not closed at the end of the exposure and they include weight loss during the cool-down period, as explained previously.) Only the condensibles, tar and water, show significant scatter and this is only with white pine. Note that a high value for water produces a low value for tar and vice versa; this is because the condensibles consist only of these two constituents and the total quantity of condensibles was very reproducible. It appears that the scatter in these percentages is more a result of scatter in the analytical technique rather than in the real tar and water proportions.

From Figure 8 onward, the emphasis is on the effects of the experimental parameters on the integrated product compositions. Table I gives all of these results in tabular form. Note that the figures show both the total mass of all products and the percentage breakdown of that total. On this type of plot, a linear increase in total amount of product with an unchanging composition would result in the dashed lines all being straight and fanning outward from a common intercept on the vertical axis.

Consider first the effect of total exposure time (Fig. 8). It was stated previously that in selecting a base case exposure time of 12 to 15 minutes, it was expected that all of the basic behavior of the wood would be seen. This

is not completely true since there is a unique transient, not seen here, when the pyrolysis zone hits the rear of the sample (see below). However, it is apparent from Fig. 8 that there are only weak quantitative changes in product composition over the exposure times examined. The only really prominent trends here are the decaying percentage of tar in the products with increasing exposure time and the increasing percentage of CO_2. This trend mirrors the tar behavior shown in Fig. 4(b); again, the former trend evidently results from partial destruction of the tar fraction of the wood pyrolysate as it passes through the increasingly thick char layer. For white pine, in the presence of oxygen here, the product that appears to replace the destroyed tar is CO_2 (consistent with Fig. 6(b)); this cannot be the sole product of tar destruction but it is one feasible product. For red oak CO_2 again grows the most but H_2O and CO show significant increases as well. Note that all of these products are probably also growing in relative amount due to increasing char oxidation as well as due possibly to tar degradation. In any event, it should be noted that after the first five minutes or so, no component changes its percentage of the total product by more than two and one half times.

Figure 9(a) shows the effect of halving the wood sample thickness. The principle impact derives from the fact that the pyrolysis zone reaches the rear surface of the sample when the thickness is halved. Because of the comparatively adiabatic behavior of the rear surface, the sample behaves as if it was increasingly pre-heated as the thermal wave reaches the back. The result is a late stage acceleration of the mass loss rate as shown in Fig. 9(b). Note the second maximum in the mass flux; it is probable that by this point this mass flux is coming in part from the rear surface as well as the front surface of the sample. The thermal wave is not very parallel to the rear surface by this stage so the intersection with the rear surface is smeared out in time widening the second mass flux peak. Figure 9(c) shows that this all has a significant impact on the instantaneous product compositions. The impact is greatest on CO_2 right at the end, probably because the pre-heating effect is greatly accelerating the char oxidation rate (and pyrolysis is nearly completed throughout the sample).

It is interesting to note that the tar content of the products from the thinner samples is about twice as high as that of the normal thickness sample.

This may be the result (in part) of pyrolyzate escape from the rear of the sample where it is not forced to pass through a hot char layer.

The effect of wood grain orientation is shown in Fig. 10. The designation "parallel" means here that the longitudinal pores in the wood were parallel to the incoming flux, i.e., these pores came straight out of the irradiated face of the sample. The designation "perpendicular" means that these pores were perpendicular to incoming flux, i.e., they ran parallel to the irradiated face. Most wood in a stove, being in log form, burns in the orientation designated perpendicular here. Figure 10(b) indicates that with red oak at the base case conditions, grain orientation has no significant impact at all on the evolved product composition. Figure 10(a) shows a small but significant effect of grain orientation for white pine on total product mass; nearly all of the added product mass in the perpendicular orientation is tar whose percentage of the total product is doubled in this case. It is not apparent why these two woods should differ with regard to grain orientation effects nor is it apparent what causes the factor of two differences in tar outputs for the two grain orientations of white pine. There are, of course, enormous differences in the gas permeabilities of woods between flow along and across the longitudinal pores [10]. Roberts, however, reports that cross-pore flow resistance decreases rapidly just above 300°C [10]. Presumably, then it is mainly water movement across the pores and not pyrolysis product movement that is influenced by sample grain orientation. Even this effect should be short-circuited here because of the finite sample width. Water vapor unable to move straight out through the irradiated surface in the perpendicular grain orientation can instead move sideways out of the sample along the pores. This would eliminate the convective cooling effect of the water normally found when it passes out through the heated zone in front of the water vaporization zone. There is not much water in the base case samples, however, and it is not clear if this diversion of a small water flux could influence the tar generation or destruction process.

Grain orientation also has a rather large effect on the thermal conductivity of wood. The conductivity in the parallel orientation (along the longitudinal pores) is roughly 2-1/2 times greater than that in the perpendicular orientation for most woods [15]. A higher conductivity tends to improve

heat flow into the bulk of the wood from the surface where the incoming radiation is absorbed. For a fixed radiation flux, this means that the sample with a higher conductivity (parallel orientation) will exhibit a lower rate of surface temperature rise; when re-radiation begins to dominate the surface temperature, conductivity effects become diminished. Below the surface, however, the effect continues to be felt. At any depth, the higher conductivity sample at first increases more rapidly in temperature but, after some minutes (increasing time with increasing depth), the local temperature lags that in the lower conductivity sample because the incoming heat is being transferred more quickly to still greater depths. The net effect of the grain orientation difference on the thermal wave depth at the end of the test or on the mass flux history is surprisingly small (~ 10%) for both white pine and red oak. One cannot assess the role of conductivity as the source of the differences in Fig. 10(a) (and the lack of differences in Fig. 10(b)) without a detailed model of the gasification process.

The effect of water content in the wood is shown in Fig. 11(a). Note that the high water content samples were made from the same wood as was used in all of the other tests; the wood was soaked in distilled water to increase its water content. Note also that the total product mass for the sample containing 30% water is somewhat high since it is based on the pre- and post-test weight, not just the constant flux exposure period.

The trends in Fig. 11(a) are somewhat more complex than those seen previously, e.g., here the variation of tar percentage is not a monotonic function. Water as a gasification product more than doubles its percentage as one would expect; CO and CO_2 decrease considerably which is not expected. This effect on CO and CO_2 is a result of the limited exposure time. This exposure time was quite adequate for all other samples, as discussed previously. However, the need to vaporize the large amount of water in the high moisture samples considerably slows the progress of the wood gasification. In the sample with 53% water there was no ash on the surface at the end of the test implying little or no oxidation of the char had as yet occurred; hence the low CO and CO_2 values.

Figure 12 shows the impact of high water loading on the temperature history in the sample with 30% water by weight. The local temperature is held down to 100°C for extended periods while water is vaporized; when the condensed phase water at the thermocouple location is finally gone, the local temperature rises rapidly. Since 30% water content is above the fiber saturation point (20-25% water content according to ref. 16), it is probable that some of the wood pores are initially filled with water which then moves toward the vaporization front by capillary action; this would be even more significant for the 53% water sample. Such a phenomenon could prove very difficult to model. In any event, the qualitative effect of this water is twofold. It places a very large heat sink just behind the wood surface; this heat sink moves inward only after the local wood is dry. In addition, the water vapors, in plentiful supply, extract heat from the layer on the outside of the vaporization zone as they move out of the sample toward the front surface. Comparison of Fig. 12(b) with Fig. 12(c) confirms that the net impact of these two effects is a considerable retardation of the processes of pyrolysis and char oxidation.

Going back to Fig. 11(b) one sees that when more exposure time is permitted, the mixture of products begins to look somewhat different due to the increasing contribution from char oxidation. The transient product evolution data reveal that even at 24 minutes, the CO_2 concentration in the gases leaving the surface is still rising at a substantial rate so the system is not in a quasi-steady state and the time-averaged composition would shift still further with exposure greater than 24 minutes. (As noted earlier, this unsteadiness in average composition is, in fact, true for all of the test results reported here but it is more pronounced for the high water cases because they extend the early highly transient phase of gasification.)

The parameters that vary the most within a wood stove are local oxygen level and heat flux; Fig. 13 and 14 show the effects of these parameters on the products of gasification.

As discussed previously, the principal effect of oxygen is that it gasifies the char left by pyrolysis. Thus the total amount of products produced at a given heat flux increases and the composition shifts to reflect

much greater amounts of CO and CO_2. This effect is apparent for white pine and red oak in Fig. 13. It is interesting to note that the combustion of the char has practically no effect on the fraction of combustible materials (CO + THC + tar) in the products; for both pine and oak it is never more than 1/4 to 1/3, a surprisingly small fraction.

Comparison of Fig. 13(a) and 13(b) shows that the impact of increased oxygen level on tar seems to vary with wood type, at least at high O_2 levels. (Because tar measurements showed greater scatter than other product measurements, one should be cautious about apparent trends based on relatively small changes.) Even though for both woods more solid is gasified in 21% O_2 than in 10-1/2% O_2, the percentage of tar and the absolute amount of tar goes down with increased O_2 in the case of white pine and up in the case of red oak. Comparing Fig. 5(b) with Fig. 3(b) confirms that the pyrolysis zone penetrates more virgin wood in the high O_2 case so that more primary tar is being generated. The peak surface temperatures for both woods are comparable in equivalent atmospheres (ca. 620°C in 10-1/2% O_2; ca. 670-680°C in 21% O_2) so this does not appear to be a factor in explaining apparent differences between wood types in the survival of the amount of primary tar that emerges as the tar actually collected. One can speculate that since oak appears to yield a more open structured char than pine (i.e., the scale of the pores and cracks is larger), more primary tar passes through but this cannot be proven at this point.

Figure 14 shows that the effect of increased heat flux is quite comparable for both wood types. For the exposure times used here, a flux of 2 W/cm^2 is just above the threshold of significant weight loss. (For longer exposures, this threshold moves downward; for example 1 W/cm^2 will cause wood in air to smolder if sustained for 45 min. or more.) Increased flux, above the threshold level, has two principal effects. It increases the heat flux reaching the pyrolysis zone through the char thus increasing the rate of pyrolytic gasification. In addition, at low fluxes, it undoubtedly accelerates char oxidation by raising the char temperature. However at high fluxes the char oxidation rate most probably becomes fully limited by the oxygen supply rate in spite of further temperature increases; thus this contribution becomes "saturated". (Referring back to Fig. 13, one sees no such

"saturation" with increased O_2 level since O_2 supply rate is proportional to O_2 level.) The combination of these two effects probably accounts for the decreasing slope of the total product weight with increasing flux in Fig. 14 for fluxes up to about 7 W/cm^2. The upturn at the higher flux is based on one experiment only (the CaF_2 window broke at this high flux). It is possible that the upturn represents an additional gasification pathway, e.g., pyrolysis of the char or gasification by CO_2 and H_2O, but this cannot be proven at this point.

Comparison of time-integrated data at a constant time exposure as flux is varied widely is potentially deceptive. As was noted previously, the product compositions are still changing at the end of the exposure. Furthermore, for a fixed integration time, the thermal wave induced by the highest flux will have progressed deeply into sample whereas the lowest flux case may be just getting started. This latter situation appears to be the case at 2 W/cm^2 but by 2-1/2 W/cm^2 the sample is well past the early rapid transient stage in its 12-15 min. exposure. The problem of being misled by time-dependent results is thus not too bad here but it should be kept in mind.

Comparing fluxes of 4 W/cm^2 and ca. 6-1/2 W/cm^2, one sees in Fig. 14 that at the higher flux level both woods appear to yield lesser percentages and absolute amounts of tar. (The 7.8 W/cm^2 case, based on single test, is anomalous with regard to tar.) These higher fluxes have a substantial impact on the char temperature near the surface; the surface temperature is raised by 100°C or more at ca. 6-1/2 W/cm^2 compared to the base cases (4 W/cm^2). One would expect this to increase fragmentation reactions in heavy tar molecules passing through the char. The amount of total hydrocarbons (THC) is not obviously enhanced by any such reactions; their percentage is essentially unchanged compared to the base case. Carbon monoxide does increase but this could come from degradation of oxygenated tar species or from CO_2 reduction on the char.

The effect of wood type has been alluded to somewhat in the previous discussion. It is shown in (a) versus (b) comparisons of the previous figures. It is also shown explicitly for three woods in Fig. 15. The most striking effect of wood type in all of the figures is on the total amount of

products evolved. It is always much greater with red oak than with white pine; yellow pine is seen in Fig. 15 to be intermediate between the two.* There are two processes responsible for the total weight loss - pyrolysis and char oxidation. The pyrolysis weight loss is proportional to the penetration depth of the pyrolysis zone. For the conditions of Fig. 15, this is about 10 mm (depth of 325°C isotherm) for red oak and about 15 mm for white pine (both measured after 15 min. of constant heating). With the assumption of equal char fractions for these two woods (25-30%), the mass pyrolyzed from these depths is proportional to the initial density of the wood. The initial wood densities are as follows: white pine, 0.36 g/cc; yellow pine, 0.66 g/cc; red oak, 0.74 g/cc. From this one infers that the mass loss of red oak due to pyrolysis alone is 1.37 times that for white pine. The actual ratio of total mass losses is 1.55 so the difference is evidently due to a slightly higher degree of char oxidation in the case of red oak. Without a detailed model of the wood gasification process one cannot be more precise as to the cause of these variations due to wood type; existing models in the literature have not been applied to such questions.

The effect of wood type on the composition of the gasified products is not large; this is apparent from Fig. 15 and from (a) versus (b) comparisons of the earlier figures. Red oak and white pine do not differ greatly in gross composition. The following data are from ref. 17:

	Northern Red Oak	Eastern White Pine
Total carbohydrates	69%	68%
Alpha cellulose	46%	45%
Klason lignin	24%	27%
Ethanol/benzene extractives	5%	6%

On the other hand, the chemical nature of the hemi-cellulose portion of the carbohydrates does differ significantly between a hardwood like oak and a softwood like pine; the lignins differ also, but to a lesser degree [18]. These detailed chemical differences appear to impact the production of

* The total product mass for white pine in Fig. 15 is for a 12 min. exposure whereas that for the other two woods is 15 min.; Fig. 8(a) shows that white pine would lose 7.8 g at 15 min.

specific compounds within the tar such as certain types of phenols, for example (see below), but they obviously do not greatly affect the gross product distribution.

3.3 Characterization of the Solid Residue

As is apparent from the previous discussion, one of the products of incomplete wood gasification is a solid sample with a continuous gradient (front to back) in its degree of degradation. It is of interest to examine this material to see what it may reveal about the overall gasification process. Samples were sliced with a fine saw into a series of layers (typically 3-5 mm thick) as parallel as possible to the pyrolysis front. This front was not flat in some cases nor was it necessarily parallel to the rear surface of the sample (in spite of the fact that the outer 6 mm of each of the four side faces was first removed and discarded to minimize edge effects). As a consequence the effective position of each slice relative to the exposed surface of the wood is uncertain to about ± 2 mm. The slices were characterized in two ways: the internal surface area was measured and the chemical functional groups were characterized by NMR spectroscopy.

The internal surface area of a solid is a factor of prime importance in its reactivity with oxygen. Here that area was measured by one point B.E.T. experiments using nitrogen at -196°C and a Quantasorb Surface Area Analyzer. (A check showed that multi-point B.E.T. measurements did not give appreciably different results.) Figure 16 shows the results. Note first that the intact wood deep within the sample starts with a surface area of about 0.4 m^2/g (the same as one finds on an unheated sample of this white pine). This area is essentially that due to the walls of the longitudinal pores in the wood. In Fig. 16(a) where only the ambient atmosphere was varied, one sees a slight increase in surface area about 1 cm below the exposed face of the sample; thereafter the increase is substantial. However up to about 4 mm (or less) below the surface, the increase is essentially independent of ambient O_2 level. At shallower depths the intermediate O_2 level (10-1/2% O_2) yields much more internal surface area near the exposed face of the sample. Interestingly, the high O_2 case (air) is back down to a surface area comparable to the zero O_2 (pure N_2) case.

When oxygen attacks a carbonaceous material it tends to bore holes into the solid, especially in locations where catalytic metal atoms exist [19]. This phenomenon, which leads to a variable surface area, has been studied extensively for coal chars [20]; the surface area typically increases and then decreases as the char approaches full consumption. Evidently what one has in the surface layer of the char here is a similarly oxygen-modified material. In the 10-1/2% O_2 case, oxygen has been reacting at a moderate rate when it encounters the char so that it penetrates to some significant depth (Zone II behavior in ref. 19). Because of the slicing technique used here one cannot say for certain what this penetration depth is except that it is ≤ 4 mm. In the 21% O_2 case, the boost in temperature accompanying the faster O_2 transport rate speeds up the local char/O_2 reaction rate and decreases the oxygen penetration depth (Zone III behavior). In the limit (ideal) no oxygen penetrates the sample face because it is consumed at the front surface; then the internal area behind the front face is undisturbed from the no oxygen case. This description, adapted from the coal char literature, appears appropriate here.

In Fig. 16(b), the O_2 level is the same in all three cases; only the water level in the sample varied. Water can participate in carbonaceous char gasification (yielding CO and H_2) but it reacts rather slowly unless heavily catalyzed [19]; its direct influence here is probably secondary since the temperature of the char is below 650°C. Given the rather rough nature of the sample slicing process, one should not take the extrapolations to zero depth in Fig. 16(b) too seriously; thus it is not clear whether differences greater than the measured factor of two in internal surface area exist in these three cases. One expected effect is clearly present: the 50% water case with its greatly compressed thermal wave (above 100°C) shows also a greatly compressed region of increased surface area.

Some of the same sample slices as were used for the surface area analyses were also characterized by ^{13}C-NMR. The solid-state, proton-decoupled spectra were acquired at 15.08 MHZ with cross-polarization and magic angle spinning techniques on a home-built instrument. The spectra shown in Fig. 17 are the result of approximately 20,000 scans with 1024 data points for scan at a dwell time of 50 μs. The time between scans was 3 s and the spinning frequency was 2300 HZ. The chemical shifts (ppm along the abscissa) are relative to tetramethylsilane.

Figure 17(a) shows successive slices from a white pine sample exposed to 4 W/cm^2 in 10-1/2 O_2. The lowest spectrum is for the unheated wood. Note that the carbohydrate portion of the wood provides a series of fairly sharp peaks (~ 60 to 110 ppm); the lignin, however, contains a variety of carbon atoms with overlapping resonances that yield a less sharply defined portion of the spectrum (110-160 ppm). The material from slice 3, centered about 7 mm below the exposed surface, varied in color from black to a medium brown. Figure 17(a) shows that despite this considerable discoloration, the carbohydrate portion of the spectrum still dominates (the relative amount of a given carbon atom in the spectrum is proportional to the area under its peak). These peaks appear even sharper in some cases, probably reflecting the disappearance (by destruction or re-arrangement) of less-ordered areas of the carbohydrate chains. The fact that the specific surface area is up by about 4x (Fig. 16(a)) implies substantial disruption of the physical structure of the wood. The temperature-time history for this condition indicates that at this position in the wood the temperature just reached about 410°C at the end of the exposure (but the gradient from back to front of the slice was nearly 100°C). Earl [21] found roughly comparable changes in oak above about 310°C but his samples were exposed to this temperature for 4-5 minutes; the present material (slice 3) progressed from 300 to 410°C over a period of about 5-1/2 minutes.

There are other significant changes in the slice 3 material (Fig. 17(a)). The broad peak between 110 and 140 ppm has grown indicating an increase in aromatic species (substituted and unsubstituted). There is also a low, broad peak below 50 ppm indicative of a range of aliphatic carbons.

Slice 2 (Fig. 17(a)) centered about 4 mm below the exposed surface is drastically different than the material immediately below it. The surface area is increased about 2x (Fig. 16(a)) indicating some further physical disruption but the chemical nature has changed enormously. Essentially all of the carbohydrate structure is gone and the spectrum is completely dominated by a broad aromatic peak. (The abruptness of the change in chemical structure is consistent with thermoanalytical data showing rapid pyrolysis of such carbohydrates as cellulose in a narrow temperature range around 300°C at 5°C/min.) Most of the persisting peak is due to unsubstituted and carbon-substituted

benzene ring structures. There is a weak shoulder at 150 ppm corresponding to oxygen-substituted aromatics; these could be due to the persistence of methoxy groups attached to aromatic rings which are present in the original lignin structure. Earl [21] found these groups to be persistent up to at least 390°C (5 min. exposure) in both oak and spruce. Here there is also some hint of persistent aliphatic carbons.

In slice 1 (Fig. 17(a)) the structure of the charred wood at and just below the sample surface (centered at about 2 mm) is further simplified, probably as a consequence of further heating. The slight aliphatic peak is gone and the oxygen-substituted shoulder on the aromatic peak is reduced to a mere hint. Recall that this is the slice that showed indications of oxygen attack in its large surface area. This spectrum implies that very little of that oxygen stays in the structure of the solid; evidently it extracts carbon in the form of CO or CO_2 and leaves.

Figure 17(b) shows comparable spectra for white pine exposed at 4 W/cm^2 in nitrogen. The deepest sample, centered about 16 mm below the exposed surface has no change in its surface area (Fig. 16(a)) and no substantial changes in its chemical structure. Figure 3(b) indicates that the 16 mm region reaches less than 250°C by the end of twelve minutes. Slice 2 (Fig. 17(b)) is centered at about 9 mm below the exposed face and reached about 350°C at the end of the exposure; it is quite similar in appearance to slice 3 from Fig. 17(a) even though that slice reached significantly higher temperatures (on average). The same chemical changes apply apparently.

The material in the next spectrum of Fig. 17(b), denoted as being between slices 1 and 2, was collected separately because it appeared to be physically homogeneous. It constituted the black frangible char-like material easily scraped off the sample leaving an intact, tough, more wood-like (though blackened) material beneath it. The NMR spectrum indicates it is in a state of transition with what appears to be some of the carbohydrate structure still present. Thus it seems that the abrupt physical transition in the sample (found also in all other sectional samples) from a woody structure to a frangible char coincides with the rapid pyrolysis of the carbohydrate portion of the wood. Even though the internal surface area undergoes no abrupt change in

this region, it seems probable that the gas flow resistance of the wood may go down rapidly in this region. Roberts [10] reported the onset of a permeability increase at 310°C (heating conditions not described). The material here has reached more than 400°C (on average), but it is most likely the coolest region of this slice (~ 350°C) that contributed the carbohydrate structure.

The top spectrum in Fig. 17(b) bears a strong resemblance to slice 2 in Fig. 17(a) and presumably represents the same chemical structure. The peak surface temperature in the N_2 atmosphere (550°C) is about 100°C less than that in 10-1/2 percent O_2. The lower temperature thus probably accounts for the persistence of the O_2-substituted aromatic shoulder on the main peak of this surface layer material.

3.4 Total Hydrocarbon (THC) Composition

The permanent gases passing through the cold trap were grab-sampled with a syringe and analyzed by gas chromatography. Identification was done by comparison with a known mixture of gases on one GC column only. The known mixture contained methane, acetylene, ethylene, ethane, propyne, propylene, propane and butane so it was these gases whose presence or absence could be sensed in the test samples. In no case were acetylene, propylene or butane seen; the other five gases were seen in varying proportions. The apparent presence of propyne is unexpected. The peak identified as this gas was seen with both white pine and red oak but it did not show up consistently (e.g., it was seen with red oak at 2-1/2 W/cm^2 and 6.2 W/cm^2 but not at 4 W/cm^2 or 6.9 W/cm^2). This raises the possibility that the peak was some kind of artifact, even though, when it did show, it was large (30-60% by weight of the measured hydrocarbons).

The measured compositions sometimes seemed to vary smoothly and weakly with some parameter, such as ambient O_2 level, then in other tests they were substantially different. It is difficult to give a typical composition other than the following. Methane was always present, usually comprising ca. 50% of the measured hydrocarbons but it varied from 20% to 80% in some cases; ethylene varied from 0 to 50% of the measured hydrocarbons from red oak but

was usually 0-10% from white pine; ethane varied from 0 to 30% from both woods; propane was seen in only one test (with white pine) in which it comprised 10-20% of the measured hydrocarbons.

3.5 Chemical Composition of the Organic Condensate (Tar)

The composition of the tar was investigated by means of capillary gas chromatography coupled with mass spectroscopy. Recall that our best estimate is that the chromatograms or fingerprints represent only about 20 percent of the mass of the tar injected; the remaining 80 percent stayed either in the injection port or in the column. Where possible, specific components of the tar which did pass through the chromatograph were identified. Figure 18(a) shows a capillary chromatogram for the base case with white pine (4 w/cm^2, 10-1/2 percent oxygen, 3.8 cm thick, wood pores perpendicular to irradiated face of sample, normal water content, 12 minute exposure). The original chromatogram which is about five feet long was recast into the form shown. For any component, the vertical ordinate is proportional to the total peak area; the abscissa is the retention time of that peak. All subsequent fingerprints like this have been normalized to the same total amount of tar as was present in Figure 18(a). The 60 or so peaks shown were those that emerged above a rather arbitrarily chosen threshold. They represent the "major" peaks present (few percent by area to a few hundredths of a percent coming through the chromatograph of the tar). A large number of minor peaks has thus been dropped.

The weight percentages reported in Fig. 18(b) are based on calculated FID correction factors. They are percentages of the material coming through the gas chromatograph; since this is only about 20% of the injected tar, their percentage of the original tar is one-fifth of that shown.

The species identifications noted in Figure 18(b) fall into two differing levels of certainty. The higher level (with no parenthetic T after the species name) were for the most part tentatively identified by mass spectroscopy and then confirmed by matching known and unknown retention times on two different capillary columns (DB-1701 and Supelcowax 10). The lower level (with a parenthetic T after the species name) emerged from the mass spectro-

scopic library search with very good scores for matching to the library spectrum.* Their identification must be regarded as tentative since they have not been checked with regard to chromatographic retention time.

Nearly all of the compounds listed in Figure 18(b) have been previously found in pyrolysis or combustion products of cellulose, lignin or wood. For example, 22 of the first 31 compounds are products of cellulose pyrolysis [22]. These include a variety of small acids (plus methyl esters possibly resulting from the methanol solvent though some small fraction of the methanol is also a pyrolysis product), aldehydes and furan derivatives; a curious feature is the nearly total lack of ketones. Some of the phenolic compounds (up to peak 31) can also be produced by cellulose pyrolysis but are more readily produced from lignin [22, 23]. Levoglucosan (peak no. 40) is a primary product of cellulose pyrolysis [22]; its decomposition may be a source of several of the smaller oxygenated species. The levoglucosan peak was always present and virtually always one of the most abundant species in the tar. However, the appearance of the peak varied considerably and it sometimes was treated by the chromatograph integrator as a series of small peaks or occasionally the integrator was fooled by its gentle leading slope and it reported only a small area value. The "pure" known compound also gave a rather complex peak of similar shape suggesting that the levoglucosan may typically be accompanied by lesser amounts of similar anhyro-sugars. Some of the more complex phenols (eugenol, isoeugenol, vanillin) have been isolated from wood decomposition products [24, 25] and are readily relatable to the

---

* There are three scores used in the matching process. Purity is a measure of the similarity between the unknown and the library mass spectrum; a score of 1,000 means the two spectra are linearly proportional to each other. Fit is a measure of the degree to which the peaks in the library spectrum are contained in the unknown spectrum; a perfect fit yields a score of 1,000. Reverse fit is a measure of the degree to which the peaks in the unknown spectrum are contained in the library spectrum; again a perfect score is 1,000. Since the species leaving the capillary columns are virtually never fully separated and 100 percent pure, scores of 1,000 are not achieved but scores above 800 (criterion used here) are highly suggestive of a species identity. Nevertheless, the identification must be scrutinized for general plausibility in light of the nature of wood and its elemental composition; e.g., species which received high scores in the library search but contained nitrogen were rejected. Compounds having other structural features seemingly incompatible with the circumstances of the experiment (e.g., a four carbon ring) were also rejected.

structure of lignin [26]. Compounds 41 to 46 (except no. 42 which was added to help stabilize the tar) appear to be derived from the extractives present in wood [26].

Some of the compounds in Figure 18(b) (nos. 18, 20, 22, and 23) were not reported in the preceding references nor in a large compilation of compounds isolated from wood distillation [27]. Of course these sources, while fairly comprehensive, are not exhaustive. Furthermore, the gasification techniques used in all of these sources differed from that used here. Nevertheless, this does add a note of caution about the tentative identification of peaks numbered 18, 20, 22, and 23.

Inspection of the compounds listed in Figure 18(b) reveals that nearly all are fairly small molecules; only the last half dozen are rather large. The only polycyclic compound on the list (no. 46) could well be derived from the resin acids in the extractive portion of the wood [26]. There is no other representative of the numerous polycyclics (benzofurans, naphthalenes, anthracenes, pyrenes, etc.) that have received so much attention in wood stove emissions [7, 25]. For the chromatographic conditions used here, one would expect that many of these compounds will be eluted though those without polar functional groups attached may not be well separated. In fact, the presence of about eight compounds in this category is suggested by the mass spectroscopic library search. They were not included in Figure 18(b) either because they fell below the threshold level (approximately 0.1 percent of the tar) or because their scores for matching the library spectrum did not meet the criterion used here (at least 800 for all three measures of matching). All of the following scored at least 900 with regard to <u>fit</u> between the unknown peak and the library spectrum (although their other scores were below 800 except as noted): naphthalene, 2,3-dihydrobenzofuran (scores for methyl benzaldehyde were as good for this peak), 7-methyl benzofuran (scores for 3-phenyl, 2-propenal were somewhat better for this peak), 1 or 2-methyl naphthalene (other scores also above 900), 3-methoxy, 2-naphthalenol (other scores were above 850), phenanthrene with extensive aliphatic substitutions ($C_{19}H_{28}$) and tetramethyl phenanthrene (3, 4, 5, 6- or 2, 4, 5, 7-). Phenanthrene itself and another highly substituted derivative also received fit scores between 800 and 900 for two other peaks. All of this suggests that a variety of polycyclic

compounds can be evolved directly from wood when it is gasified. It is possible that other bigger polycyclics are present but fall below the detection limits for the techniques used here. The threshold level for Figure 18 corresponds to about 100 mg of a given species per kilogram of wood gasified. Formation of this much of a given polycyclic during wood combustion (in a stove) is evidently highly unlikely; typical levels appear to be one or two orders of magnitude less [25].

3.6 Variability of the Organic Condensate (Tar)

In the discussion of Figures 7 to 15, all of the condensible organic materials were lumped into a single category called tar. The amount of this tar varies only by a factor of four over all of the parameter ranges indicated; most of the parameters altered total tar quantity by a factor of two or less. Thus, tar would appear to be no more variable than the other major constituents. On the other hand, when one considers the origin of the tar in the pyrolytic break-up of cellulose, hemicelluloses and lignin coupled with the harsh environment through which it must pass on leaving the wood (hot char sometimes containing hot oxygen), one anticipates a greater variability in at least some of the constituents of the tar. Since they comprise the products of a large number of parallel degradation reactions, their relative amounts should vary with the heating rate of the wood. Furthermore, some species should be more thermally or oxidatively labile than others.

First it should be noted that the fingerprint for the tar from a given test was found to be reproducible but this reproducibility required certain precautions. As noted previously, the methanol solution of the tar frequently yielded two liquid phases. These had to be uniformly interdispersed before they could be reliably sampled with a syringe. An ultrasonic bath was used for this purpose.

The reproducibility of a tar fingerprint for separate samples of the same wood exposed to the same gasification conditions was good though not nearly as good as that just noted above. Figure 19 shows an example. The qualitative reproducibility is very good; it is even better than it appears because most of the peaks missing from Figure 19(b) are present in the original chromato-

gram but fell below the threshold for inclusion.* One peak seems to be genuinely absent (or too small for detection) in Figure 19(b), that between peaks 26 and 27 in Figure 18(a). Presumably the missing peak is a phenolic compound.

The quantitative reproducibility is not as good as the qualitative reproducibility. Some of the variation in relative peak areas is due to variability in the amounts of minor species that, in effect, confused the chromatograph integrator as to when larger peaks were beginning and ending. However, some of the peak areas vary by a factor of two between Figure 19(a) and 19(b); e.g., the group including peak no. 16 (furaldehyde), peak 17 (furfuryl alcohol), peak 22 (tentatively, 1-acetyl cyclohexene), and peak 32 (cresol). Peaks missing from Figure 19(b) that are greater than two relative area units in Figure 18(a) (and conversely) also must have varied by a factor of two or more. The reason for this kind of relative peak size variability must lie in the wood and/or the gasification process itself.† Probably the most variable feature of the latter is the pattern of cracks in the char. The larger cracks provide cooler pathways out through the hot char for pyrolysis products generated behind the char. The proportion of products going this way versus through the finer pores in the char where they would be heated to the char temperature depends on the statistical variability of the crack pattern. Such a mechanism could lead to a random variation in the concentrations of those tar species most subject to thermal degradation (and, conversely, in the products of such degradations).

---

* There are some systematic differences in retention times of equivalent peaks that result mainly from small variations in column carrier gas flow rate. Comparisons discussed below are all based on superimposing two fingerprints and aligning characteristic patterns of peaks irrespective of retention times which can vary by a few minutes.

† There is also significant scatter in the absolute size of all peaks in the fingerprint as a whole. It was noted previously that all of the fingerprints have been normalized to the same amount of tar as that injected for Figure 18(a). However the absolute tar determinations are subject to an uncertainty of about ± 30 percent on average since the tar was the minor component in a mixture with methanol and water and could only be determined by difference.

Figure 20 shows the effect of exposure time to the thermal radiation for otherwise base case conditions; the wood is white pine. The first two fingerprints in the series (1-1/2 minutes, 2-1/2 minutes) show differences that appear to be significant (greater than the sample-to-sample variability). In the following discussion, the retention times are those for the base case (Figure 20(d)). The acetic acid peak (#13, ca. 8 minutes) is greatly suppressed. The group of small to medium peaks between 12 and 16 minutes, including #14 and #15 (tentatively, ethyl benzene and propionic acid, respectively) is suppressed (all are present in trace amounts). The group of peaks between 20 and 24 minutes is strongly suppressed except that #17 (furfuryl alcohol) is present just below the threshold. Essentially all of the other differences represent changes in relative proportions rather than total suppression of a peak since all peaks in the base case are present at least at the trace level. From exposure times of 6 minutes to 24 minutes, the differences are less and less significant, with corresponding peaks falling mostly within a factor of two with regard to absolute or relative size.

The reasons for the differing fingerprints at short times are at least twofold. First, the surface temperature is still climbing significantly: it is 525°C at 1-1/2 minutes, 580°C at 2-1/2 minutes, and it then rises only another 40°C to 620°C by 6 minutes. This means that in the first few minutes, the relative proportions of products arising from the different wood constituents is changing more rapidly than it does after the thermal wave becomes more "quasi-steady", penetrating inward with a nearly fixed peak temperature. Relative thermal stability of the wood constituents counts more with regard to gaseous product emissions in these first few minutes than it does subsequently. Second, there is no char layer initially so any reactions in such a layer are suppressed. Unfortunately, in the absence of more specific information on degradation rates and products, we cannot discern which of these mechanisms is primarily responsible for the product variations noted above.

Figure 21 shows the effect of ambient oxygen level on the fingerprints of the tar from white pine. The fingerprints from pure nitrogen and from 10-1/2 percent O_2 are extremely similar (as good as the reproducibility of a fingerprint from one sample to the next). The fingerprint from the ambient air case has all of the same peaks (though several fall below the threshold). However,

there are substantial differences in the sizes of most of the peaks with the air case yielding peaks half the size of those in 10-1/2 percent O_2. Given the uncertainties here, this difference is on the borderline of being significant so it is difficult to assign a meaningful interpretation.

Figure 22 shows the effect of incident heat flux varied about the base case (4 w/cm^2) for white pine. In this series, virtually all of the same peaks are present; those that appear to be missing fell below the threshold for inclusion. Most of the relative peak height variations fall near or just outside a factor of two and therefore cannot be judged to be significant. One apparent exception is compound number 32 (cresol) which shows peak height variations of a factor of four among the various cases. In fact, the very large cresol peak for the base case (Figure 22(b)) is exceptional; other base case runs show this peak reduced by about a factor of two relative to the other peaks present. Red oak showed a similar lack of significant effects due to flux level.

Sample thickness and grain orientation had a similar mild impact on the tar fingerprints. Figures 23 and 24 are included for completeness.

Figure 25 shows the tar fingerprints obtained with white pine where only the water content of the wood was varied about the base case value. The difference between the oven dry case and the base case is not significant; this is not surprising since the base case water content was only about 5 percent. The presence of 30 percent or more of water in the wood has a significant impact on the tar composition. Comparison of Figures 25(b) and (c) shows that the higher water case yields a fingerprint where many of the peaks are suppressed. Note that the phenols are less suppressed (the decreases are of borderline significance) than the numerous oxygenated species probably arising in large part from the carbohydrate portion of the wood (cellulose and hemi-celluloses). Most, if not all of these latter degradation products are in fact present but their relative quantities are decreased by factors of 4 to 10. About half dozen of them re-emerge above the threshold in the case with ca. 50 percent water (Figure 25(e)).

It was noted earlier that the base case 12-15 minute exposure times may have been too short in some cases such as with high water content because the early transient is distended. The case of ca. 30 percent water was repeated with a 24 minute exposure (Figure 25(d)) and it shows essentially no significant changes in the tar fingerprint as a result of this longer time even though greater char oxidation was clearly evident in the test. Thus, relatively short exposure time is not the cause of these fingerprints differing from the base case.

The peak surface temperature (ca. 650°C) is about the same for 33 percent water and for the base case. Furthermore, in the extended exposure case just mentioned, the char layer is ultimately comparable to the base case as well. Thus, there would appear to be no reason to expect differing degrees of tar alteration upon passage through the char. However, there are some differences here that may count in this regard. Recall that most of the tar is evolved in the first few minutes (Figure 4(b)). During this time, the high water content does indeed keep the char substantially cooler as a comparison of surface temperature histories shows:

Time (min)	Base Case Surface Temp.(°C)	33% Water Surface Temp.(°C)
2	575	325
4	600	495
6	625	590
8	630	620

In addition there is a physical difference in the chars that may well yield differing degrees of thermal contact; the char in the high water cases always was perforated by a fairly regular array of cracks (1-2 mm wide). This yielded 2-3x more large crack area for sub-surface volatile escape than was seen in low water cases (all cases are for the wood pores perpendicular to the irradiated sample face).

It is tempting to infer that it is levoglucosan degradation (or the lack thereof) that accounts for the bulk of the differences in the high water/low water tar fingerprints. While some of the high water cases do indeed show high levoglucosan levels, there is not a consistent significant trend.

One expects some significant differences in the tar fingerprints when different types of wood are compared, particularly hard wood versus soft wood. Figure 26 compares base case fingerprints for white pine, yellow pine and red oak. Hard wood lignin contains many more dimethoxy phenolic moieties than does soft wood lignin [28]. The hemi-cellulose constituents also differ significantly [26]. The degradation products from the latter probably cover a very large spectrum of species and may not yield distinctive differences between hard and soft woods. The lignin, on the other hand, is the major precursor of the various phenols so one anticipates significant changes in the range of such species in the tar. Figure 26 does show some significant changes in the phenolic make-up between the two types of pine and red oak but the changes are not very dramatic. Once again, peaks not shown are present below the threshold. The biggest identified change is in the quantity of species no. 39 (vanillin). Contrary to expectation, since this is mono-methoxy phenol, the red oak yields significantly more than either type of pine. The other large change is the tall peak at about 59-1/2 min in the red oak fingerprint. This is a complex peak and it is unclear whether the bulk of it is due to compound no. 36 (eugenol) or to eugenol plus some other species (likely another phenol in this region of the chromatogram). In any event it is surprising to note that no dimethoxy phenol is definitely identified in the red oak fingerprint. The other differences among wood species are of borderline significance.

In summary, the preceding results imply that, except for the case of wet wood or of normal wood exposed only briefly, the chromatographable portion of the organic condensate does not vary in the relative concentrations of most of its constituent species by more than a factor of two or three.

3.7 Other Fingerprinting Techniques for the Organic Condensate

The preceding result is more than a little surprising given the wide range of conditions under which the tars were generated. Recall that the capillary GC fingerprints only represent about one-fifth of the tar. This being the case, it is highly desirable to attempt to confirm this apparent invariance by some other technique that does not select a portion of the tar in the same way as does the gas chromatograph. Three further techniques were

tried, gel permeation chromatography, fast atom bombardment mass spectrometry and liquid chromatography. Neither of the first two techniques is very satisfactory in that the fingerprint is relatively featureless. Both look essentially at the distribution of molecular sizes in the tar and not at functional groups on the molecules. The third technique produces a detailed fingerprint but it has other limitations.

Gel permeation chromatography (GPC) is a form of liquid chromatography that separates molecules based on their effective size in a given solvent. The stationary phase, in this case Waters Microstyragel, has a graded microporosity that retards the forward motion of molecules through the column to varying degrees as a function of the molecules size-dependent ability to penetrate the pores. The injected sample thus elutes from the column as a function of time with the smaller molecules exiting last. The concentration of the eluting molecules is measured by a differential refractometer. The calibration of elution time with molecular weight is done with known compounds. In the present case this calibration was done with narrow molecular weight fractions of polystyrene so the calibration is not exact; it could easily be off by a factor of two but that is not crucial for the present purpose.

Figure 27 shows GPC results for the organic condensate from two white pine samples exposed differently, one in nitrogen (Fig. 27(a)) and the other in air; other exposure conditions are those of the base case. These two cases were chosen because one might expect significant differences in the composition of the condensate; inspection of Fig. 3 and Fig. 5 indicates that the peak sample surface temperatures differ by more than 100°C. Both spectra are qualitatively quite similar showing a main peak at MW $\simeq$ 220-250; both also show a significant number of molecules of MW > 1000. (Recall, however, that the absolute molecular weight calibration is approximate here.) Both GPC chromatograms have been truncated at just below MW=100 because the water and methanol present cause a large negative peak. It should be noted also that about 15% of the height of the lower molecular weight peak is due to solvent impurities. Quantitative differences between the two cases can be seen but they are probably not significant; they fall within the spread of results seen when condensate from two different wood samples, exposed identically, is

subjected to GPC analysis. The same ambiguity about the significance of quantitative differences also was found with condensate from samples exposed at very low and very high radiant fluxes (2-1/2 W/cm^2 vs. 7.8 W/cm^2).

Fast atom bombardment (FAB) mass spectroscopy provides a measure of the molecular weight distribution of a sample as well. The sample is coated on a metal surface (along with some glycerol) and bombarded with fast neutral atoms (cesium in the present case) which both vaporize and ionize the molecules. The ions (positive or negative) are then sorted according to mass/charge ratio as in normal mass spectroscopy. Fragmentation of the molecules is relatively small but it does yield some distortion of the molecular weight distribution, biasing it toward smaller sizes.

Figure 28 shows FAB mass spectra of the organic condensate from the same two white pine samples as were used for Fig. 27. Figure 28 does not show a significant difference in the FAB spectra. Both samples yield a broad flat distribution of ions extending to 1000 amu and beyond (note that the inset graphs provide magnified views of the high end of the mass unit scale). The tall peaks at 93 and 185 amu are due to the glycerol; the peak at 133 amu is due to cesium ions; the peak at 43 amu is a common hydrocarbon fragment that could arise from many different parent molecules.

An interesting feature here, as with the GPC chromatograms, is the indication of an appreciable amount of high molecular weight material. The capillary gas chromatograms did not reveal material heavier than about 200 amu. Figure 28 implies that perhaps 40-50% of the organic condensate mass lies above this value. (Figure 27 implies a high molecular weight portion more like 25-30%.) One might at first infer that such material is largely polycyclic organic material. While some of it undoubtedly is, it seems unlikely that the majority is. Polycyclic aromatic hydrocarbons become rapidly less volatile with increasing size; coronene (M.W.=300) has a boiling point of 525°C. Unlike the wood stove situation in the radiative heating experiments such molecules cannot form in the gas phase away from the wood. They must form in the wood sample and then leave; the temperatures are not adequate for the requisite vaporization in most of the sample.

A more probable explanation of these large molecules is that they are polymers (oligomers) of some of the smaller species. The furans, phenols and aldehydes are capable of reacting together to form condensation polymers [29]. Such polymerization of the organic condensate from wood gasification has been previously reported [24,30]; acid or base catalysis can be involved. Such large molecules would be equally unlikely to vaporize from the wood during radiative heating. They could conceivably form in the aerosol droplets as the cooler temperatures away from the wood surface allow condensation; in this case they would not be artifacts. The alternative is that they are artifacts which formed in the sampling system or during sample storage. The capillary GC chromatograms have not changed systematically with age over many months; this implies that any such polymerization would have to go essentially to completion fairly soon after sample generation, perhaps during the process of being extracted from the cold trap (the samples spend up to two hours at room temperature). Unfortunately, we do not have enough information to resolve this issue.

Liquid chromatography, based on a solute's chemical interaction with a stationary phase (rather than a physical interaction as in GPC), can produce a more detailed fingerprint. In the form used here (reverse phase), the tar/solvent sample is injected on the head end of a high pressure liquid chromatographic column (HPLC) where it is subjected to a flow of an eluting solvent whose composition is slowly changed. An important advantage here is the lack of any sample heating such as occurs in gas chromatography; this method is non-destructive so the losses that occurred in the capillary GC inlet are absent here. The HPLC column was a Vydac 201 TP C_{18} column; the eluting solvent was initially 10% methanol in water and it was programmed to 100% methanol over a 30 min. period. The net solvent polarity thus decreased with time so the first eluted components are the most polar. Since 100% methanol is still fairly polar, non-polar constituents of the sample would not be eluted; it is not expected that any great amount of totally non-polar species is present anyway.

A difficulty with HPLC is the lack of a highly sensitive universal detector. A refractive index detector, such as that used in the GPC studies, is universal but here it showed only two or three peaks (probably solvents

present). An ultraviolet absorption detector (254 nm) was used to generate the fingerprints in Figure 29. Such a detector is 10^3-10^4 times more sensitive but it is selective for species absorbing at the wavelength chosen. Generally this means species with conjugated double bonds or aromatic resonance. This could include, for example, the various phenols, furans, polycyclic aromatics and carbonyl compounds with β unsaturation. Since ultraviolet absorbance peaks are quite broad, many compounds whose absorbance does not peak very near 254 nm will be seen anyway but the apparent peak height will be relatively suppressed.

What this means is that HPLC with an ultraviolet detector should definitely produce a fingerprint with a differing set of biases from those in gas chromatography. Since it relies on solubility and not volatility, it seems reasonable to expect that it also will elute nearly all of the sample, i.e., the higher molecular weight species (at least those soluble in methanol, which appear to be a majority) should elute as well as the smaller species.

Figure 29 presents HPLC fingerprints for two of the same samples as were used in the other techniques. It is clear that HPLC lacks the resolution of capillary gas chromatography, however, the fingerprint has a good deal of detail. Comparison of the fingerprints for the condensate obtained from two substantially differing gasification conditions (white pine in air and in nitrogen) shows very little difference. As with the other techniques, the most obvious differences (which are few) are in relative peak heights only.

These additional fingerprinting techniques tend to confirm the borderline significance of variations in the composition of the organic condensate as the conditions of its generation are varied. The first two indicate that the bulk of the material missing from the capillary GC fingerprints is of high molecular weight (MW $\geq$ 200), most likely polymers of some of the smaller molecules. If these (presumed) polymers were prevented from forming, the capillary GC fingerprints would look different because some of the furan, aldehyde and phenol peaks would be enlarged (we cannot say which at this point). However, since the amount of high molecular weight material apparently does not vary greatly with the conditions of condensate formation, we can only infer at this point that the fingerprints with polymerization suppressed would not vary much

differently with sample exposure conditions from those obtained here. The mechanism for such comparative invariance of the condensible organic species remains unclear.

3.8 Comparison with Wood Stove Organic Condensate

It is of interest to see to what degree the fingerprints of the tar from the radiative heating tests correspond to those for similar woods burned in a wood stove. The stove used for this purpose was airtight and non-baffled with a firebrick lining; it had a glass window on one side that allowed limited viewing of the combustion of the wood load. Duplicate runs with two kinds of wood were made under the "overnight burn" conditions mentioned earlier, i.e., the air supply was choked down to the point that flaming was absent more than 95% of the burn time. The resultant stack temperature (about two feet from the stove exit) was in the range 100-115°C. The stove was filled to about two-thirds of full capacity after a bed of coals was first established. Smoke from the stack centerline (about two feet from the stove exit) was sampled continuously during the next 5-1/2 to 6 hours of burning. The stove air vents were adjusted manually during this time to keep the stack temperature in the range indicated. The sampling system was essentially identical to the cold trap and aerosol filter used in the radiative heating tests except that a second spiral cold trap was added in series with the first to preclude break-through at long times; this proved to be unnecessary. The sampling rate was kept low (500 cc/min) so as not to warm up the cold traps excessively at long times. About 5 g of material was collected over the test duration. Extraction and fingerprinting techniques were identical to those for the radiative heating tests. Two runs were made with mixed oak wood (red, white and pin oak) and two were made with yellow pine. The logs were split pieces with a minimum thickness dimension in the range of one to three inches; bark was included in the oak but not the yellow pine tests. Moisture content of the wood, checked with an impedance meter, was 8-10%.

Figure 30 shows the fingerprint of the organic condensate from a stove burn with mixed oak and that of the condensate from radiative heating of red oak at the base case conditions. It should be noted that the heating rate and ambient oxygen history around the wood in the stove most probably differ

substantially from point to point in the stove and also, of course, they differ from that seen by the red oak sample in the base case radiative heating test. However, the preceding discussion of the fingerprints from the radiative heating tests implies that these differences will not have a major impact on the condensate composition. In fact Fig. 30 shows that the fingerprint from the stove is generally quite similar to that from the radiative heating apparatus. At the same time there are a few differences that are more definite than those existing among the radiative heating fingerprints. Several of the peaks in the retention time range of 14 to 17 min (Fig. 30(a)) are present only at trace levels in the stove fingerprint. The peaks at 28.14 (tentatively, solketal) and 28.35 min (3 or 5-methyl furan 2-aldehyde) (Fig. 30(a)) are completely absent in the stove fingerprint. The peak at 55.8 min (2-tert butyl phenol) (Fig. 30(a)) is suppressed by an order of magnitude. Three or four other peaks due to unidentified products are similarly suppressed by an order of magnitude. Levoglucosan (79-80 min) is present in substantially reduced amounts though this compound varied widely in the radiative heating tests. The reasons for the absences noted is not clear. Presumably these compounds were generated in the wood but were preferentially degraded as the smoke underwent recirculation through the smoldering bed of wood before leaving the stove.

Figure 31 shows a similar comparison for yellow pine. Again the two fingerprints are largely alike although here the stove case has a few both added and subtracted peaks. For the identified species the major differences are as follows. The peak at 28.41 min (3 or 5 methyl furan 2-aldehyde) (Fig. 31(a)) is much less in the stove as it was for oak above. The peak at 29.58 min (butyrol lactone) (not shown in Fig. 31(a) because it is below the threshold) is an order of magnitude bigger in the stove. The peak at 59.34 min (eugenol) (again below the threshold in Fig. 31(a)) is about 5x bigger in the stove. Contrary to the oak case, the levoglucosan peak (79-80 min) is somewhat bigger in the stove than in the radiative heating situation. There are about half a dozen other unidentified peaks which differ in size by a factor of 5 to 10 between the two heating situations.

The major implication of this result is that, in this "overnight burn" condition, the majority of the products leaving the wood stove (and becoming

air pollutants) arise directly from the wood surface during its self-sustained smoldering process. Passage through the stove for the most part involves dilution and cooling of the wood gasification products. Some recirculation through the smoldering bed of wood is inevitable and this causes some re-contact with the hot wood surfaces but the net alteration is comparatively small. It is possible that the differences between the stove and radiative heating fingerprints seen here have more to do with the differences in the mode of wood gasification rather than any further reactions in the stove. This point will be checked in future experiments on two-dimensional, self-sustained smolder of wood.

4. CONCLUSIONS

The products of the gasification of wood have been extensively characterized for a wide range of conditions incorporating those in wood burning stoves. The major products (CO, CO_2, water, tar, THC) vary rapidly with time only in the first two or three minutes but their rate of emission continues to vary more slowly with prolonged heat exposure. When time-averaged major product compositions are compared as a function of the conditions of wood gasification (varying heat flux, ambient oxygen, sample thickness, grain orientation, exposure time, water content and wood type, one variable at a time about a base case), they are found to change by no more than a factor of four for all conditions examined; in many cases the variation is within a factor of two.

The organic condensate or tar is extremely complex in composition, probably exceeding two hundred constituents above trace levels in the chromatographable portion alone. Twenty-nine species were positively identified by a combination of gas chromatography and mass spectroscopy. An additional fifteen species were tentatively identified by the same techniques. Nearly all of these species have been previously seen in other types of wood and/or wood component gasification processes. Except in the cases of very short time exposures or high water content in the wood, the relative levels of the main constituents in the chromatographable portion of the tar (ca. 20% of the mass) varied by no more than a factor of two or three despite the wide variations in sample exposure conditions. In the former two cases, there was

some hint (but no definitive evidence) that the significant differences could be due to lesser degradation of primary tar components in the hot char through which they must pass in order to leave the gasifying wood.

An interesting finding is the general similarity between the fingerprints from the radiative heating experiments and those from "overnight burning" of the same woods in a stove. This implies that, for this type of burn condition, most pollutants issuing from a woodstove are coming directly from the smoldering wood.

The results of this study (and others preceding it) imply that predicting even the major components (CO, CO_2, H_2O, tar, THC) of wood gasification in the presence of oxygen requires a chemically complex model. Kinetic descriptions are needed for the temperature (and possibly oxygen) dependent rate of gasification of the three major component classes (cellulose, hemi-celluloses, lignin). For ignition studies where the most volatile components count heavily, the extractives may also be important. Strictly speaking each of these major wood components requires a multi-step description of the degradation and gasification in order to be broadly applicable and this still neglects any interactions among the basic wood constituents. A complete description of the stoichiometry of major product formation from each wood component is also necessary. The char oxidation process may be fairly simple chemically but it has physical complications inherent in it; the char is porous and it goes through large changes in internal surface area as it is consumed. Some description of this is needed. Secondary gasification reactions (CO_2, H_2, H_2O attack) complicate the char behavior at temperatures above about 650°C. Finally there is the ambiguous issue of reactions between primary tar products and the hot char (forming either smaller molecules or more char). More direct evidence on this is needed. Presumably the same experiments which could provide the direct evidence could also provide some empirical rate information. Secondary tar reactions are also coupled to the physical state of the char - the degree to which it contacts the primary tar passing through or largely bypasses material through cracks. Prediction of char cracking patterns is a fundamentally intractable problem so some appropriate empirical description of this process would be required.

5. ACKNOWLEDGMENTS

Mr. William Wooden and Dr. Arvind Attreya helped extensively in carrying out the radiative heating experiments. Dr. Attreya also provided extensive assistance in the tedious job of installing the fine surface thermocouples.

Dr. William Manders ran the ^{13}C-NMR experiments on the wood residue and interpreted the spectra.

Mr. Robert Smith of the West Virginia University Mass Spectroscopy Center performed all of the mass spectral analyses.

Mr. James Brown ran the gel permeation chromatograms on the organic condensate. Dr. Michael Welch ran the Fast Atom Bombardment mass spectral analyses. Dr. Stephen Wise ran the liquid chromatography analyses. Mr. Frank Guenther provided helpful advice from time-to-time on the capillary gas chromatographic analyses.

6. REFERENCES

[1] Cooper, J. and Malek, D., Residential Solid Fuels; Environmental Impacts and Solutions, (Proceedings of the 1981 International Conference, Portland, Oregon), published by Oregon Graduate Center, Beaverton, Oregon, 1982.

[2] Bendersky, C., "Results of the Residential Wood Program Emissions Think Shop", Pyros Inc. Report 1011.R1, August 1980.

[3] Gann, R., "Comparison of Principal Combustion Products from a Wood Stove as a Function of Height in the Chimney", Final Report for FY 1982 on DOE Project No. 133A, DE-AOI-76PR06010 from the National Bureau of Standards (October 1982).

[4] Murphy, M., Allen, J. and Longanbach, J., "Residential Heating with Solid Fuels, Task 2: Characterization of Wood Charge Utilization in Woodstoves", Final Report to USDOE from Batelle Columbus Laboratories, Columbus, Ohio (April 1984).

[5] Dyer, D., et al., "Improving the Efficiency, Safety and Utility of Woodburning Units", Quarterly Report WB-4, Vol. II on ERDA Contract EC-77-S-05-5552, Auburn Univ. Dept. of Mech. Eng., September 1978.

[6] Attreya, A., "Pyrolysis, Ignition and Fire Spread on Horizontal Surfaces of Wood", Ph.D. Thesis, Harvard University (1983).

[7] DeAngelis, D., Ruffin, D. and Reznik, R., "Preliminary Characterization of Emissions from Wood-Fire Residential Combustion Equipment", Environmental Protection Agency Rept., EPA-600/7-80-040, March 1980.

[8] Rose, M. and Johnstone, R., Mass Spectroscopy for Chemists and Biochemists, Cambridge University Press, Cambridge, England, 1982, p. 54 ff.

[9] Lee, C., Chaiken, R. and Singer, J., "Charring Pyrolysis of Wood in Fires by Laser Simulation", Sixteenth Symposium (International) on Combustion, The Combustion Institute, Pittsburgh, PA (1976), p. 1459.

[10] Roberts, A.F., "A Review of Kinetics Data for the Pyrolysis of Wood and Related Substances", Combust. Flame 14, p. 261 (1970).

[11] Kung, A.C., "A Mathematical Model of Wood Pyrolysis", Combust. Flame 18, p.185 (1972).

[12] Kansa, E., Perlee, H.E. and Chaiken, R., "Mathematical Model of Wood Pyrolysis Including Internal Forced Convection", Combust. Flame 29, No. 3, p. 311 (1977).

[13] Madorsky, S., Thermal Degradation of Organic Polymers, Interscience, New York (1964) p. 238.

[14] Kanury, M. and Blackshear, K., "Some Considerations Pertaining to the Problem of Wood Burning", Comb. Sci. Technol. 1, (1970) p. 339.

[15] Summitt, R. and Sliker, A. (eds.), CRC Handbook of Materials Science, Vol. IV, Wood, CRC Press, Boca Raton, Florida, 1980, p. 38.

[16] ibid, p. 26.

[17] Rowell, R. (ed.), The Chemistry of Solid Wood, ACS Advances in Chemistry Series No. 207, American Chemical Society, Washington, DC, 1984, p. 78 ff.

[18] ibid, p. 62 ff.

[19] McKee, D., "The Catalyzed Gasification Reactions of Carbon", Chemistry and Physics of Carbon, Vol. 16 (P. Walker and P. Thrower, eds.), Dekker, New York (1981), pp. 1-118.

[20] Laurendeau, N., "Heterogeneous Kinetics of Coal Char Gasification and Combustion", Prog. Energy Combust. Sci. 4, (1978), p. 221-270.

[21] Earl, W., "An Investigation of Wood Pyrolysis Using Solid State ^{13}C Nuclear Magnetic Resonance", in Residential Solid Fuels, op. cit., p. 772.

[22] Molten, P. and Demmitt, T., "Reaction Mechanisms in Cellulose Pyrolysis: A Literature Review", Batelle Pacific Northwest Laboratories Report BNWL-2297, Richland, Washington, 1977.

[23] Milne, T., "Pyrolysis - The Thermal Behavior of Biomass Below 600°C" in "A Survey of Biomass Gasification, Vol. II - Principles of Gasification", Solar Energy Research Institute SERI/TR-33-239, Vol. II, July 1979.

[24] Goos, A., as quoted in Jahnsen, V., "The Chemical Composition of Hardwood Smoke", Ph.D Thesis, Purdue University, 1961.

[25] Hubble, B., et al., "Experimental Measurements of Emissions from Residential Wood-Burning Stoves" in Residential Solid Fuels; Environmental Impacts and Solutions, op. cit. p. 79.

[26] Sjostrum, E., Wood Chemistry; Fundamentals and Applications, Academic Press, New York, 1981, Chap. 4 and 5.

[27] Hawley, L., "Combustion of Wood" in Wood Chemistry, Vol. 2 (2nd ed.), L. Wise and E. Jahn (eds.), Reinhold, New York, 1952, pp. 846-850.

[28] Rowell, R. (ed.), op. cit., p. 66.

[29] Roberts, J. and Caserio, M., Basic Principles of Organic Chemistry, W.A. Benjamin, New York (1965) pp. 1102-1103.

[30] Polk, M. and Phingbodhippakkiya, M., "Development of Methods for the Stabilization of Pyrolytic Oils", EPA Report EPA-600/2-81-201, Atlanta University, Atlanta, Georgia, September 1981.

Table 1

Summary of Test Results

Wood Type	Grain Orientation	Sample Thickness (cm)	Water Content	Exposure Time (Min)	Atmosphere	Incident Flux (W/Cm^2)	Total Mass Of Products (g)	(Product Mass) (Weight Loss)	%Water	%CO	%CO_2	%THC	%Tar
White Pine	Flux || To Pores	3.87	Normal	12	10 1/2% O_2	4.0	6.42	1.27	30.6	11.5	30.8	4.8	22.2
White Pine	Flux || To Pores	3.75	Normal	12;Shutter not closed	10 1/2% O_2	4.0	6.47	1.21	46.1	13.6	28.9	5.3	6.0
White Pine	Flux || To Pores	3.85	Normal	12;Shutter not closed	10 1/2% O_2	4.0	6.52	1.10	38.4	13.0	28.5	5.5	14.5
White Pine	Flux || To Pores	3.80	Normal	15	10.5%O_2	4	8.61	1.23	45.1	11.8	31.0	4.9	7.2
White Pine	Flux || To Pores	3.89	Normal	12:Shutter not closed	N_2	3.37	3.37	0.92	64.4	7.5	8.4	5.6	14.0
White Pine	Flux || To Pores	3.71	Normal	15	N_2	4	4.64	0.99	69.7	6.7	8.8	5.0	10.0
White Pine	Flux || To Pores	3.81	Normal	12	Air	4.0	10.32	1.45	34.4	15.4	38.9	4.0	7.3
White Pine	Flux || To Pores	3.70	Normal	15	Air	4	13.70	1.41	33.1	13.7	41.1	6.0	6.1
White Pine	Flux || To Pores	3.84	Normal	12	10.4% O_2	2.5	3.90	1.14	54.6	10.0	21.5	1.9	12.0
White Pine	Flux || To Pores	3.77	Normal	15	10.5%O_2	2.5	5.27	1.13	51.4	9.5	24.5	2.8	11.8

Table 1 (Continued)

Summary of Test Results

Wood Type	Grain Orientation	Sample Thickness (cm)	Water Content	Exposure Time (Min)	Atmosphere	Incident Flux (W/Cm^2)	Total Mass Of Products (g)	(Product Mass) (Weight Loss)	%Water	%CO	$\%CO_2$	%THC	%Tar
White Pine	Flux || To Pores	3.9	Normal	13' 19"	10 1/2% O_2	6.7	7.05	1.29	45.4	13.0	30.2	4.7	6.6
White Pine	Flux || To Pores	3.85	Normal	12	10.4% O_2	6.9	10.68	1.23	38.9	16.3	28.8	8.7	7.3
White Pine	Flux || To Pores	3.80	Normal	12	10.5% O_2	6.9	11.02	1.22	40.8	15.8	29.4	7.9	6.1
White Pine	Flux || To Pores	4.03	Normal	12	10.6% O_2	7.85	10.62	1.19	28.6	19.0	27.9	9.6	14.6
White Pine	Flux || To Pores	3.84	0	12;Shutter not closed	10 1/2% O_2	3.95	6.50	1.29	31.6	14.9	30.9	6.3	16.2
White Pine	Flux || To Pores	3.95	0	15	10.5% O_2	4	8.58	1.29	31.6	14.9	35.2	6.4	11.9
White Pine	Flux || To Pores	3.40	53%	12	10.4% O_2	4.0	11.50	0.92	77.3	2.3	5.0	0.5	15.0
White Pine	Flux || To Pores	3.87	53%	10' 41"	11% O_2	4	10.97	0.88	73.5	3.6	8.8	0.9	13.3
White Pine	Flux || To Pores	3.80	~ 30% Water	15	10.6% O_2	4	10.97	0.80	70.9	1.7	4.9	0.6	21.9
White Pine	Flux || To Pores	3.80	~ 33% Water	24	10.6% O_2	4	16.39	1.11	68.4	6.7	18.4	2.0	4.6
White Pine	Flux ⊥ To Pores	3.8	Normal	12	10 1/2% O_2	4.0	7.59	1.21	36.5	9.2	27.7	3.7	22.9

Table 1 (Continued)

Summary of Test Results

Wood Type	Grain Orientation	Sample Thickness (cm)	Water Content	Exposure Time (Min)	Atmosphere	Incident Flux (W/Cm^2)	Total Mass Of Products (g)	(Product Mass) (Weight Loss)	%Water	%CO	$\%CO_2$	%THC	%Tar
White Pine	Flux ⊥ To Pores	3.75	Normal	15	10.5% O_2	4	8.99	1.17	51.3	8.1	28.8	3.6	8.2
White Pine	Flux ⊥ To Pores	3.78	Normal	15	10 1/2% O_2	4	-	-	50.4	-	-	-	29.3
White Pine	Flux ∥ To Pores	4.02	Normal	1 1/2	10 1/2% O_2	4	0.87	1.09	46.6	5.8	11.5	3.0	33.1
White Pine	Flux ∥ To Pores	3.85	Normal	2 1/2	10 1/2% O_2	4	1.54	1.08	38.4	7.8	11.7	2.5	39.5
White Pine	Flux ∥ To Pores	4.02	Normal	6	10 1/2% O_2	4	3.79	1.13	34.2	12.2	20.6	4.4	28.7
White Pine	Flux ∥ To Pores	3.85	Normal	6	10 1/2% O_2	4.0	3.69	1.10	43.4	11.4	19.5	4.1	21.6
White Pine	Flux ∥ To Pores	3.87	Normal	24	10.4% O_2	4.0	11.08	1.31	34.1	13.5	35.2	5.8	11.4
White Pine	Flux ∥ To Pores	4.02	Normal	24	10 1/2% O_2	4	12.29	1.30	36.8	13.2	34.5	5.9	9.5
White Pine	Flux ∥ To Pores	1.96	Normal	12; Shutter not closed	10 1/2% O_2	3.95	6.35	1.18	35.5	13.1	25.7	5.4	20.5
White Pine	Flux ∥ To Pores	1.83	Normal	15	10.6% O_2	4	8.55	1.19	27.8	13.2	28.0	5.6	25.4
Red Oak	Flux ∥ To Pores	2.90	Normal	15	10.4% O_2	4.0	11.94	1.15	48.0	10.4	23.4	4.4	13.8

Table 1 (Continued)

Summary of Test Results

Wood Type	Grain Orientation	Sample Thickness (cm)	Water Content	Exposure Time (Min)	Atmosphere	Incident Flux (W/Cm^2)	Total Mass Of Products (g)	(Product Mass) (Weight Loss)	%Water	%CO	$\%CO_2$	%THC	%Tar
Red Oak	Flux || To Pores	2.90	Normal	15	10.5%O_2	4	13.26	1.07	49.8	10.9	23.4	3.8	12.0
Red Oak	Flux || To Pores	2.90	Normal	15	N_2	4.0	8.00	0.98	68.6	5.8	12.1	4.8	8.8
Red Oak	Flux || To Pores	2.90	Normal	15	N_2	4	7.87	0.88	58.4	5.8	12.6	3.9	19.2
Red Oak	Flux || To Pores	2.82	Normal	15	Air	4.0	15.68	1.26	27.3	12.6	33.2	4.9	22.1
Red Oak	Flux || To Pores	2.88	Normal	15	Air	4	18.93	1.20	36.6	13.2	32.0	4.8	13.4
Red Oak	Flux || To Pores	2.87	Normal	15' 20"	10.5%O_2	2 1/2	5.40	1.01	62.2	4.8	14.1	2.2	16.6
Red Oak	Flux || To Pores	2.93	Normal	15	11%O_2	2.5	5.99	0.94	66.2	4.8	13.5	2.0	13.4
Red Oak	Flux || To Pores	2.98	Normal	12	10.5%O_2	6.9	14.69	1.19	44.6	17.0	23.1	6.5	8.7
Red Oak	Flux || To Pores	2.90	Normal	12	10 1/2%O_2	6.2	14.25	1.07	54.5	14.9	22.7	5.5	2.3
Red Oak	Flux ⊥ To Pores	3.12	Normal	5' 35"	10.4%O_2	4.0	3.78	-	43.1	6.9	14.8	3.2	32.0

Table 1 (Continued)

Summary of Test Results

Wood Type	Grain Orientation	Sample Thickness(cm)	Water Content	Exposure Time(Min)	Atmosphere	Incident Flux(W/Cm^2)	Total Mass Of Products(g)	(Product Mass) (Weight Loss)	%Water	%CO	$\%CO_2$	%THC	%Tar
Red Oak	Flux $\perp$ To Pores	3.12	Normal	7' 54"	10.4%O_2	4	5.39	-	40.6	8.9	17.4	4.1	29.0
Red Oak	Flux $\perp$ To Pores	3.05	Normal	15	10.5%O_2	4	12.01	1.12	48.6	10.2	25.5	4.2	11.5
Red Oak	Flux $\perp$ To Pores	2.88	Normal	15	10.5%O_2	4	13.68	1.02	47.8	9.2	22.9	3.7	16.4
Yellow Pine	Flux $\parallel$ To Pores	3.80	Normal	15	10.4%O_2	4.0	9.40	1.19	43.2	10.7	24.7	4.8	16.6
Yellow Pine	Flux $\parallel$ To Pores	3.87	Normal	15	10.5%O_2	4	8.81	1.12	49.3	9.8	23.7	4.1	13.1

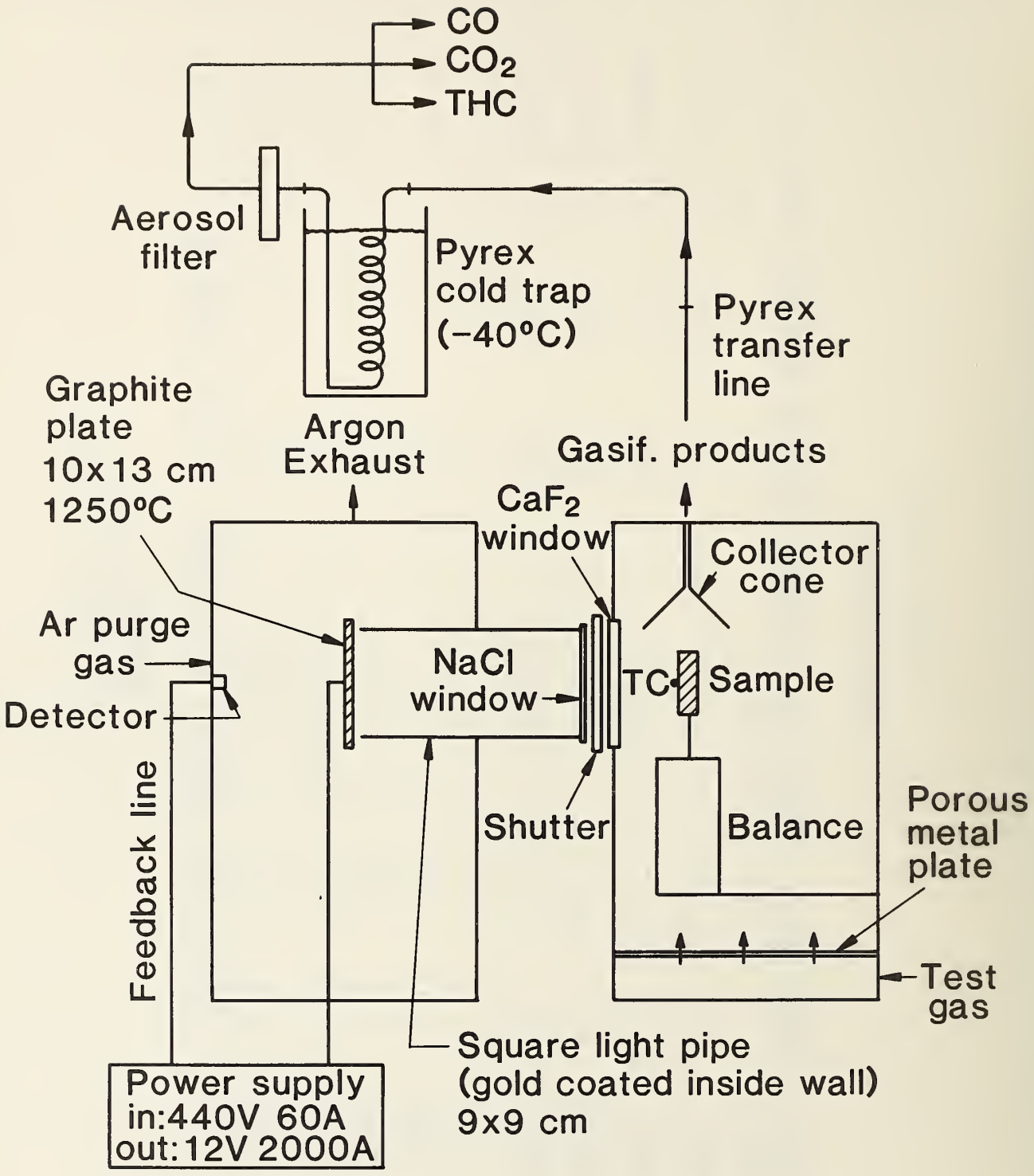

Figure 1. Schematic of apparatus showing details of radiation source and sample chamber

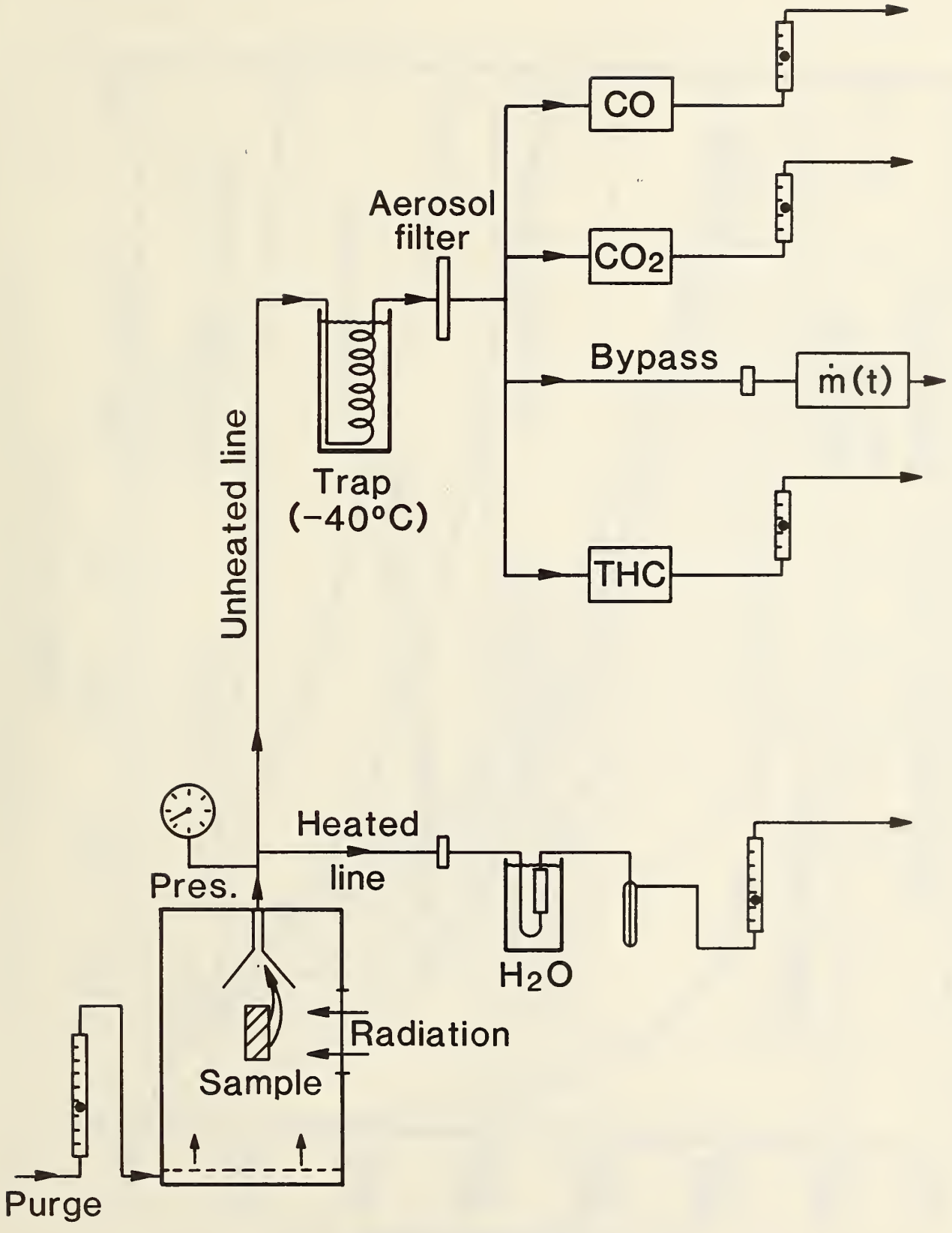

Figure 2. Schematic of apparatus showing details of product monitoring

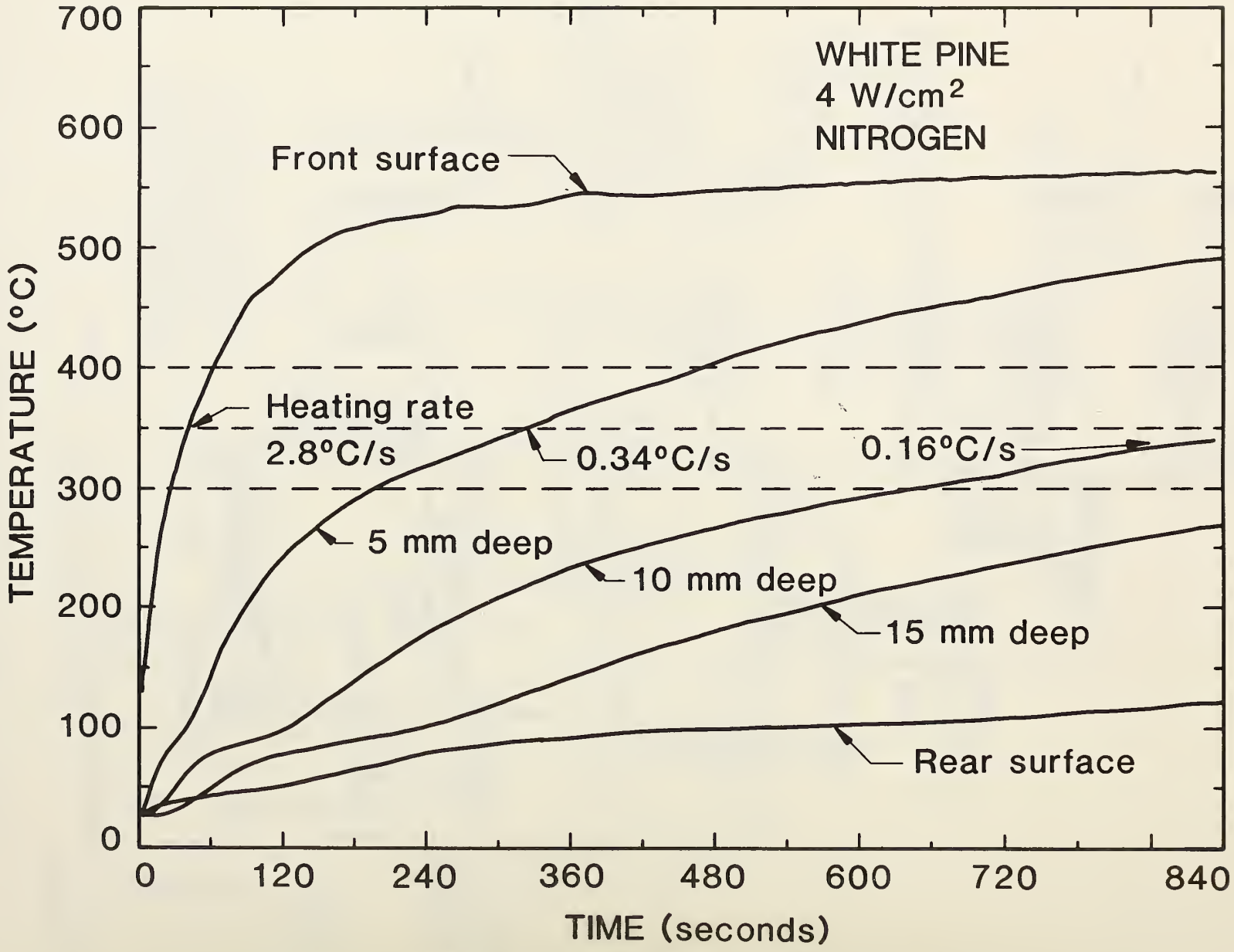

Figure 3(a). Temperature vs time from five thermocouples in a white pine sample: base case conditions except N_2 atmosphere

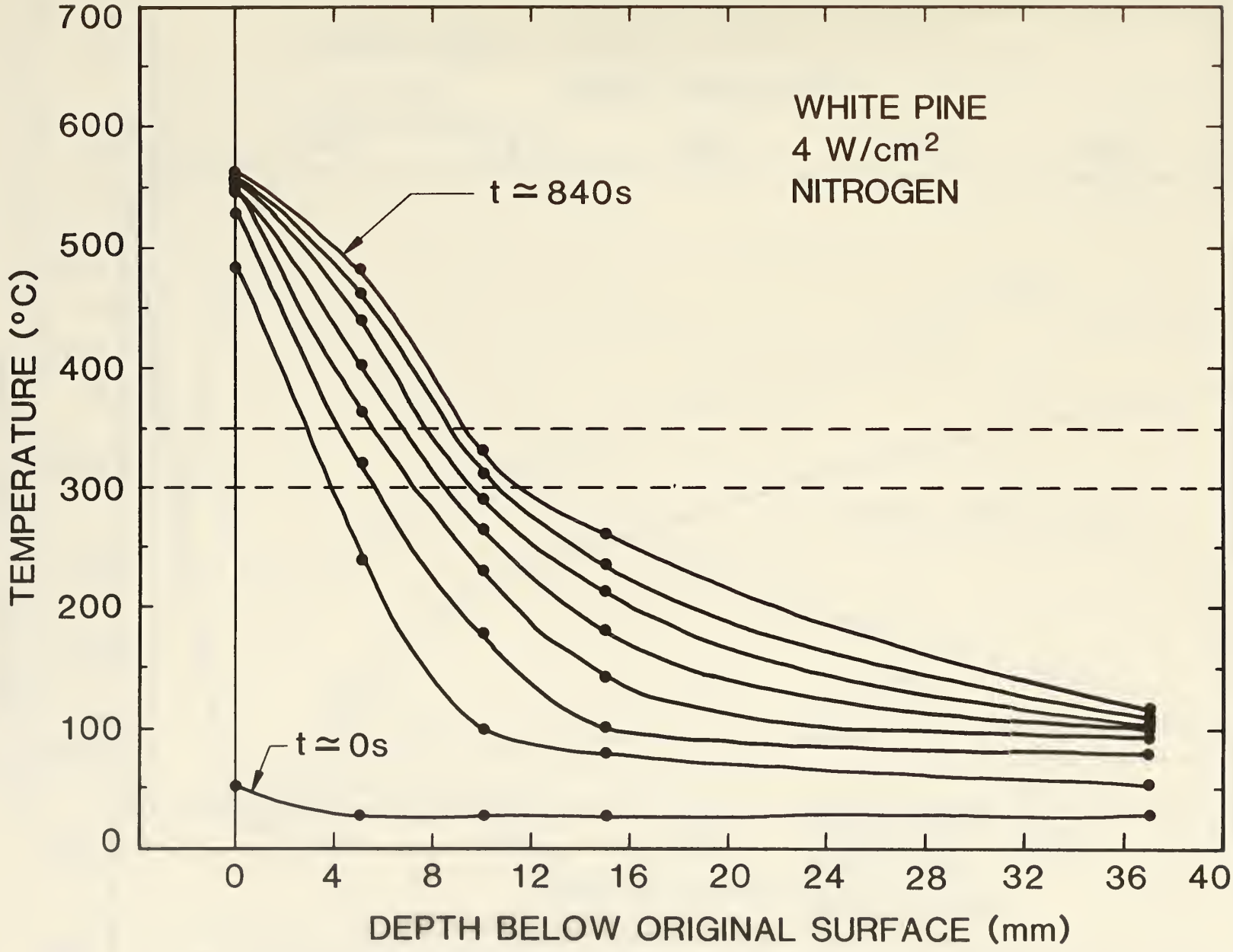

Figure 3(b). Temperature vs depth and time; cross-plotted from Fig. 3(a)

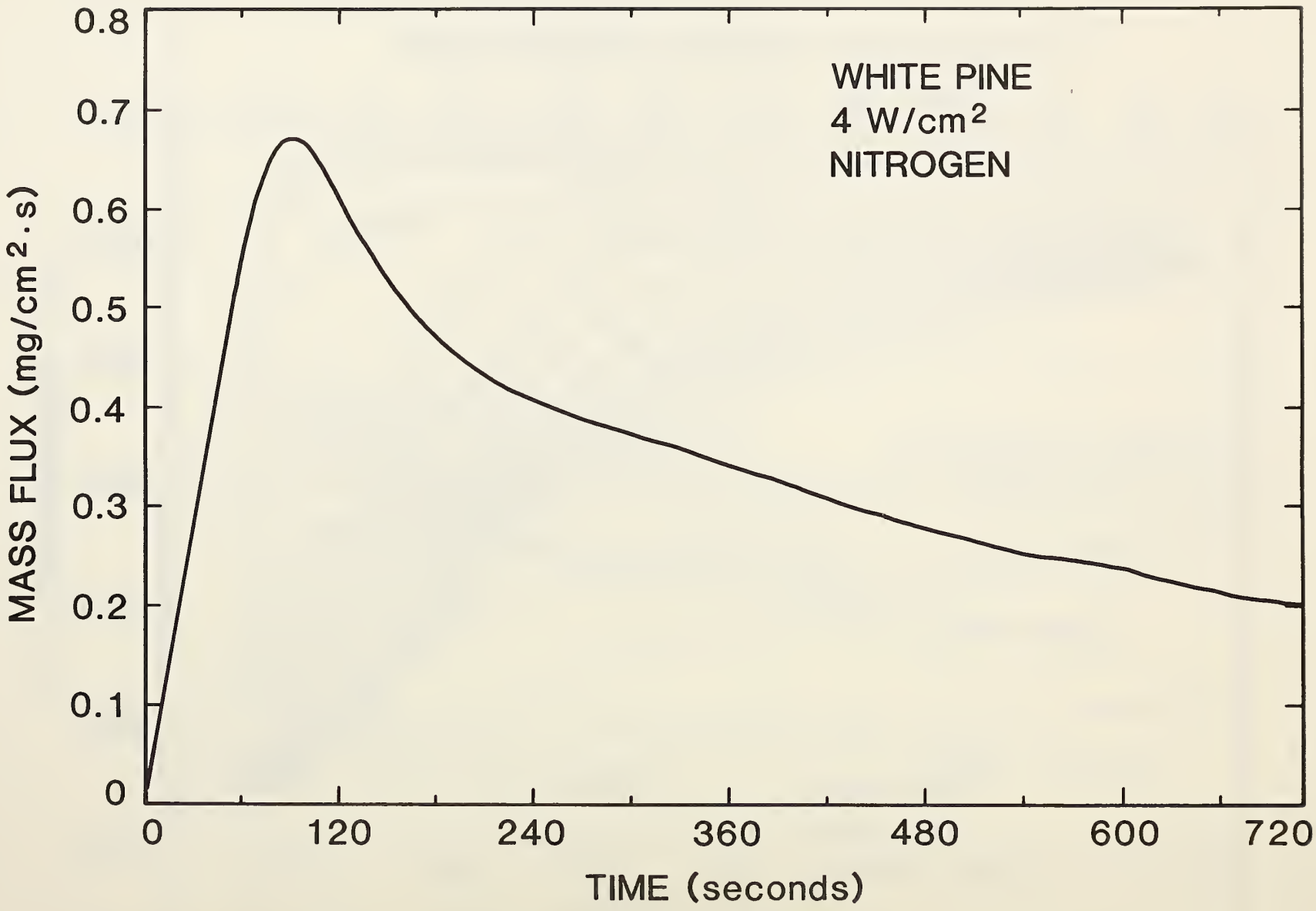

Figure 4(a). Surface mass flux vs time; white pine at base case conditions except N_2 atmosphere

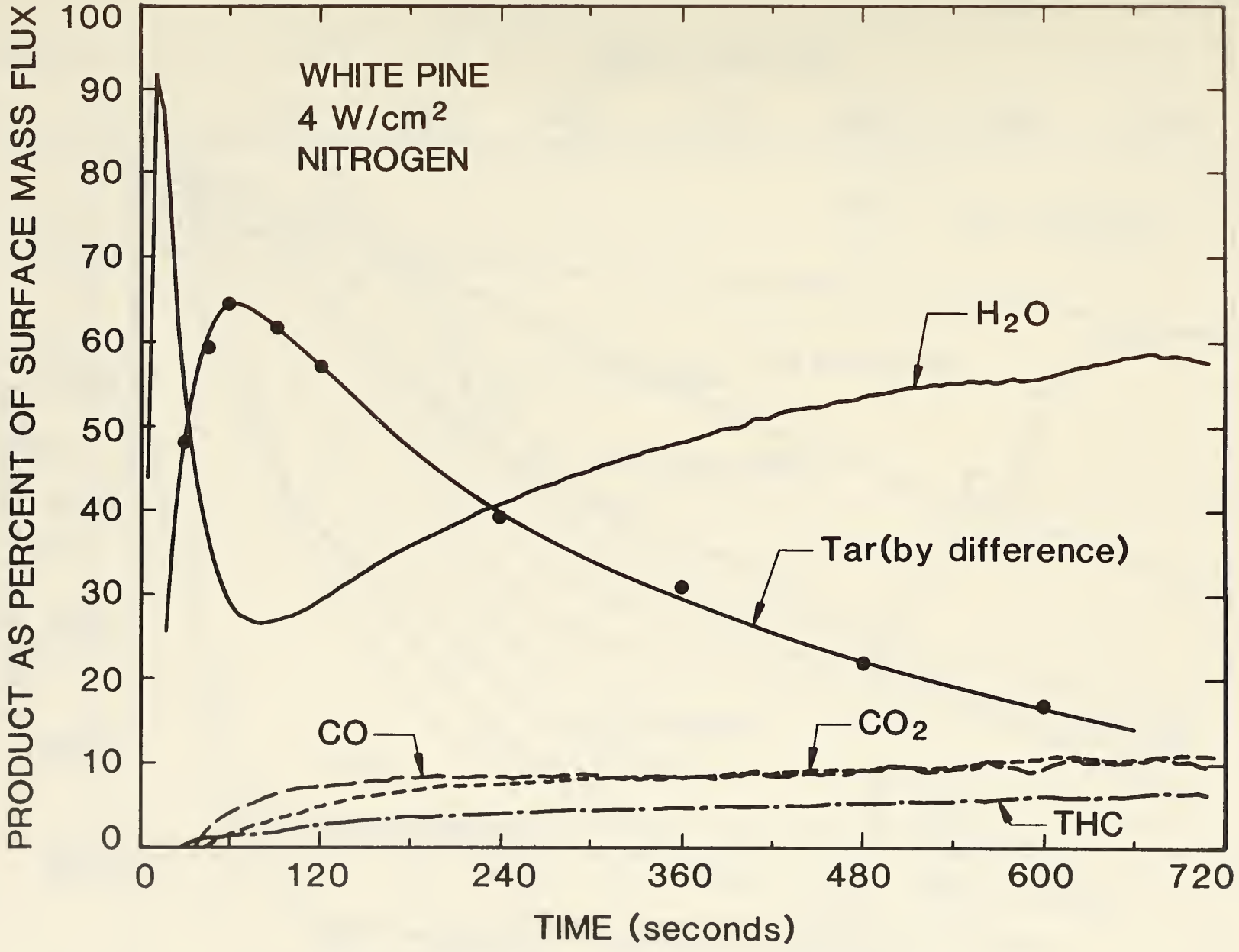

Figure 4(b). Composition of evolved products; white pine at base conditions except N_2 atmosphere. Tar curve is computed at points shown by subtracting the sum of the other products from 100%.

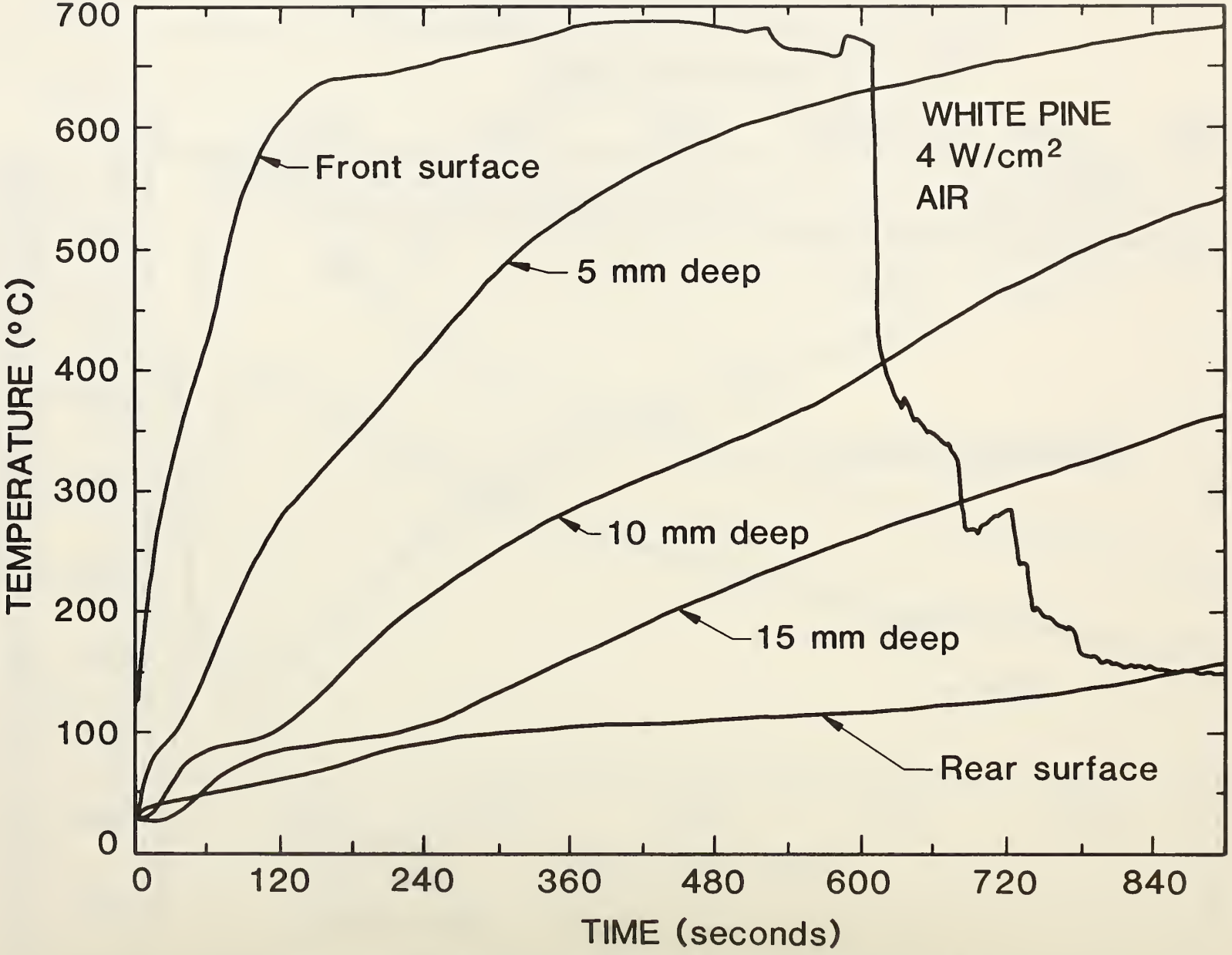

Figure 5(a). Temperature vs time from five thermocouples in a white pine sample; base case conditions except air atmosphere

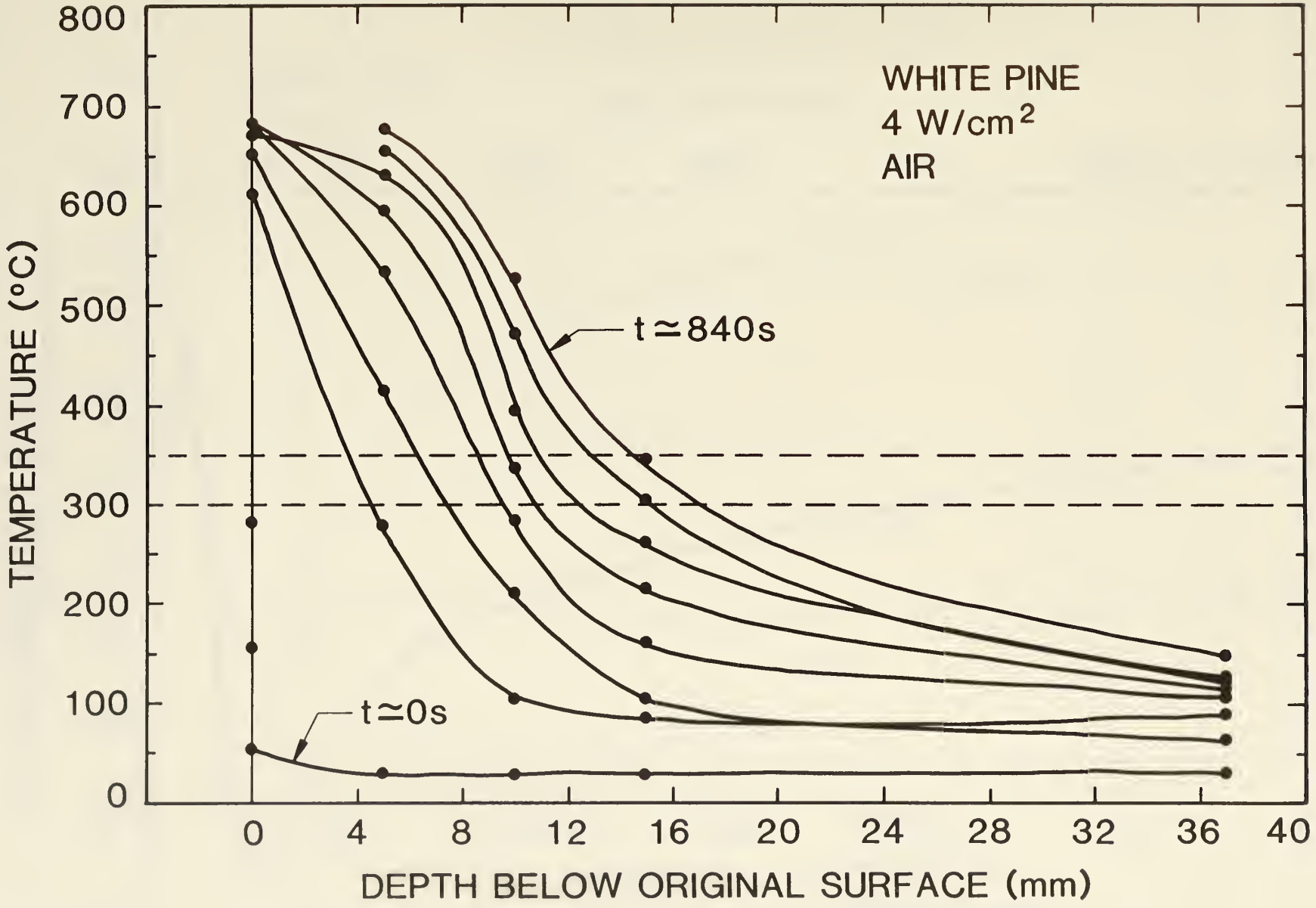

Figure 5(b). Temperature vs depth and time; cross-plotted from Fig. 5(a)

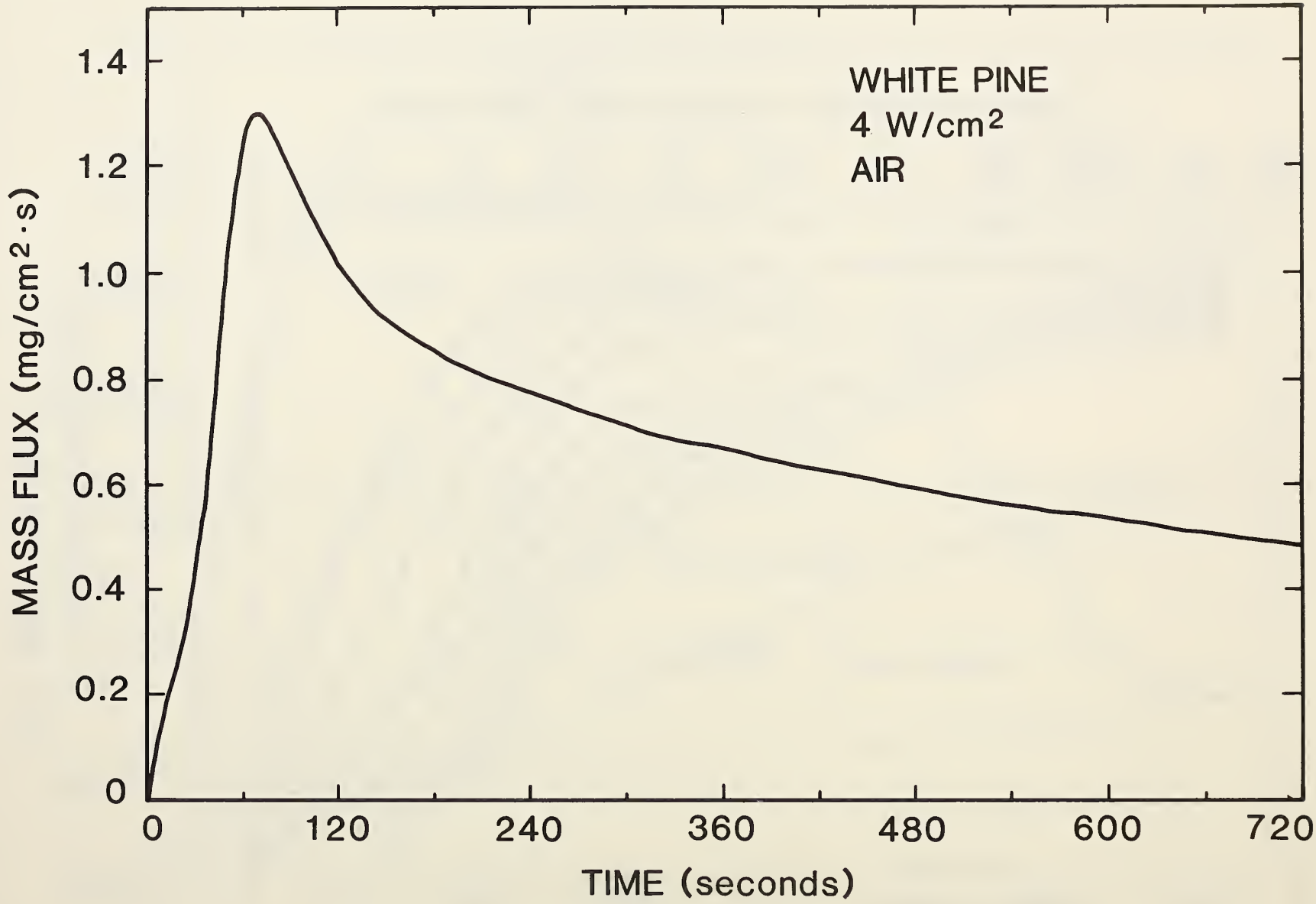

Figure 6(a). Surface mass flux vs time; white pine at base case conditions except air atmosphere

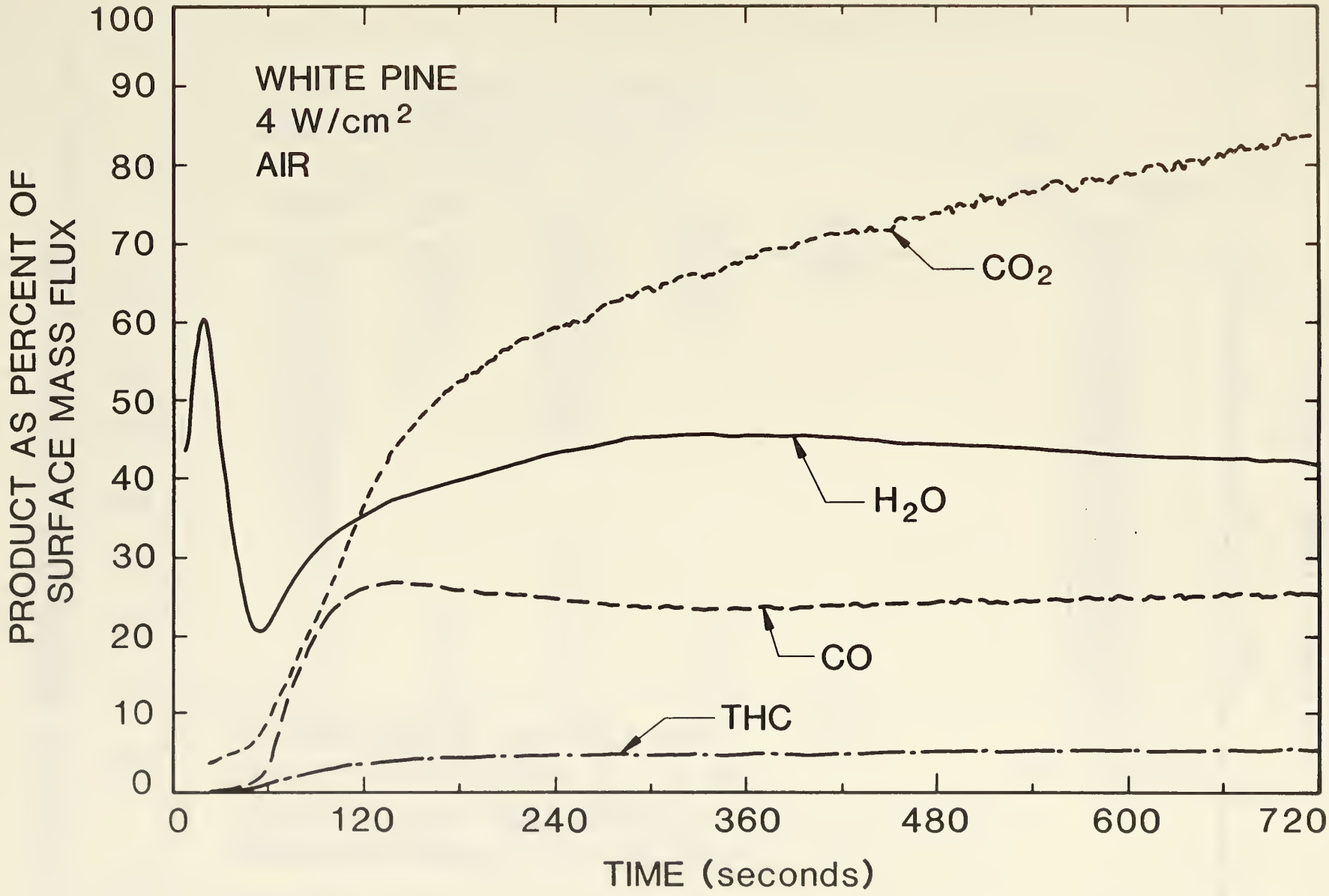

Figure 6(b). Composition of evolved products: white pine at base case conditions except air atmosphere

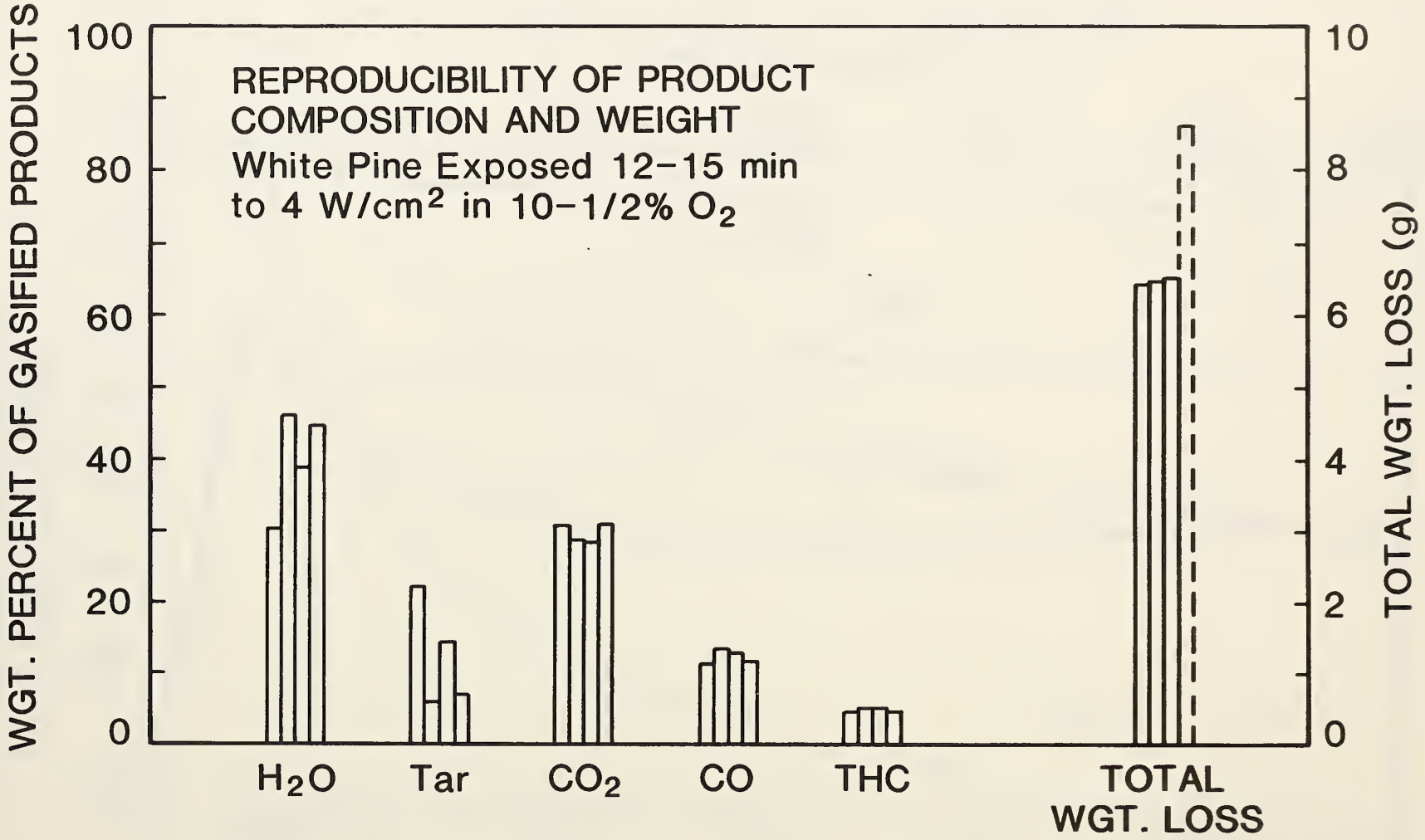

Figure 7(a). Reproducibility of integrated product composition and weight loss for white pine at base case conditions. Dashed weight loss is based on pre- and post-test weights, not just weight loss during constant heat flux period.

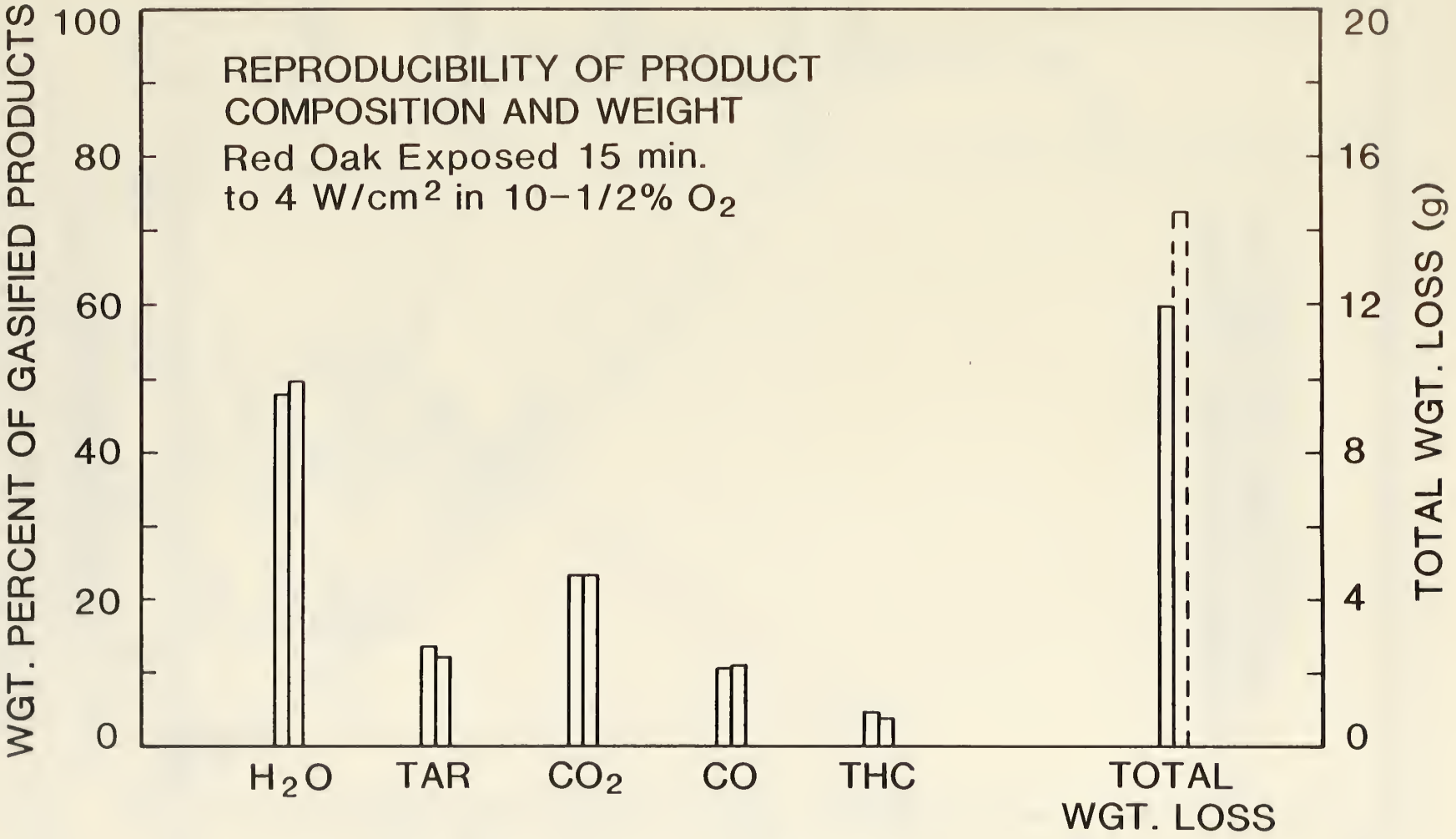

Figure 7(b). Reproducibility of integrated product composition and weight loss for red oak at base case conditions

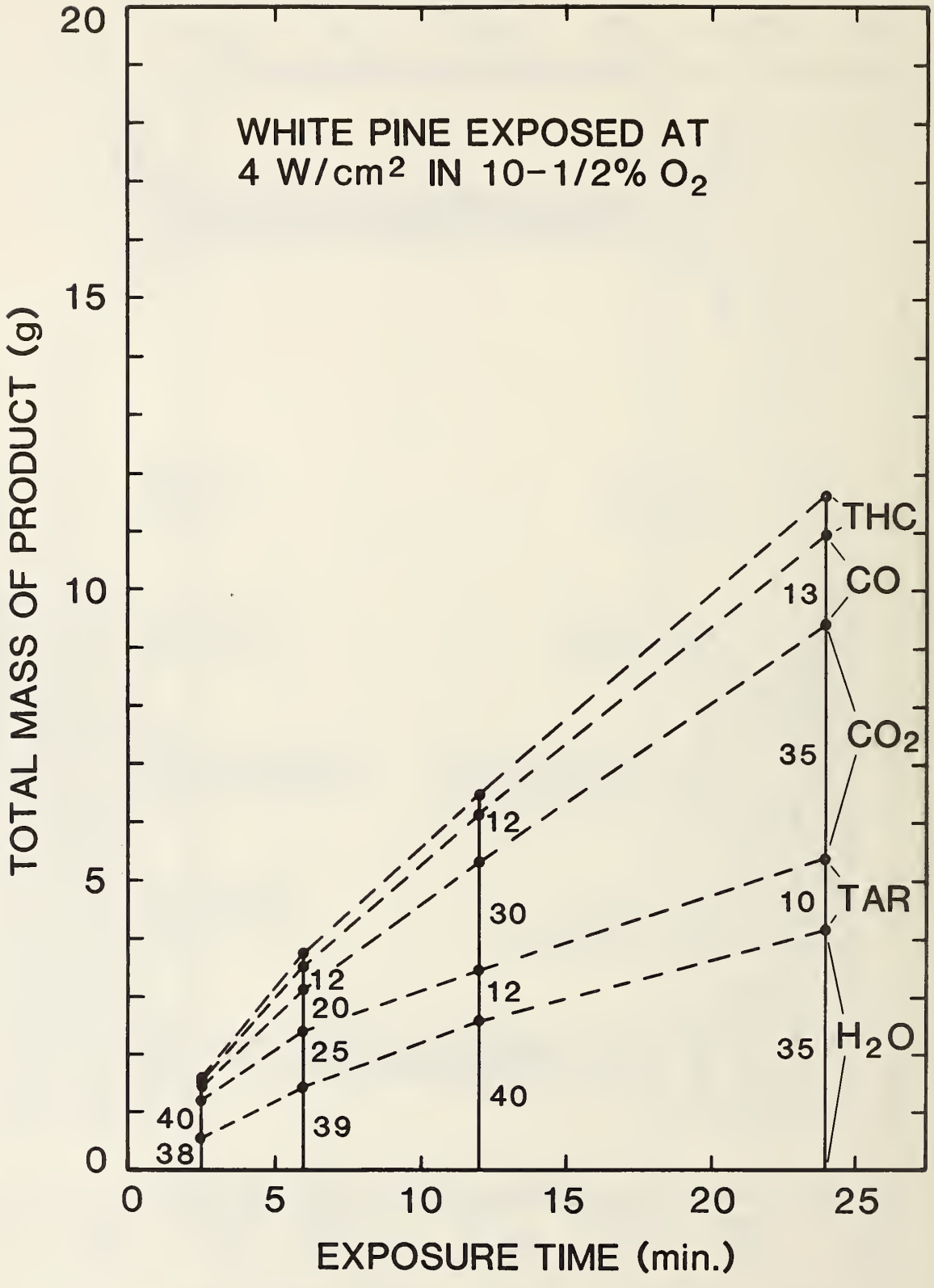

Figure 8(a). Integrated product mass and composition as a function of exposure time; white pine at base case conditions except for exposure time

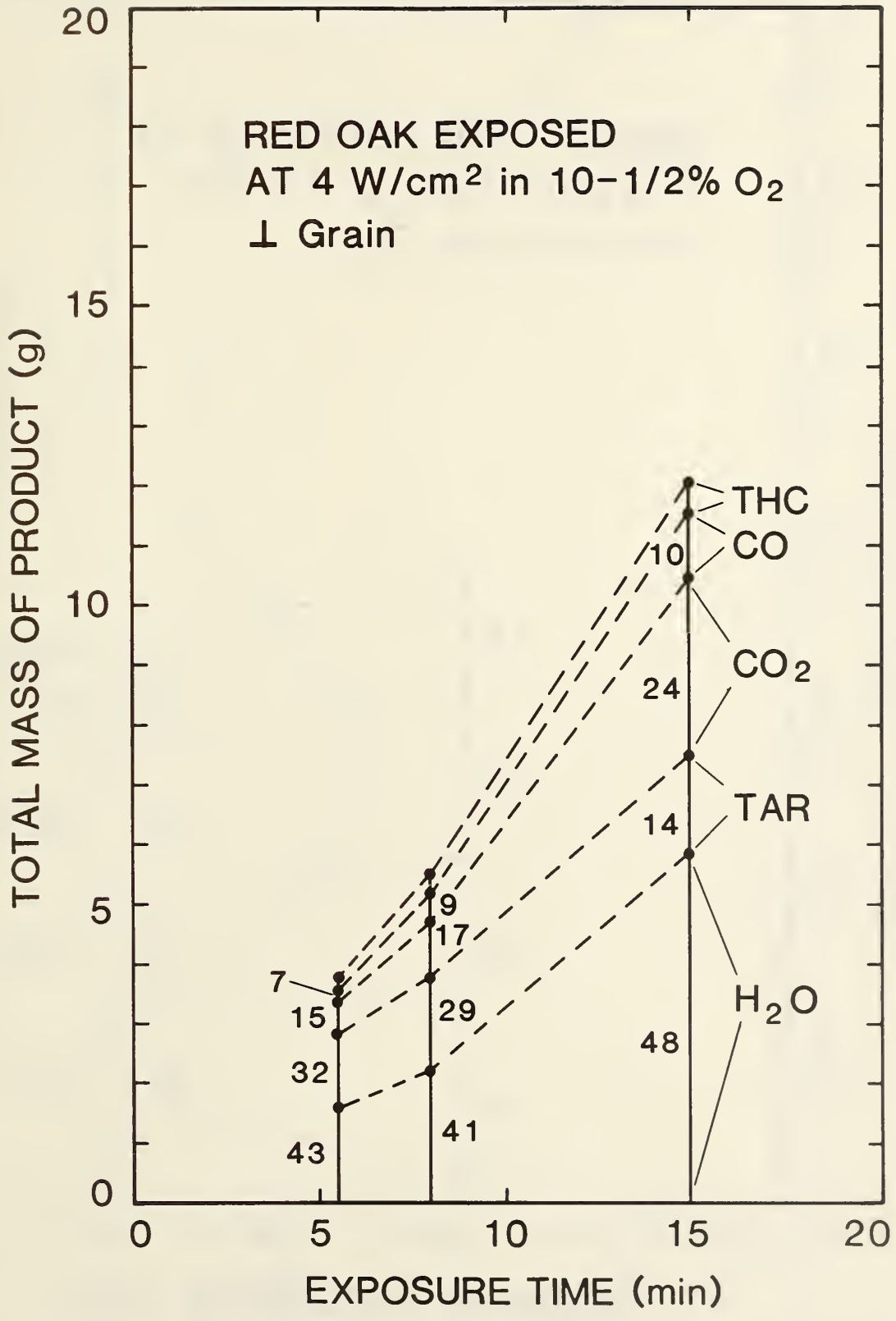

Figure 8(b). Integrated product mass and composition as a function of exposure time: red oak at base case conditions except for exposure time

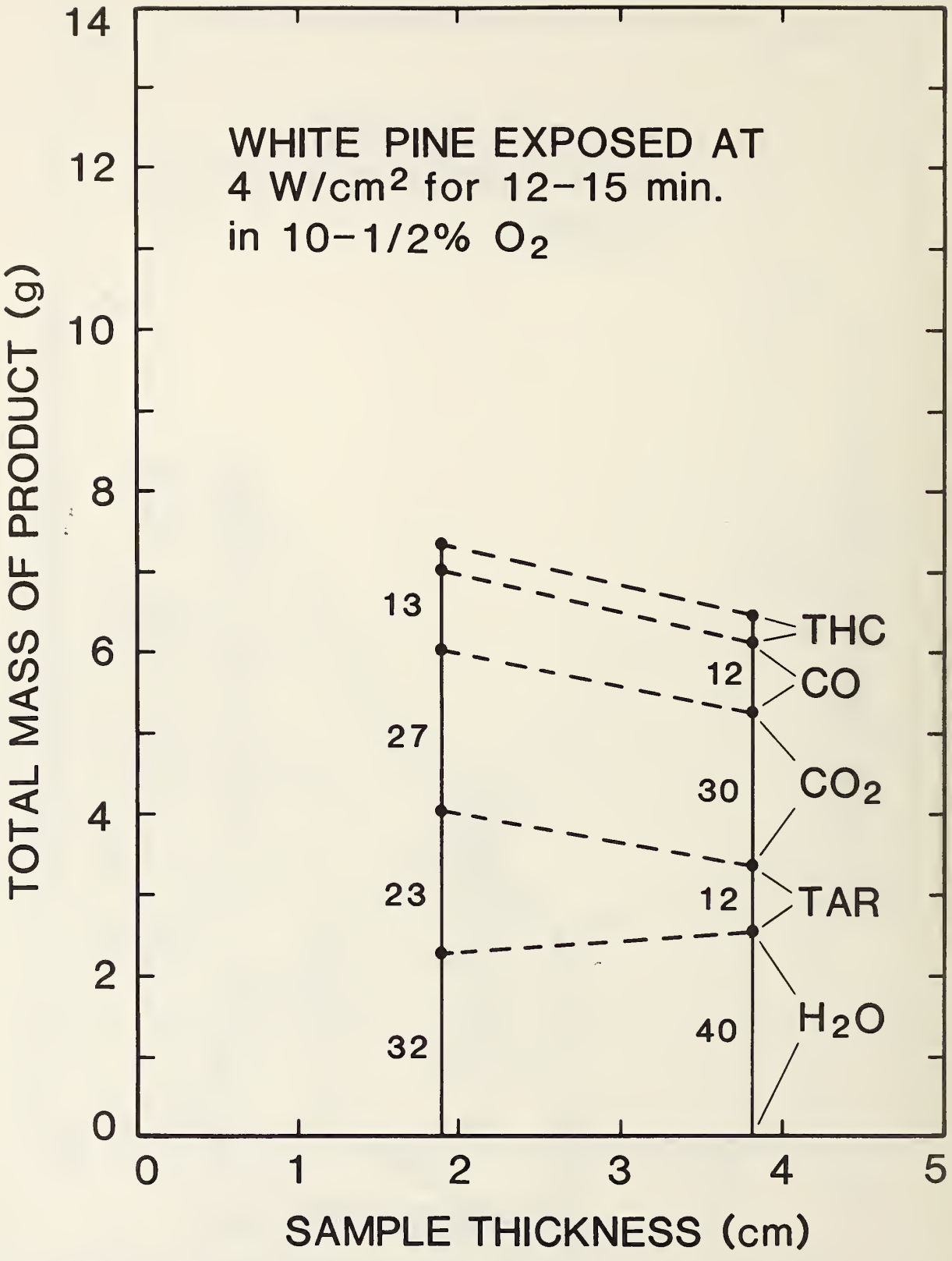

Figure 9(a). Integrated product mass and composition as a function of sample thickness: white pine at base case conditions except for thickness

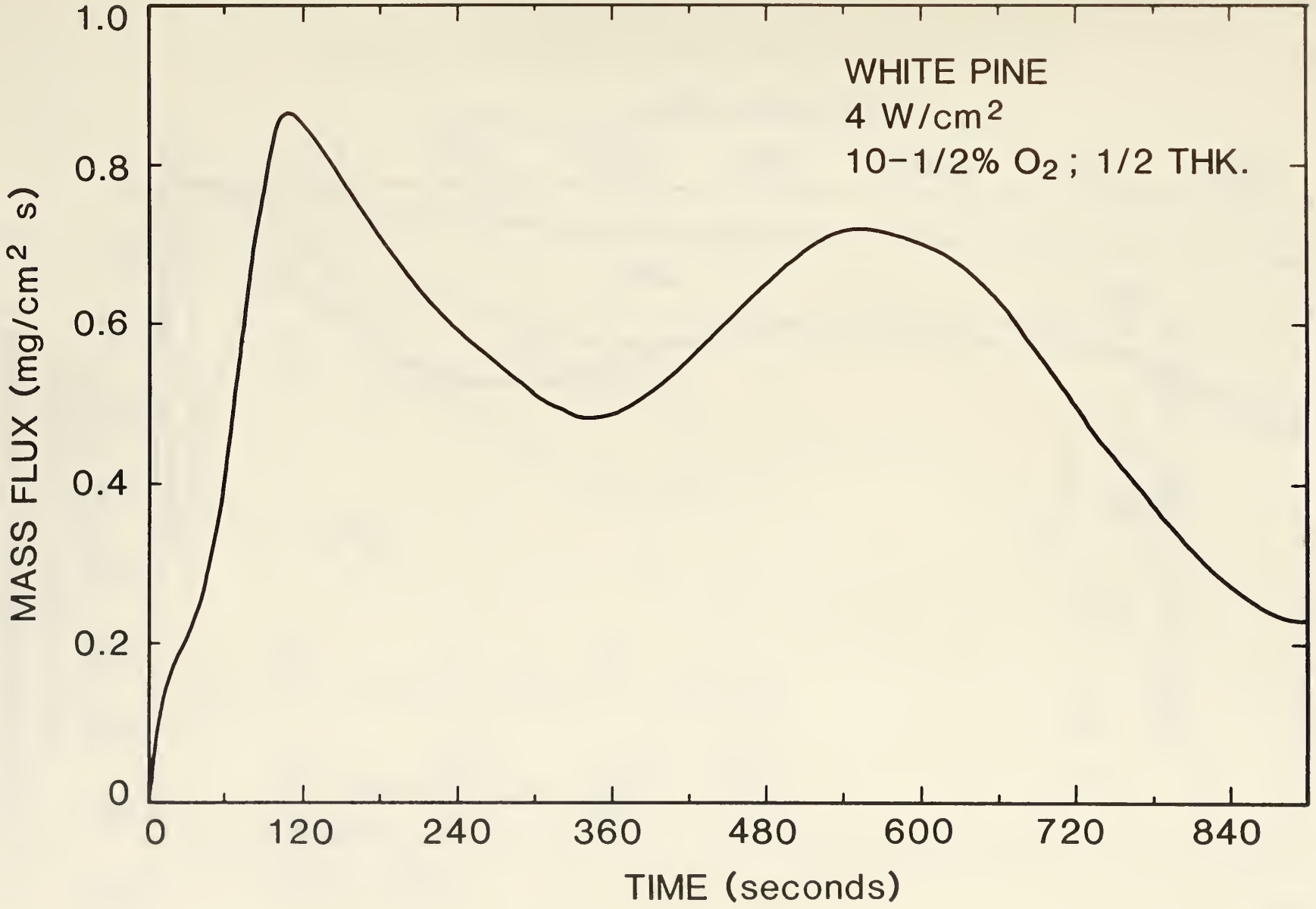

Figure 9(b). Surface mass flux vs time: white pine at base case conditions except sample thickness is halved

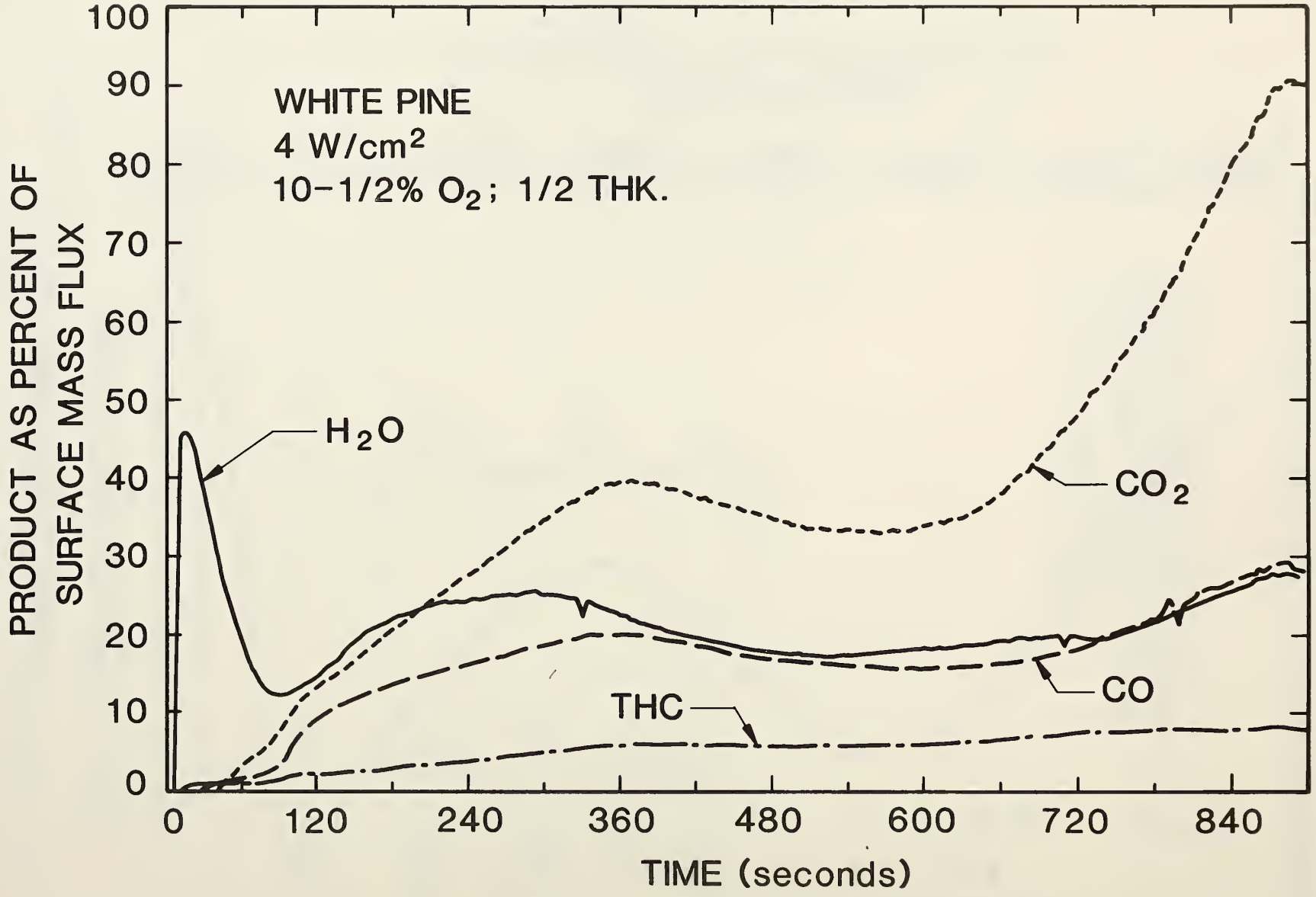

Figure 9(c). Composition of evolved products; white pine at base case conditions except sample thickness is halved

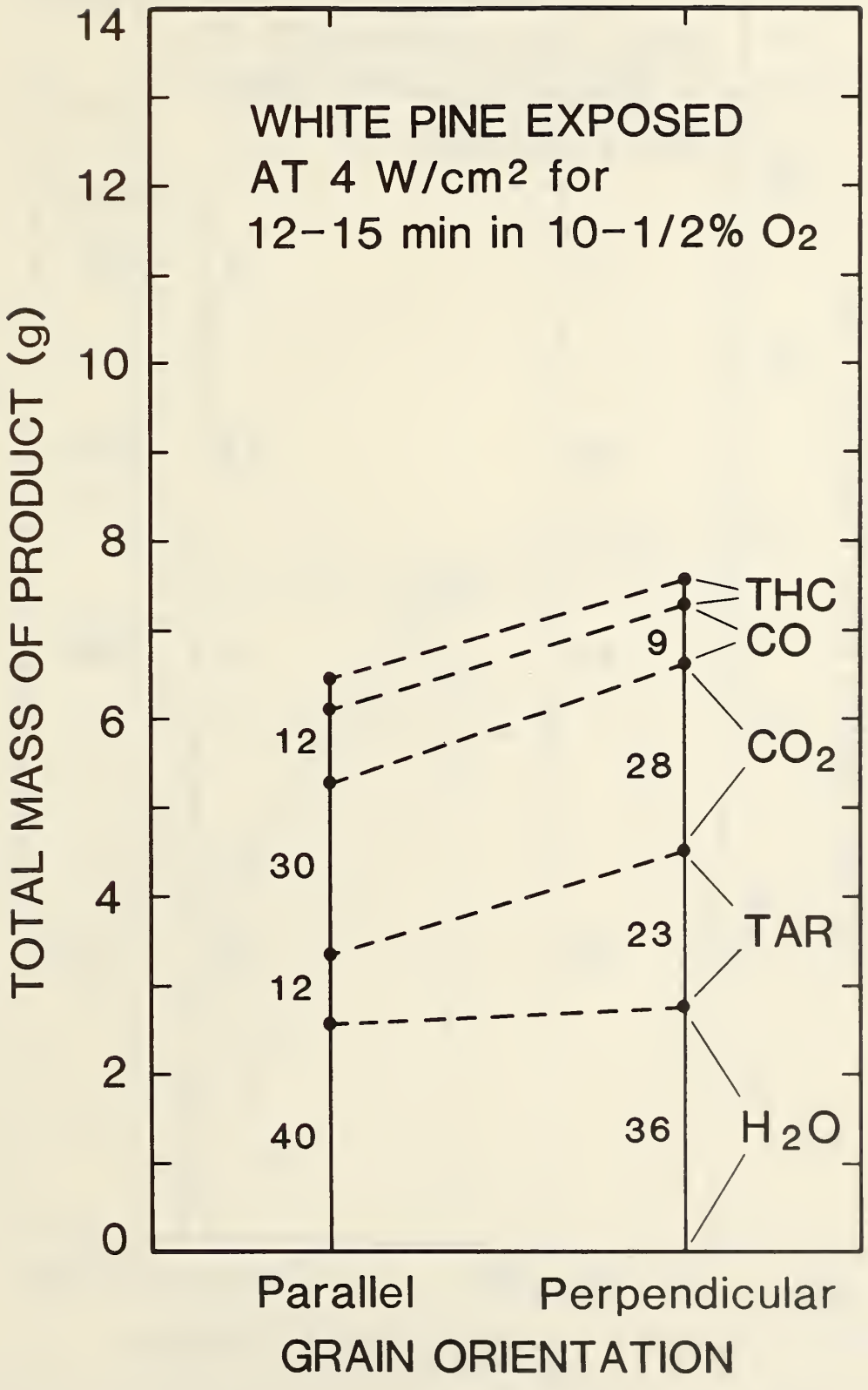

Figure 10(a). Integrated product mass and composition as a function of wood grain orientation; white pine at base case conditions

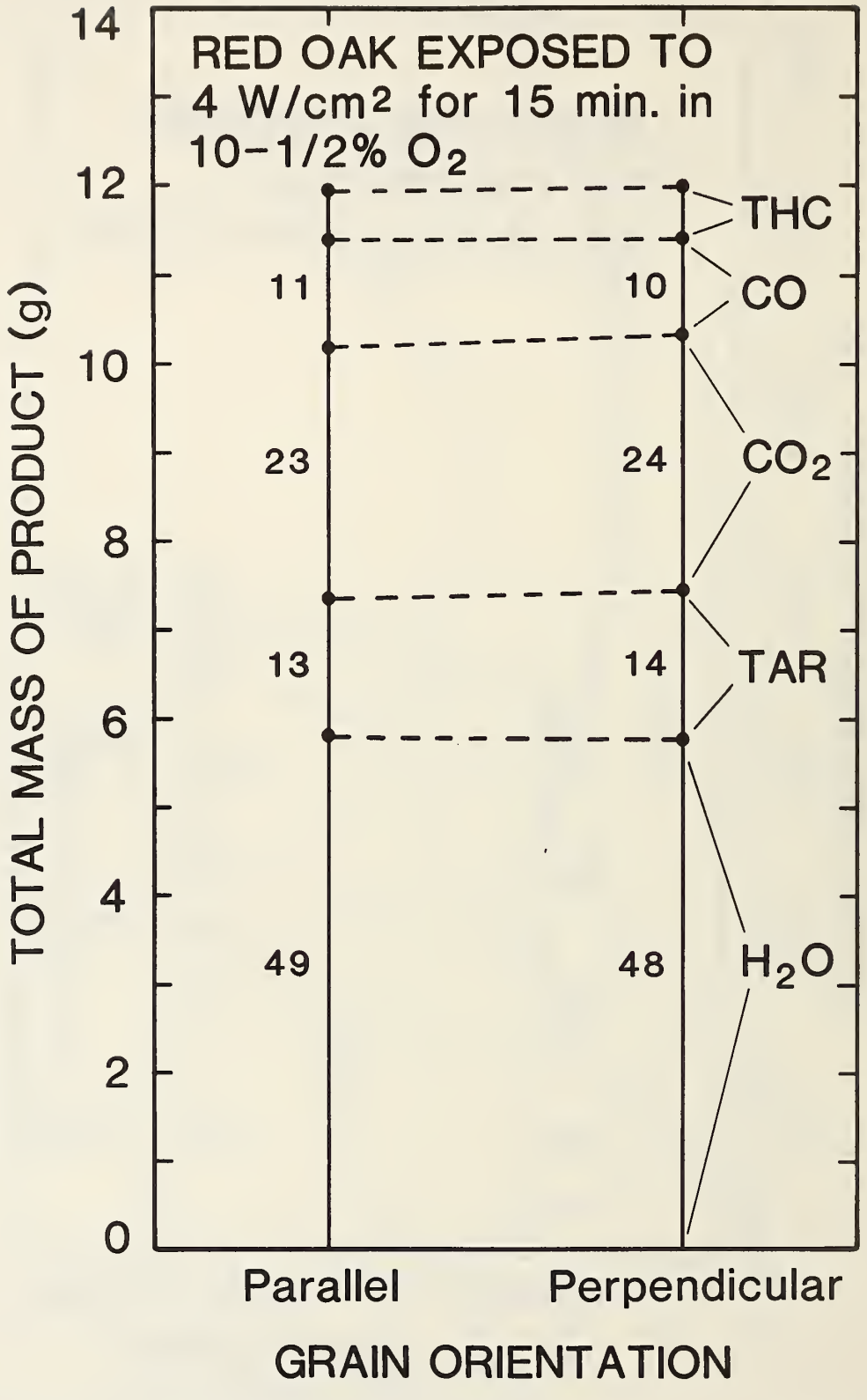

Figure 10(b). Integrated product mass and composition as a function of wood grain orientation; red oak at base case conditions

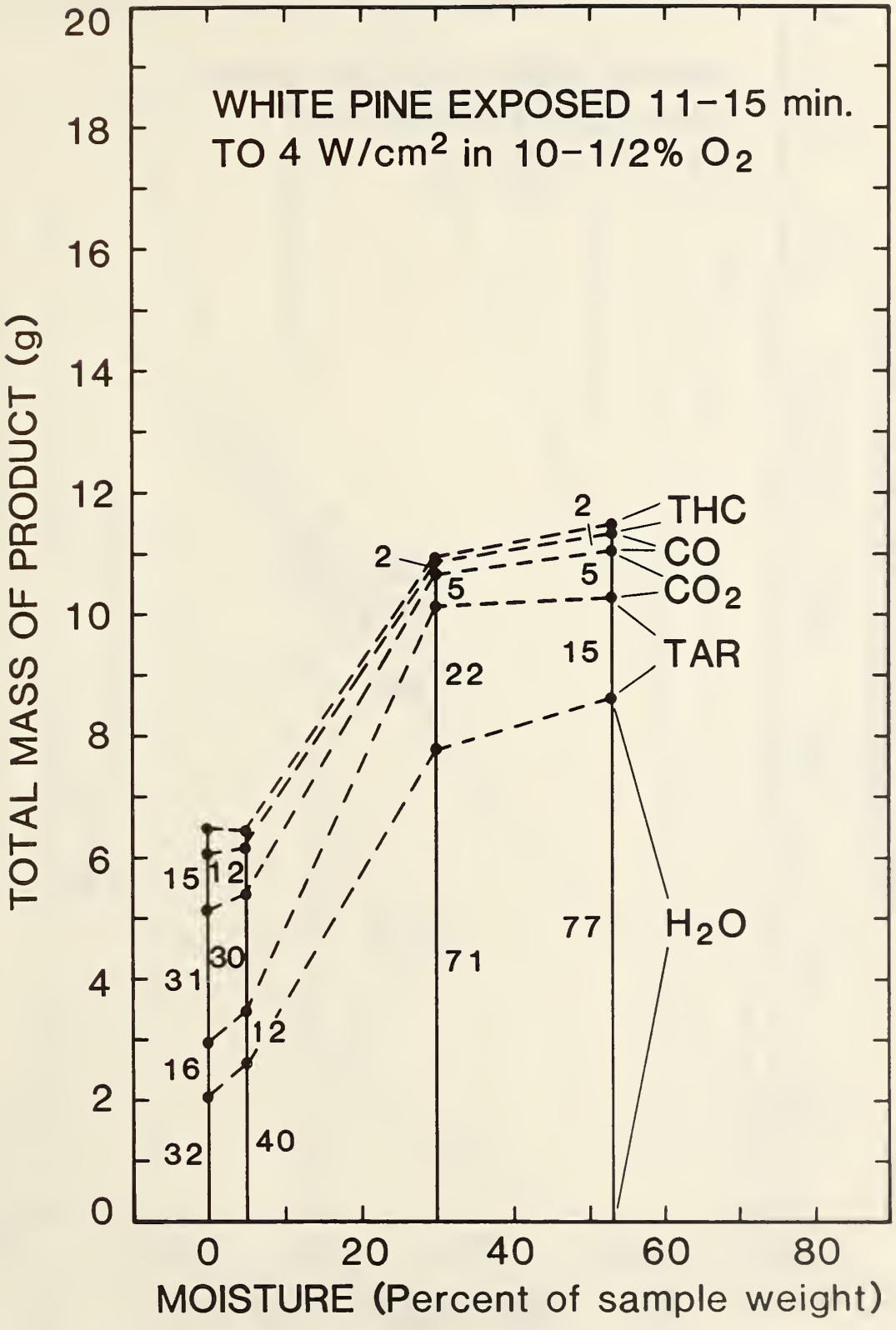

Figure 11(a). Integrated product mass and composition as a function of sample moisture content; white pine otherwise at base case conditions

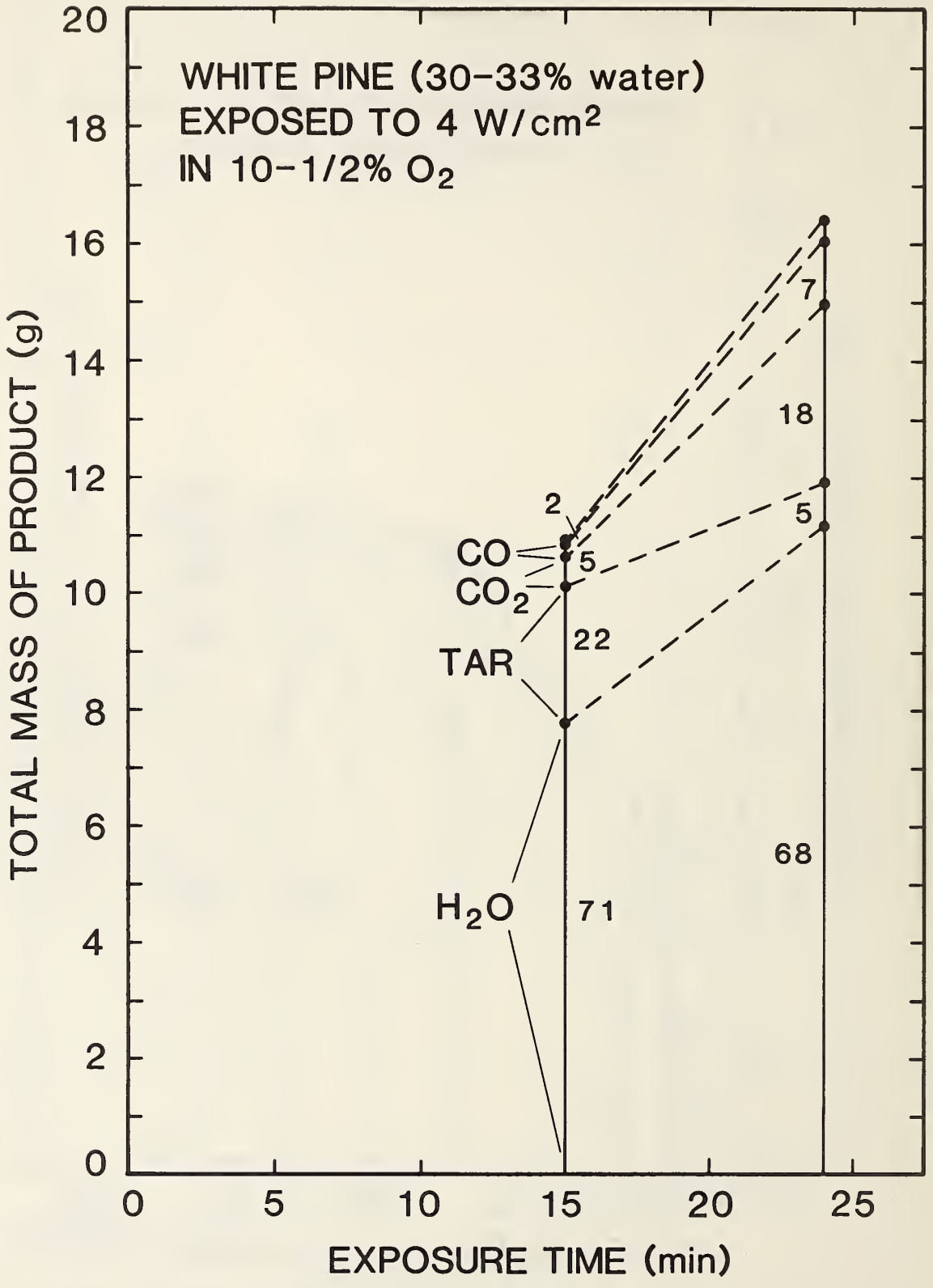

Figure 11(b). Integrated product mass and composition for wet white pine as a function of exposure time

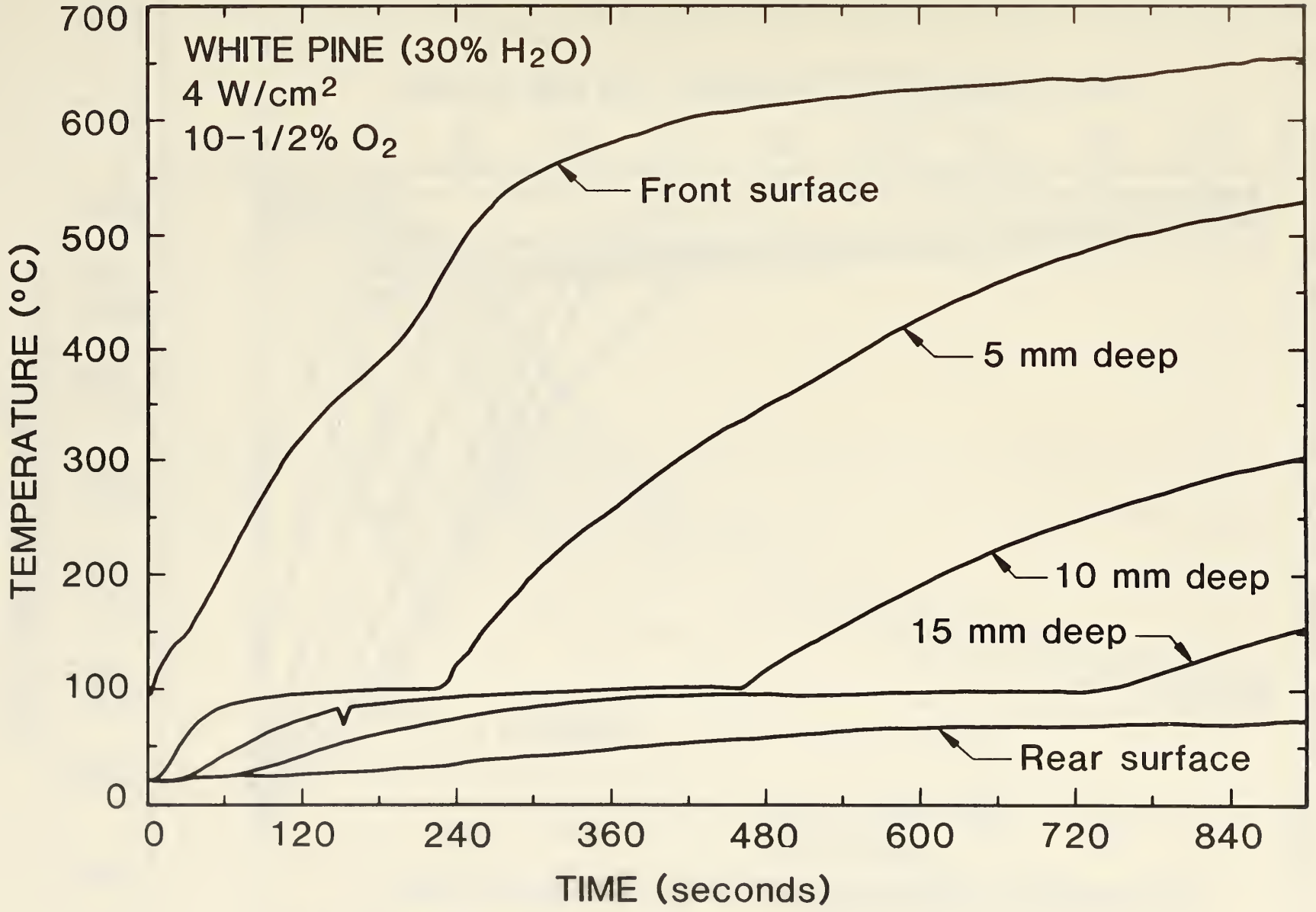

Figure 12(a). Temperature vs time from five theromcouples in a white pine sample: base case conditions except for moisture content

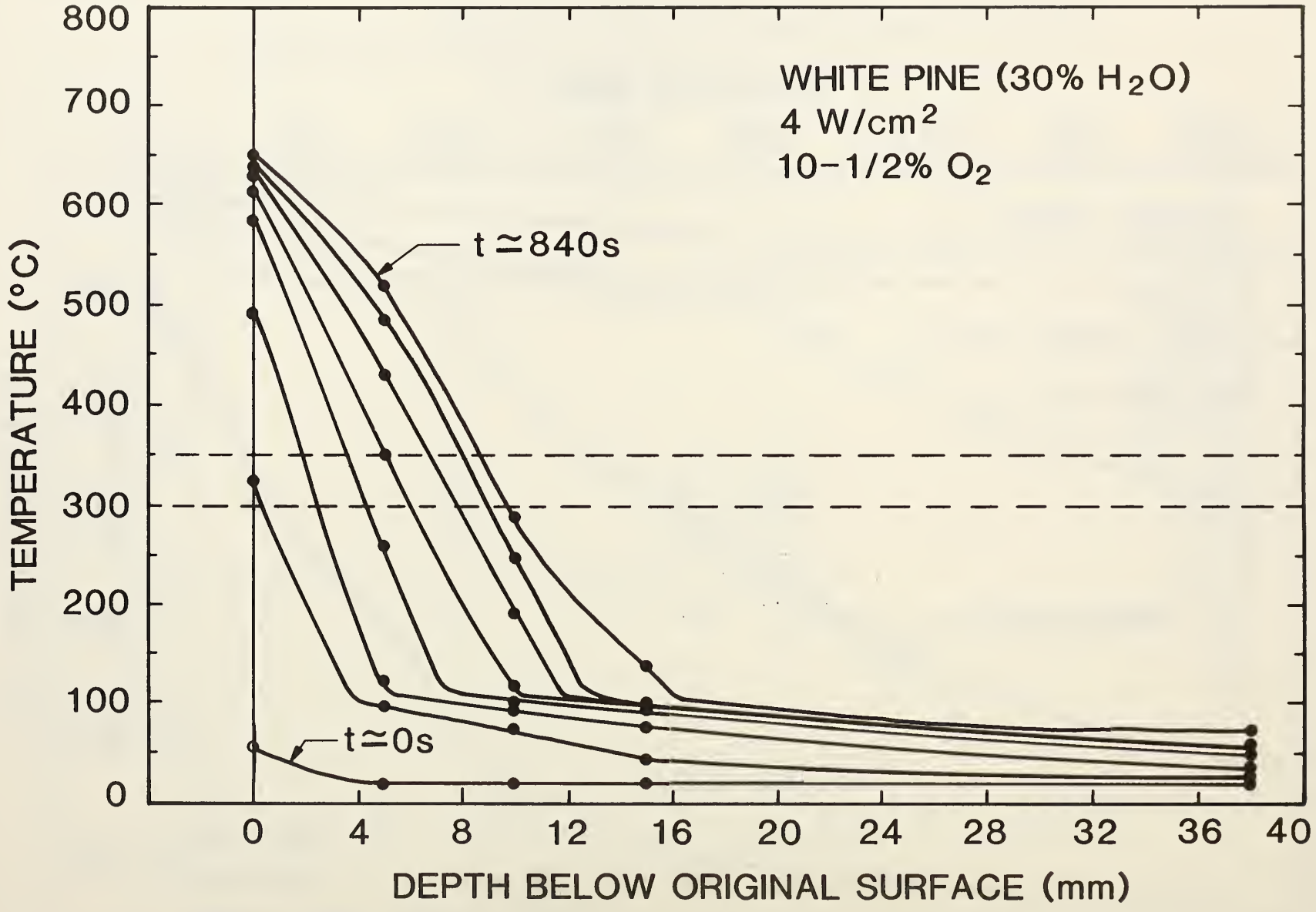

Figure 12(b). Temperature vs depth and time; cross-plotted from Fig. 12(a)

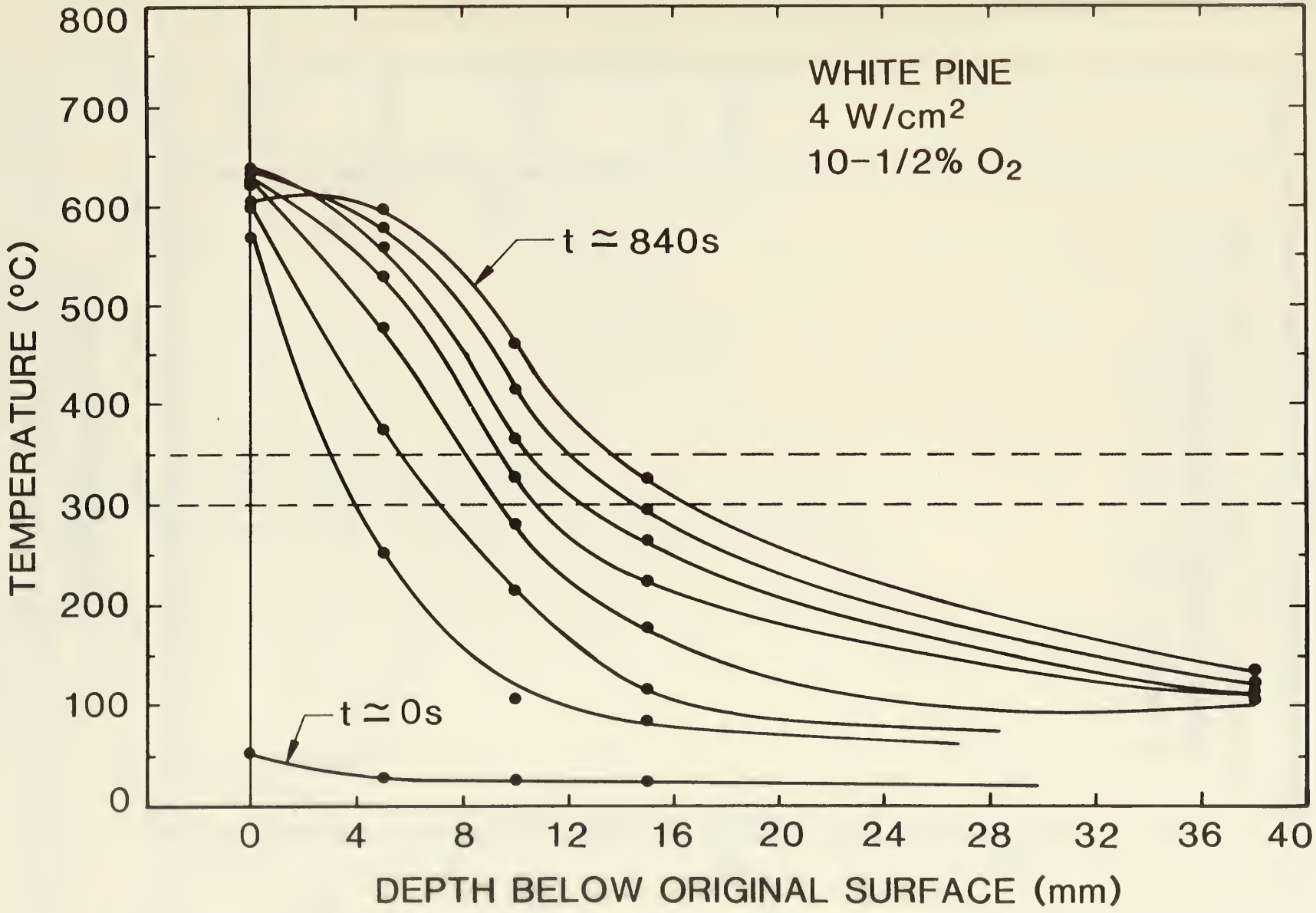

Figure 12(c). Temperature vs depth and time; white pine base case conditions

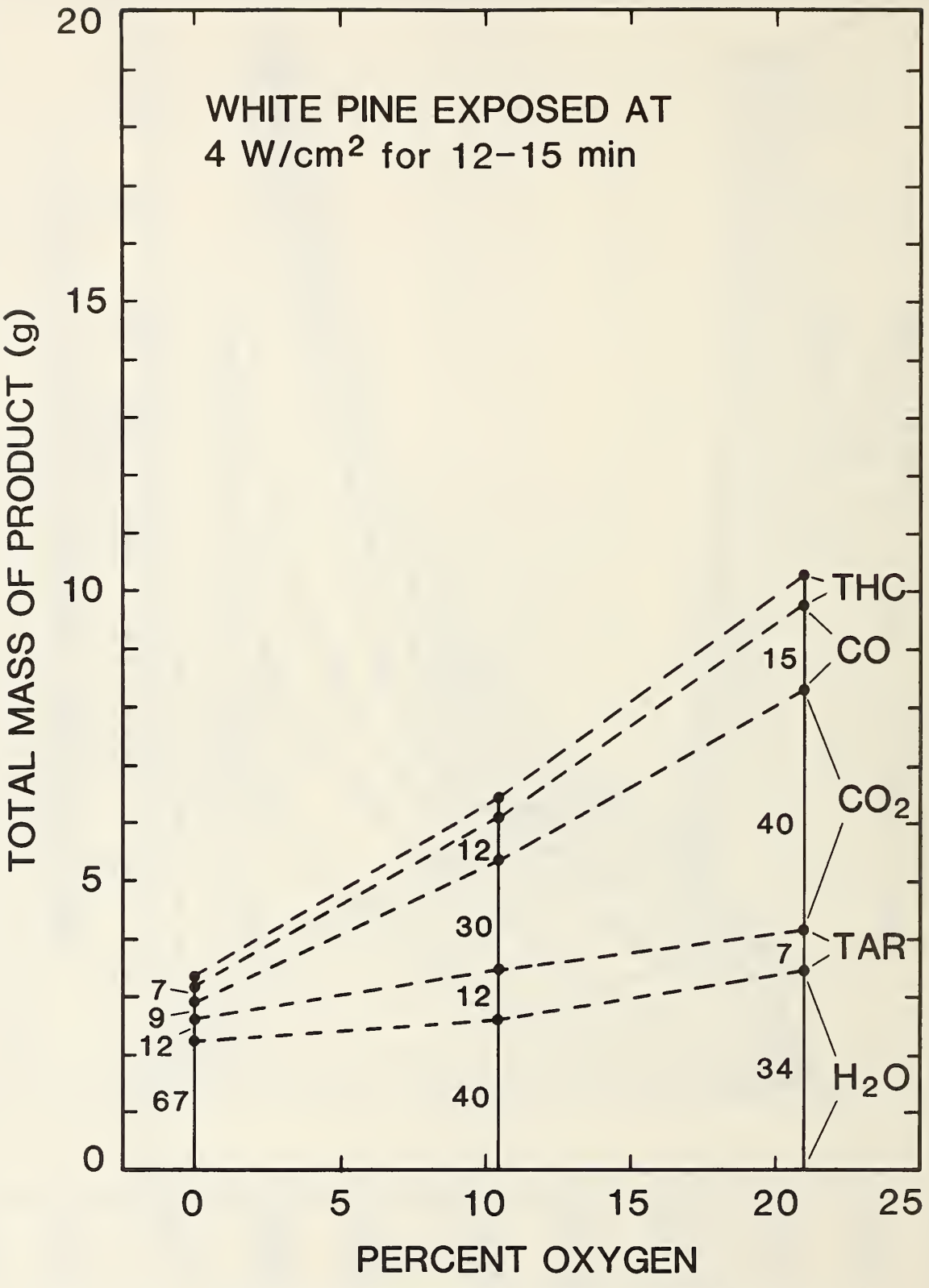

Figure 13(a). Integrated product mass and composition as a function of ambient oxygen percentage: white pine at otherwise base case conditions

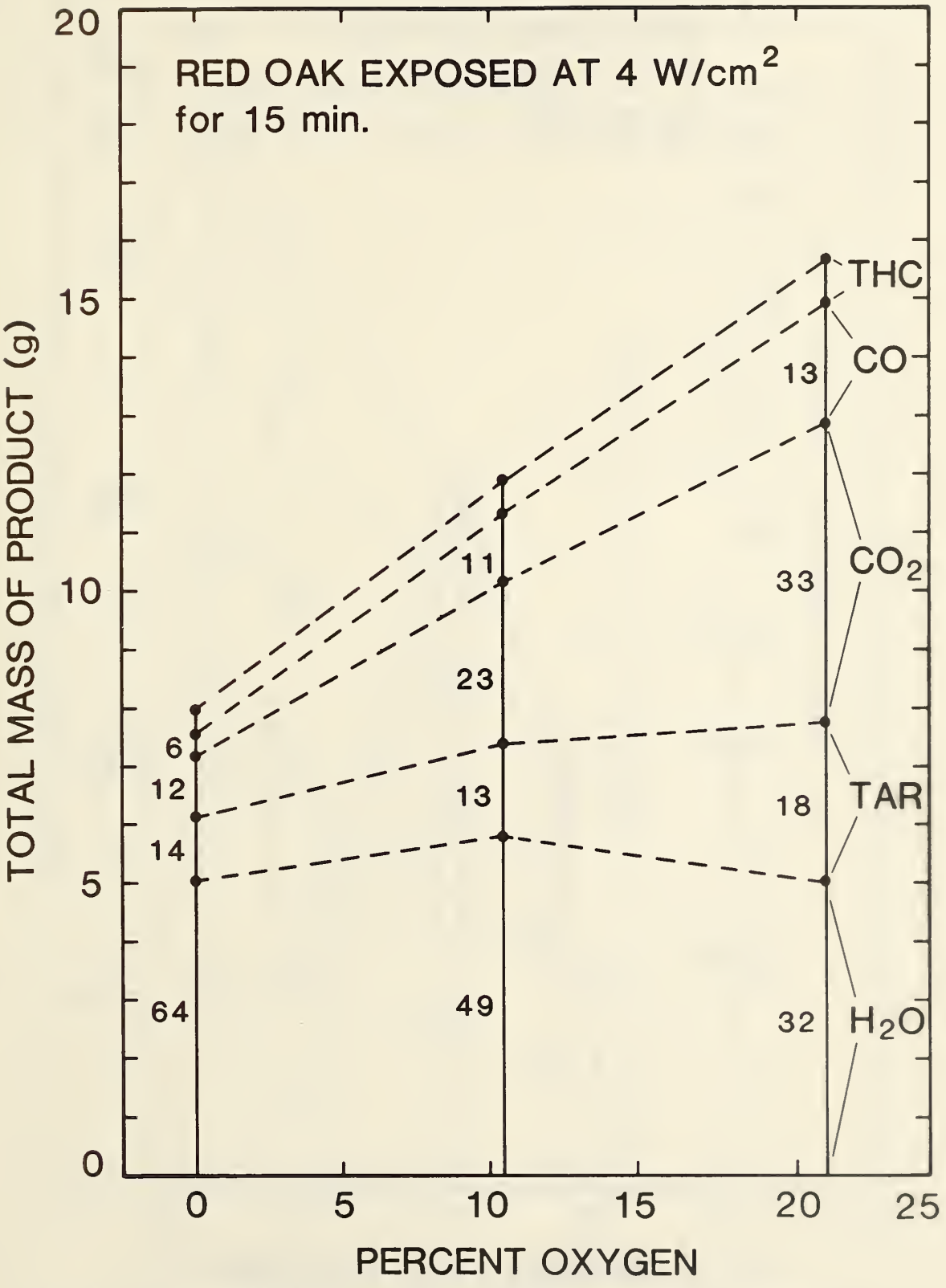

Figure 13(b). Integrated product mass and composition as a function of ambient oxygen percentage: red oak at otherwise base case conditions

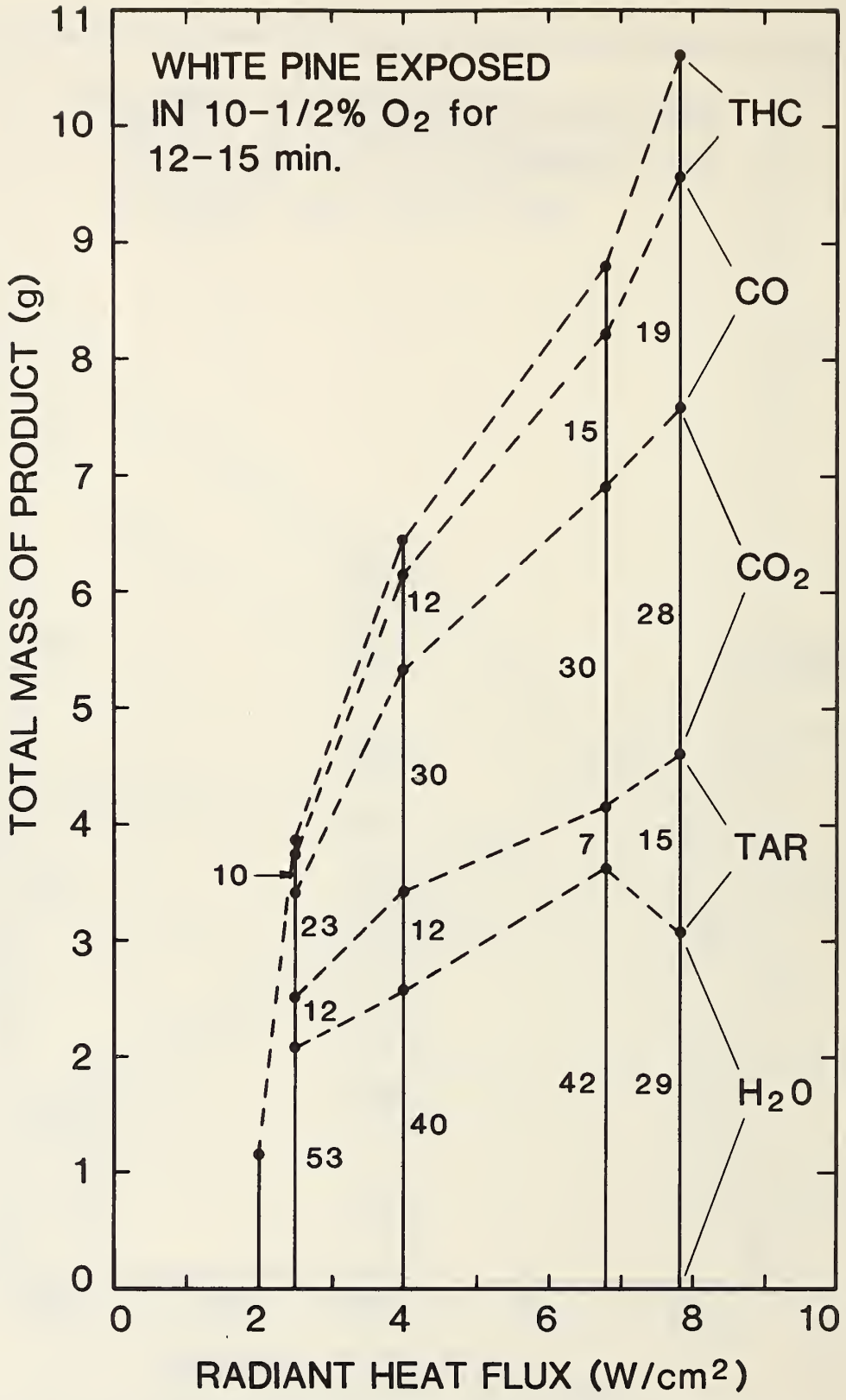

Figure 14(a). Integrated product mass and composition as a function of incident radiant flux; white pine at otherwise base case conditions

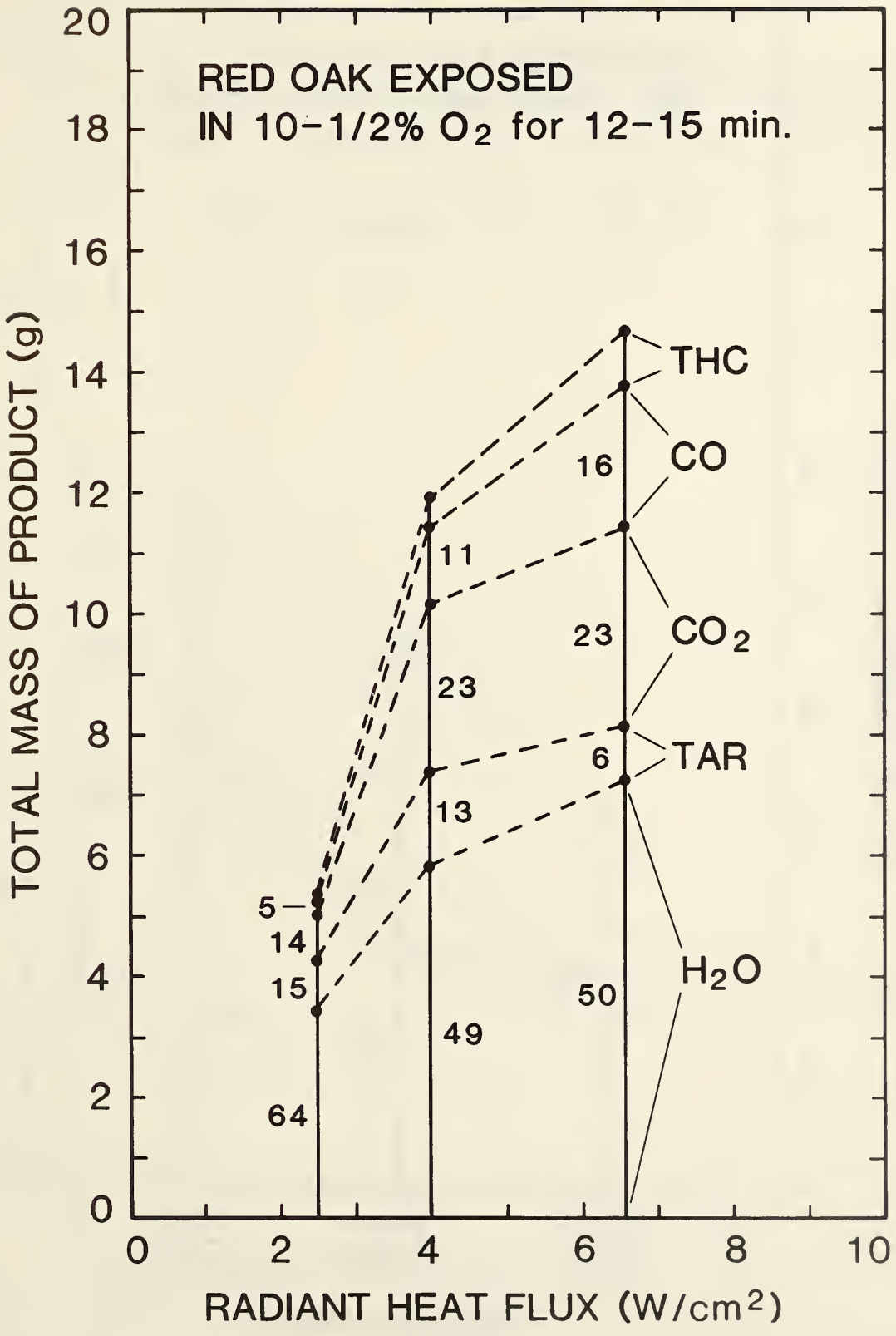

Figure 14(b). Integrated product mass and composition as a function of incident radiant flux; red oak at otherwise base case conditions

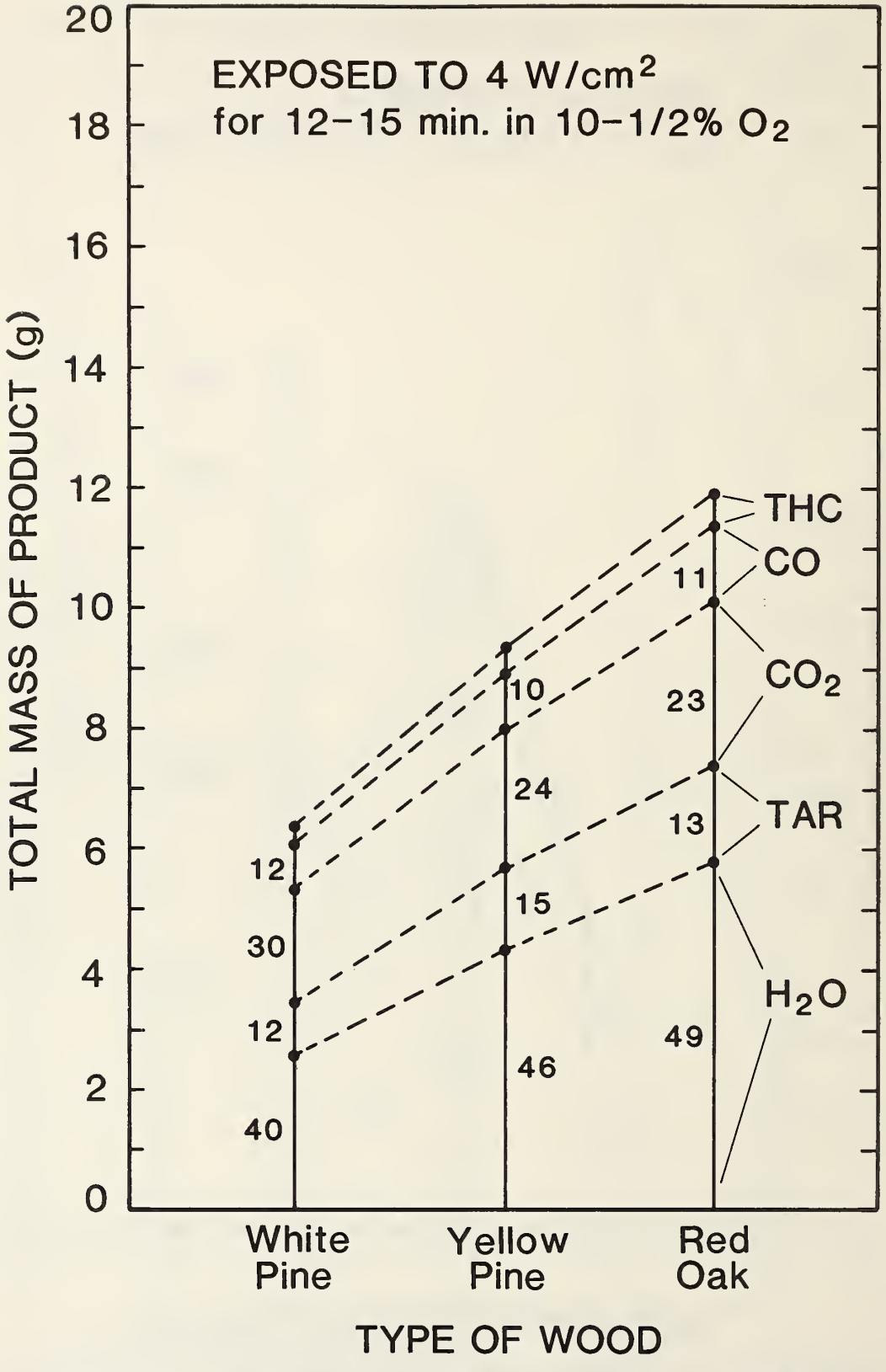

Figure 15. Integrated product mass and composition as a function of wood type: all at base case conditions

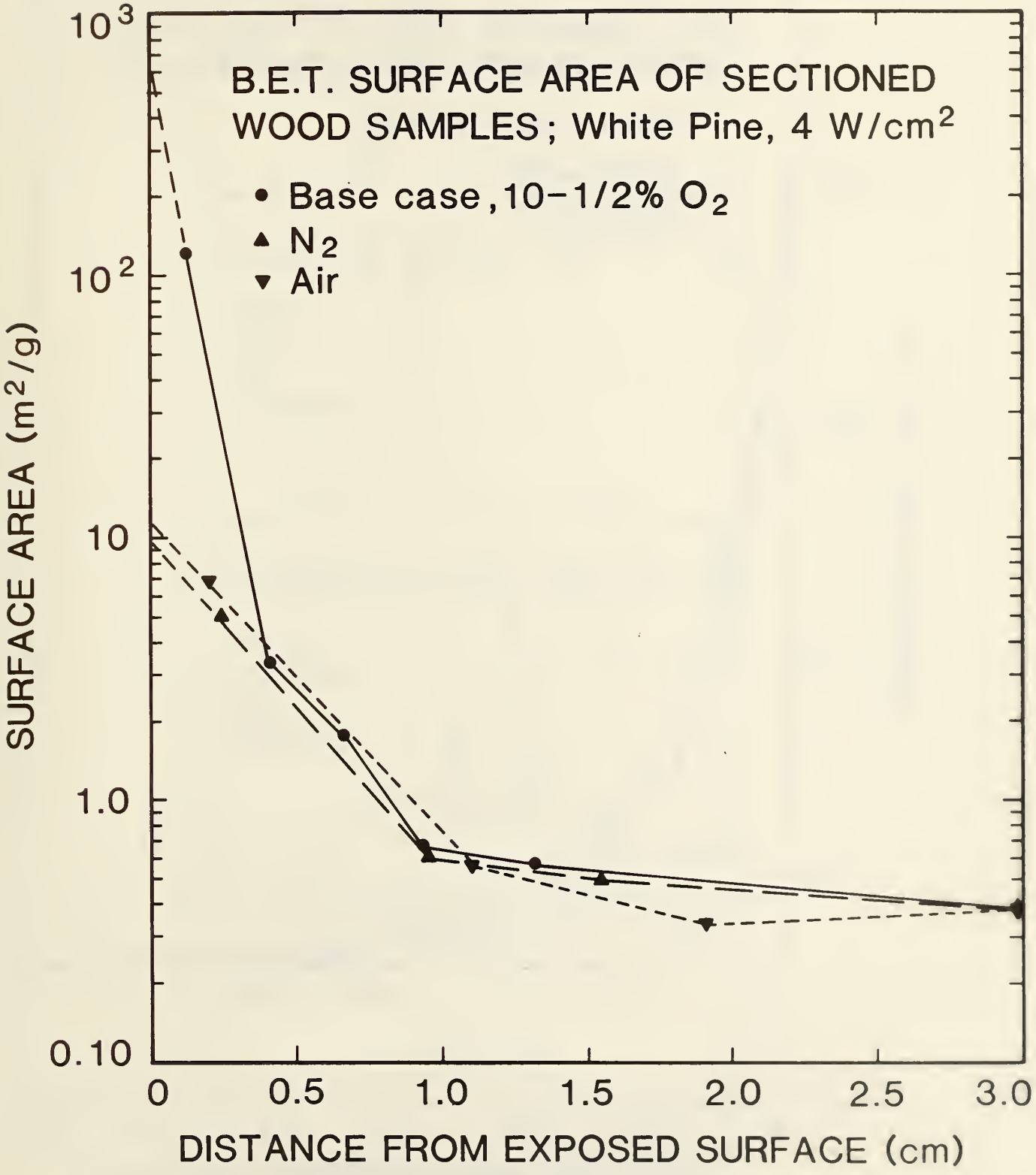

Figure 16(a). B.E.T. surface area vs depth for white pine in three atmospheres; otherwise base case conditions

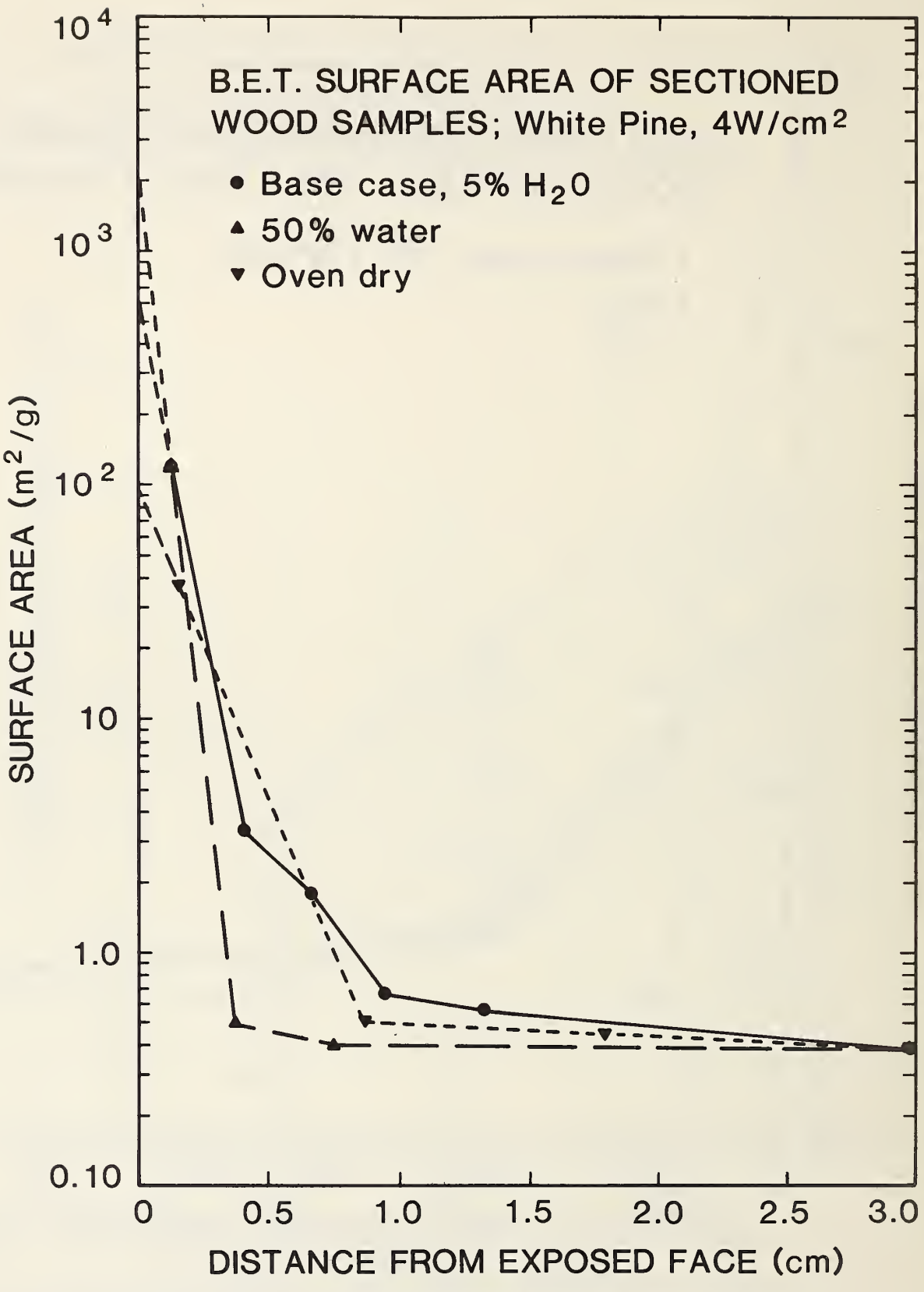

Figure 16(b). B.E.T. surface area vs depth for white pine of three moisture levels: otherwise base case conditions

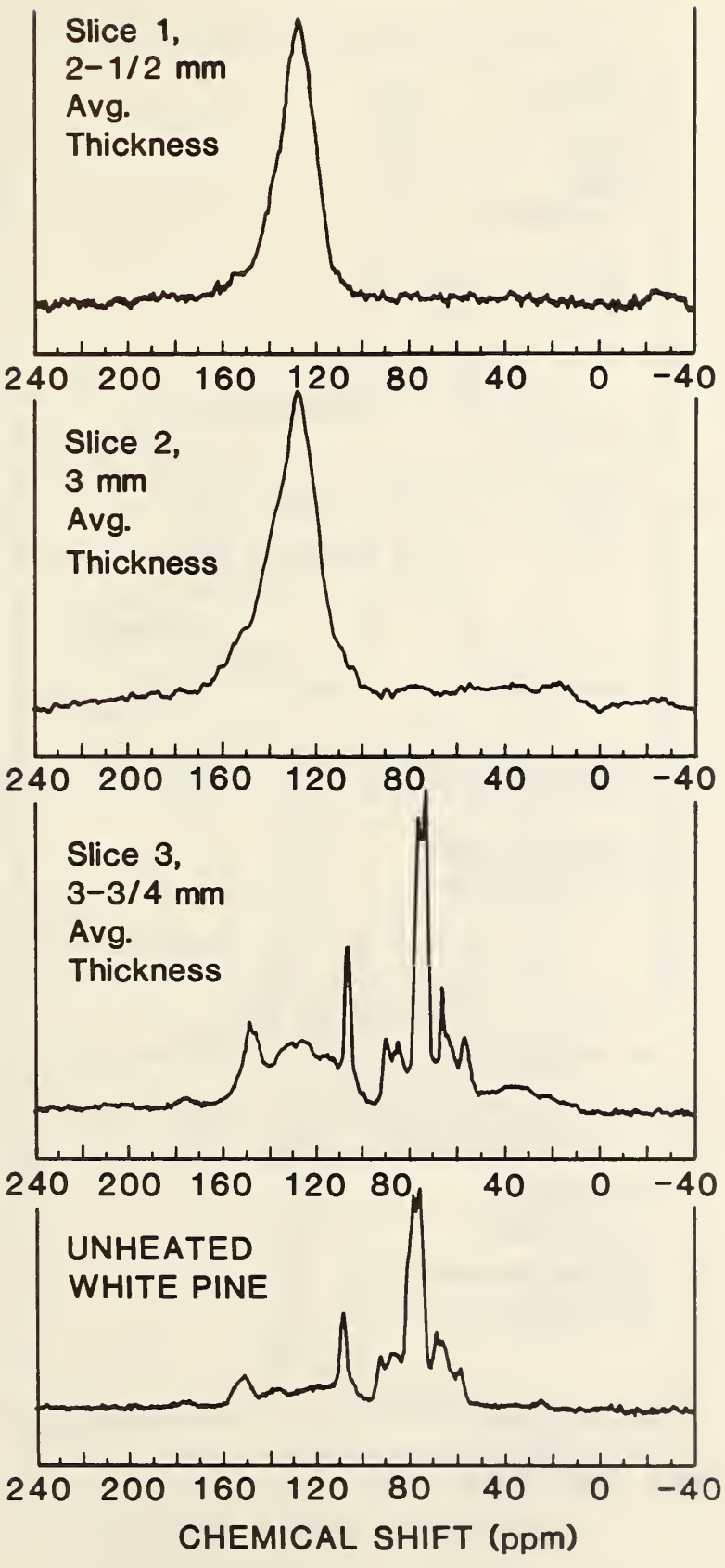

Figure 17(a). ^{13}C-NMR spectra vs depth; white pine at base case conditions

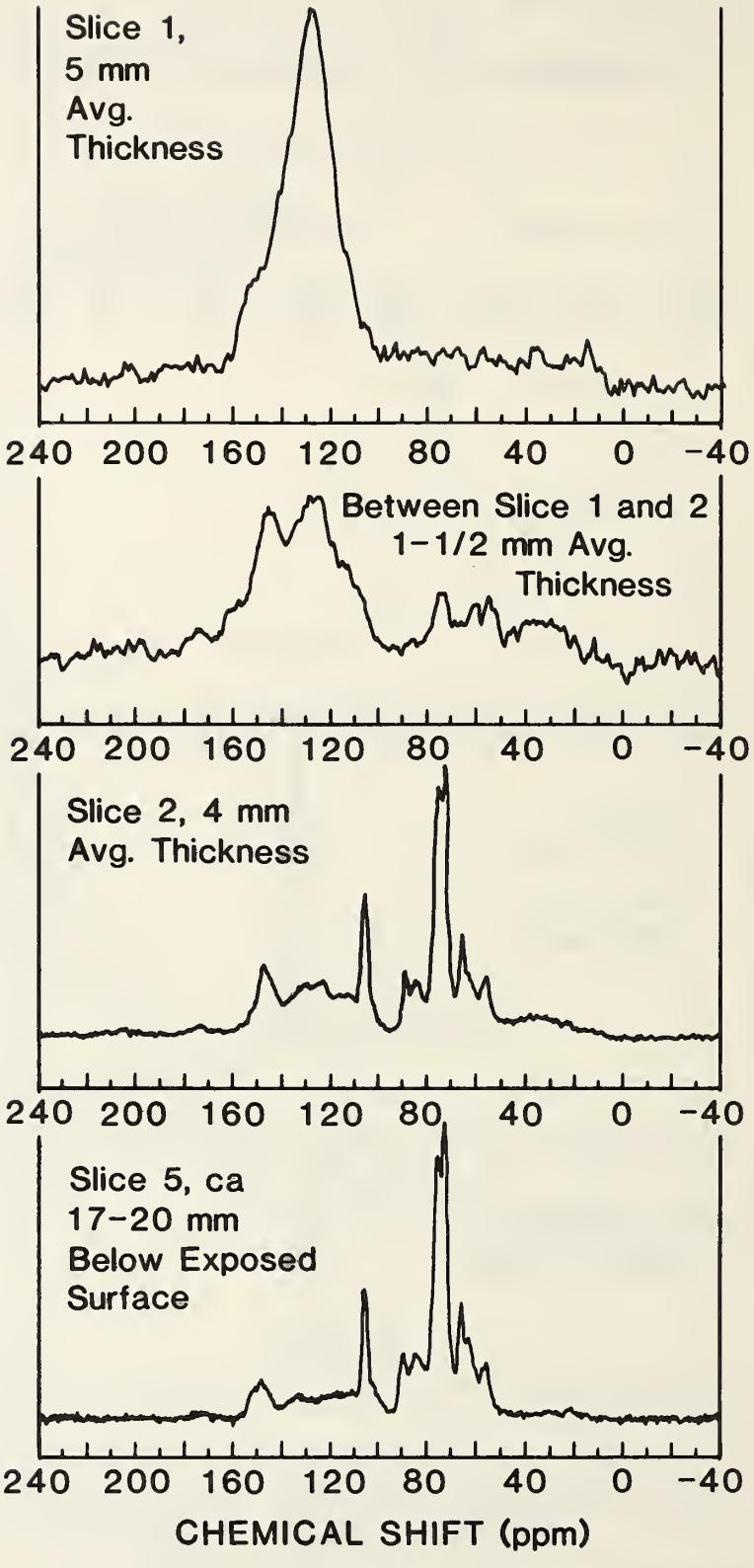

Figure 17(b). ^{13}C-NMR spectra vs depth: white pine at base case conditions except exposed in nitrogen

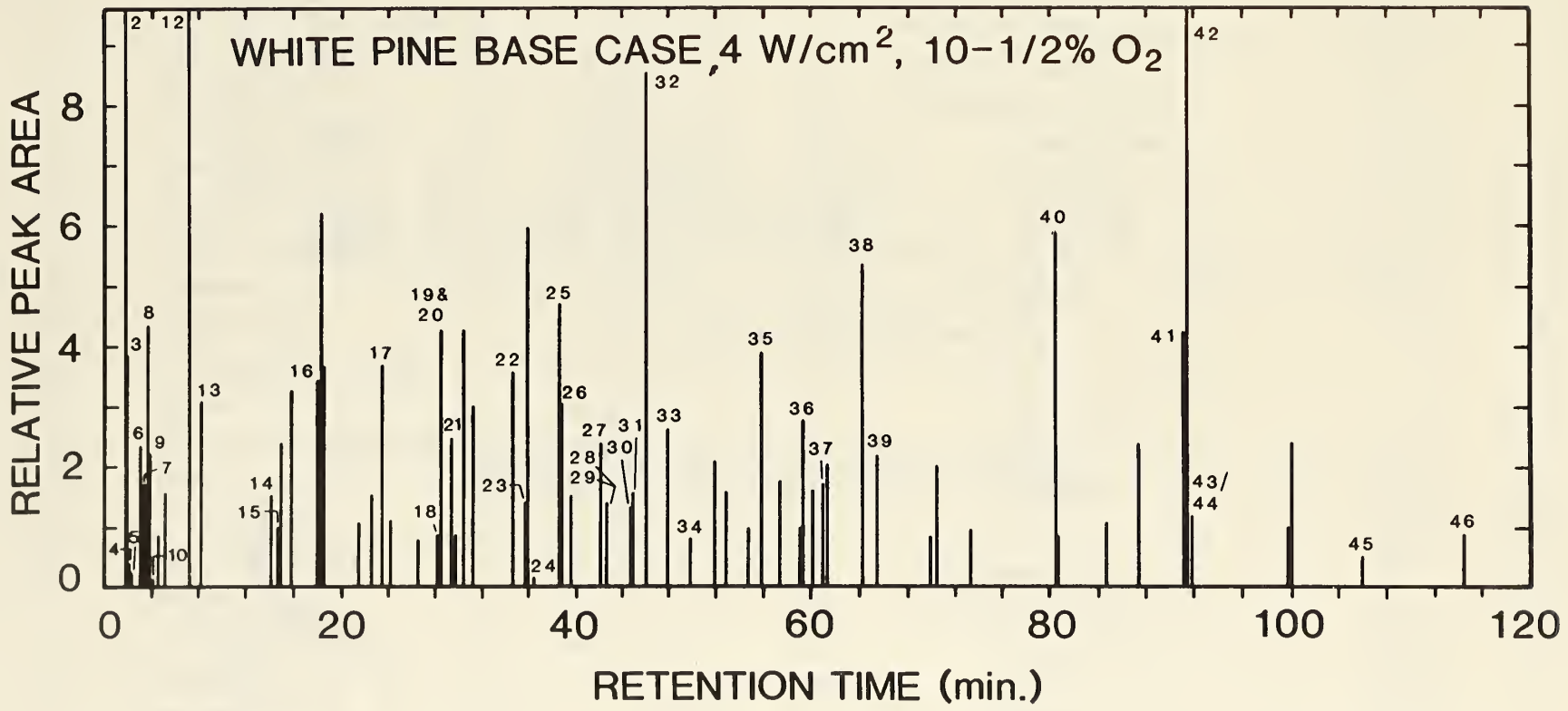

Figure 18(a). Capillary GC fingerprint of tar from white pine at base case conditions; areas not corrected for FID response factors; nearly all of peak #2 is the methanol solvent; peak #42 (triphenyl methane) was added as a stabilizer.

Fig. 18(b) Identified peaks in base case capillary GC fingerprint of white pine; (T) means identification is tentative. Percentages are based on amount of material that passed through chromatograph; all are corrected for calculated FID response factor.

Peak No.	Name	Weight Percent	Peak No.	Name	Weight Percent
1	Methyl Formate	0.08	24	2-OH, 3-CH_3, 2 Cyclopentene 1-One	0.04
2	Methanol		25	Guaiacol	1.37
3	Acrolein	1.64	26	Phenol	1.05
4	Propionaldehyde (T)	0.04	27	o-Cresol	0.69
5	Methyl Acetate	0.08	28	2,3 Dimethyl Phenol (T)	0.41
6	Methyl Propionate	2.25	29	2,5 Dimethyl Phenol (T)	
7	Acetaldehyde	0.70	30	m-Cresol	0.42
8	2 Methyl Furan (T)	0.36	31	p-Cresol	0.46
9	2,5 Dimethyl Furan (T)	0.79	32	Creosol	2.82
10	Crotonaldehyde (T)	0.04	33	2,4 Xylenol	0.76
11	1,1 Dimethoxy Ethane	0.37	34	Furoic Acid (T)	0.46
12	Acetic Acid	8.08	35	2-Tert Butyl Phenol	1.12
13	Toluene	0.70	36	Eugenol	0.90
14	Ethyl Benzene (T)	0.44	37	1,2 Benzene diol	0.52
15	Propionic Acid (T)	0.50	38	Isoeugenol	1.74
16	Furaldehyde	1.72	39	Vanillin	0.85
17	Furfuryl Alcohol	1.62	40	Levoglucosan	4.87
18	Solketal (T)	0.44	41	Hexadecanoic Acid (T)	1.28
19	5 Methyl Furan 2 Aldehyde	1.90	42	Triphenyl Methane	
20	3 Methyl Furan 2 Aldehyde		43	Methyl 10 Octadecenoate (T)	0.37
21	Butyrolactone	1.59	44	Methyl 9 Octadecenoate (T)	
22	1 Acetyl Cyclohexene (T)	1.17	45	Methyl Linoleate	0.19
23	Benzyl Alcohol (T)	0.43	46	Phenanthrene Carboxylic Acid Deriv. (T)	0.25

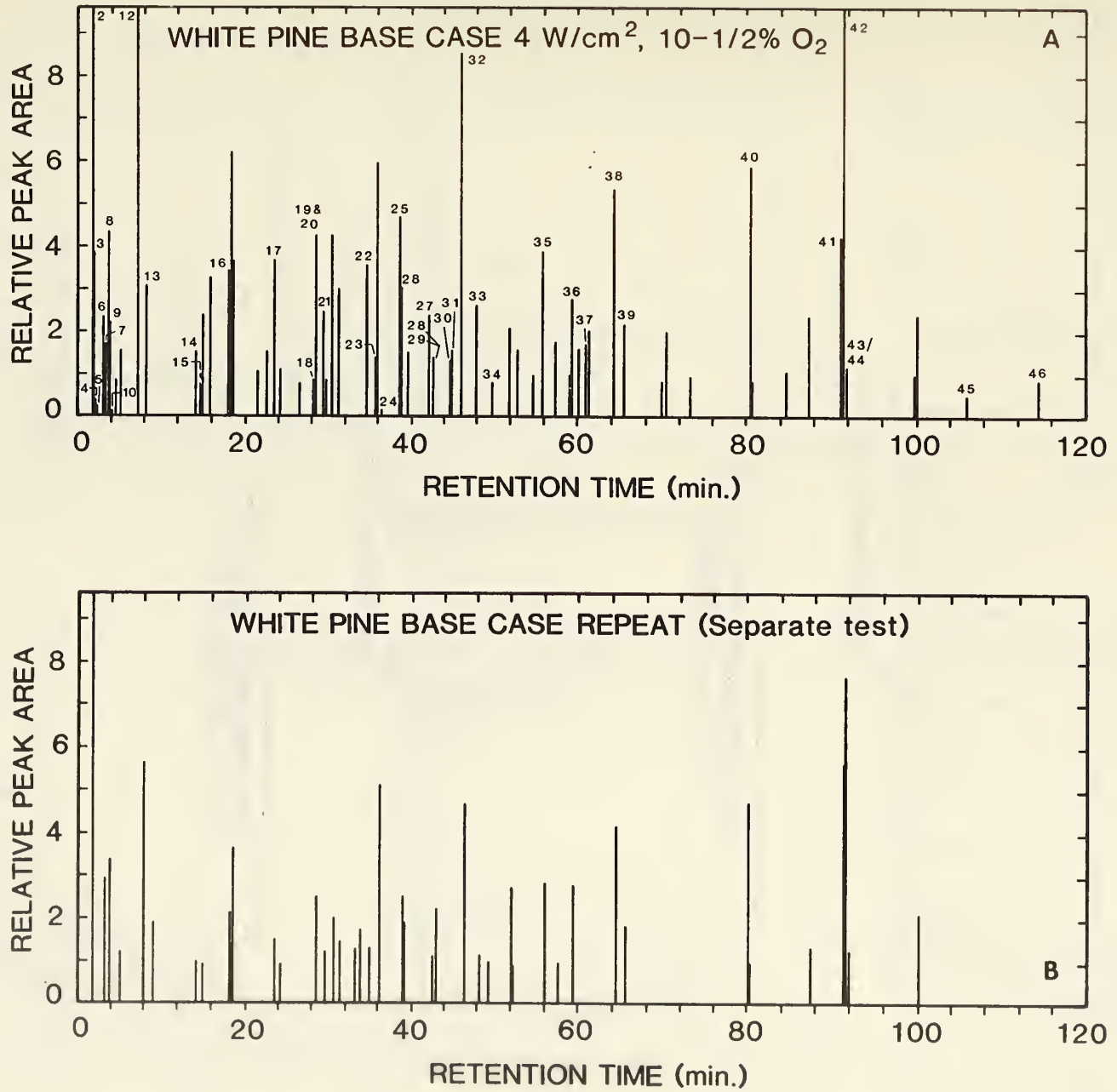

Figure 19. Reproducibility of capillary GC fingerprint; tar from two separate tests on white pine at same base case conditions

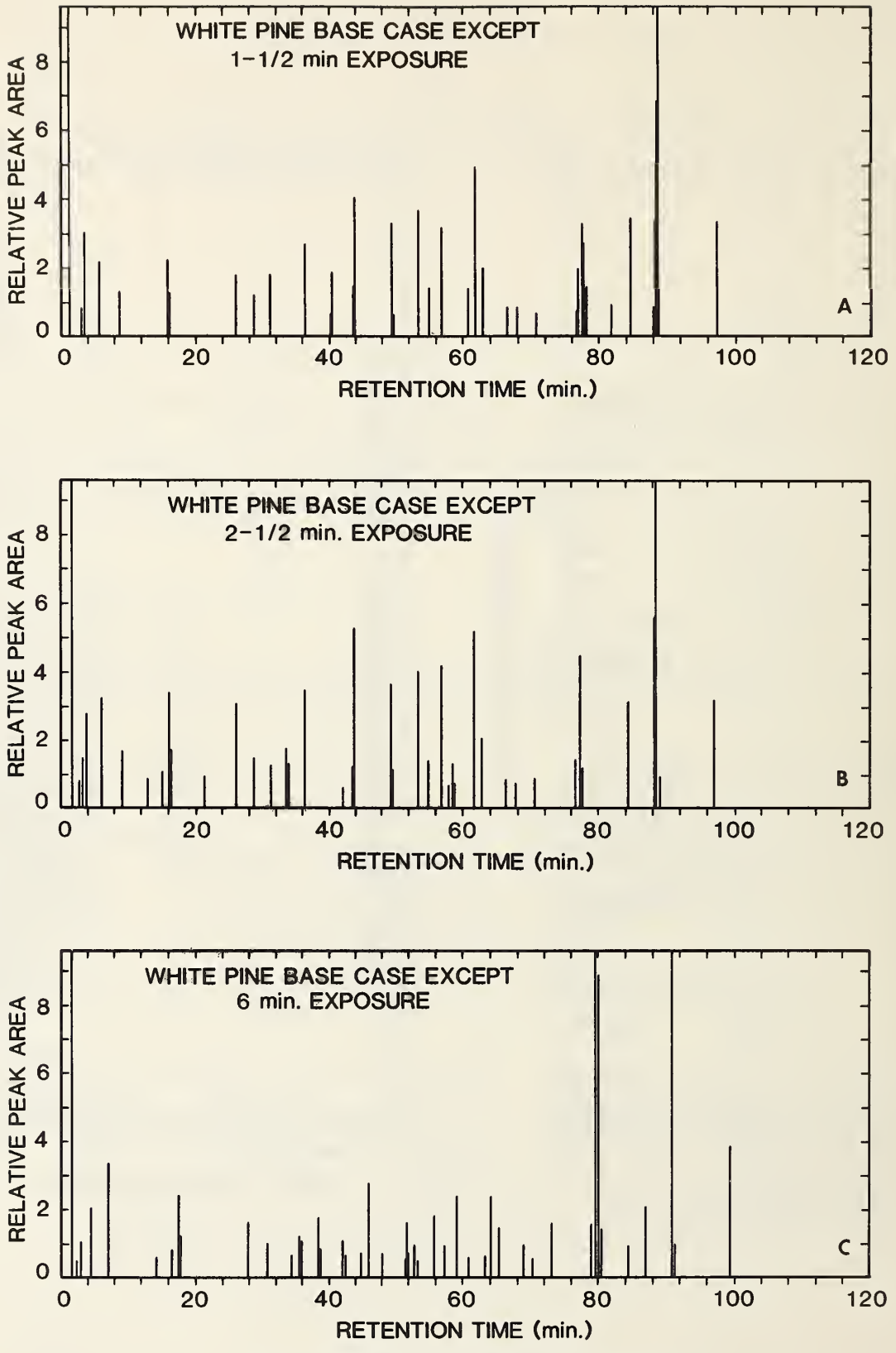

Figure 20. Capillary GC fingerprints of tar as a function of exposure time; white pine at base case conditions except: (a) 1-1/2 min, (b) 2-1/2 min, (c) 6 min, (d) 12 min, (e) 24 min exposure

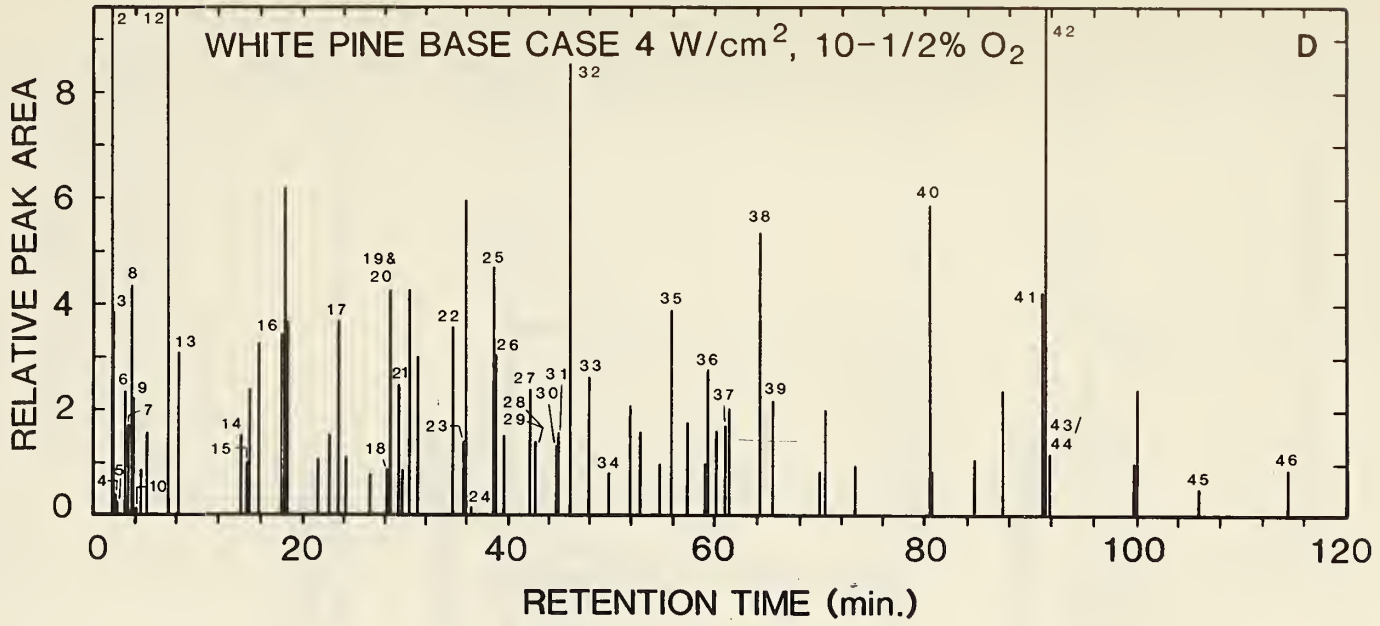
WHITE PINE BASE CASE 4 W/cm^2, 10-1/2% O_2
D
RELATIVE PEAK AREA
RETENTION TIME (min.)
0
2
4
6
8
0
20
40
60
80
100
120
1
2
3
4
5
6
7
8
9
10
11
12
13
14
15
16
17
18
19&
20
21
22
23
24
25
26
27
28
29
30
31
32
33
34
35
36
37
38
39
40
41
42
43/
44
45
46

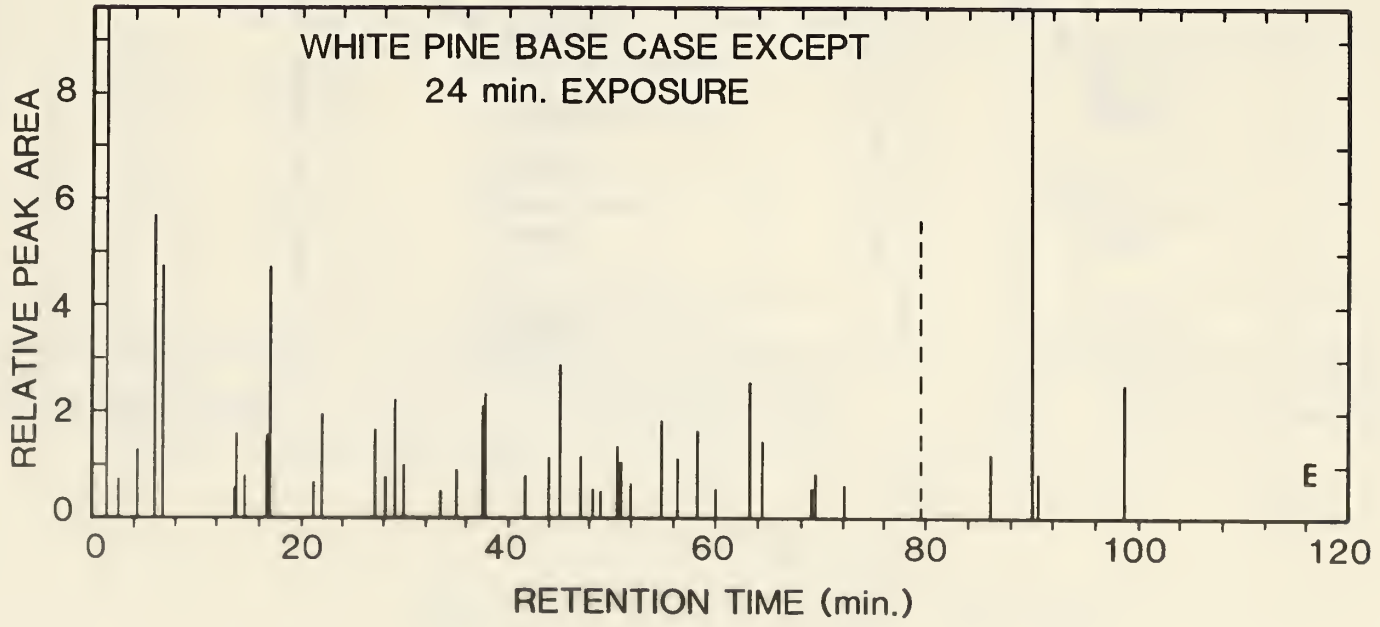
WHITE PINE BASE CASE EXCEPT
24 min. EXPOSURE
E
RELATIVE PEAK AREA
RETENTION TIME (min.)
0
2
4
6
8
0
20
40
60
80
100
120

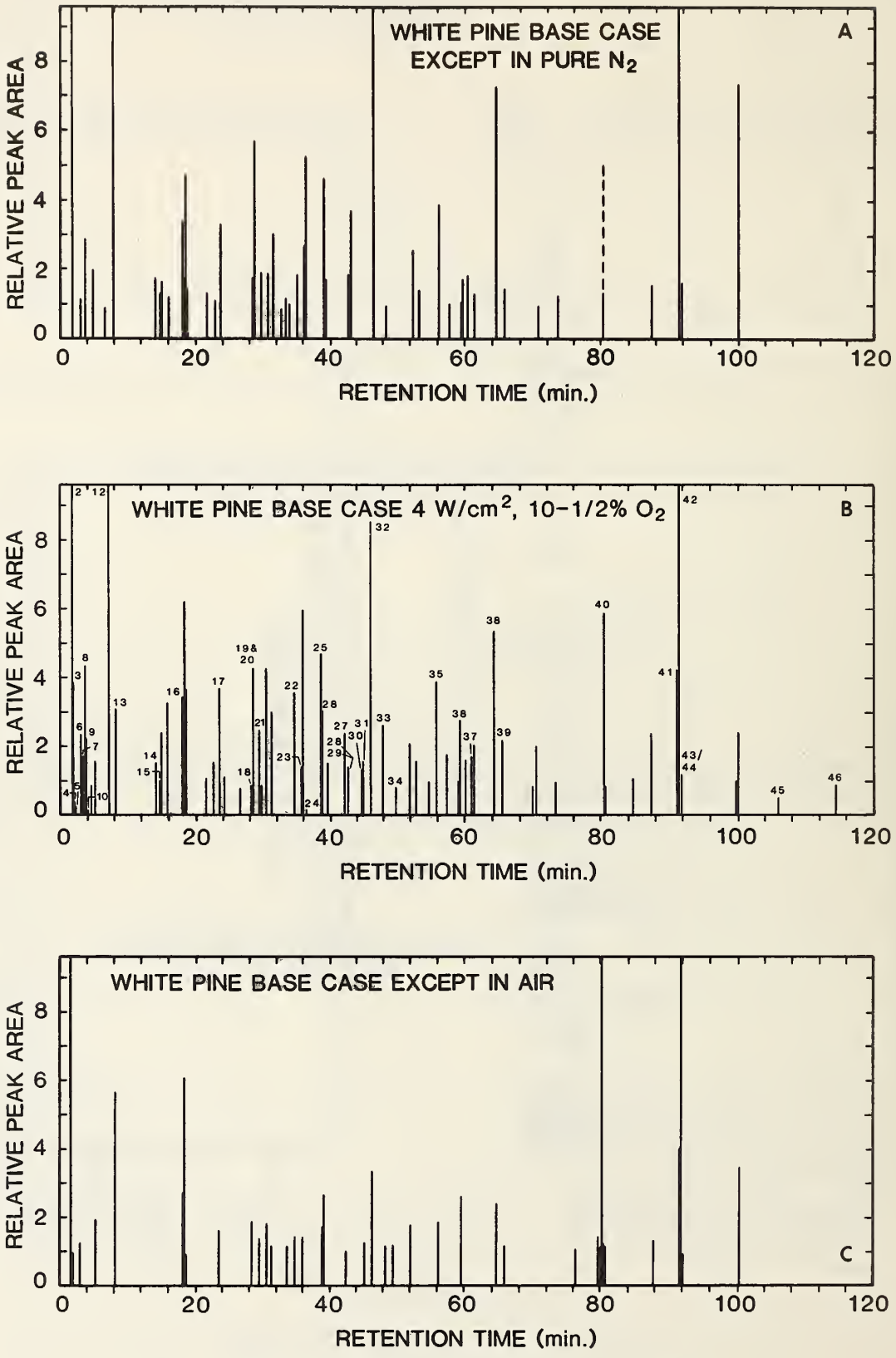

Figure 21. Capillary GC fingerprints of tar as a function of ambient oxygen level: white pine (a) 0% O_2, pure N_2; (b) 10-1/2% O_2; (c) 21% O_2

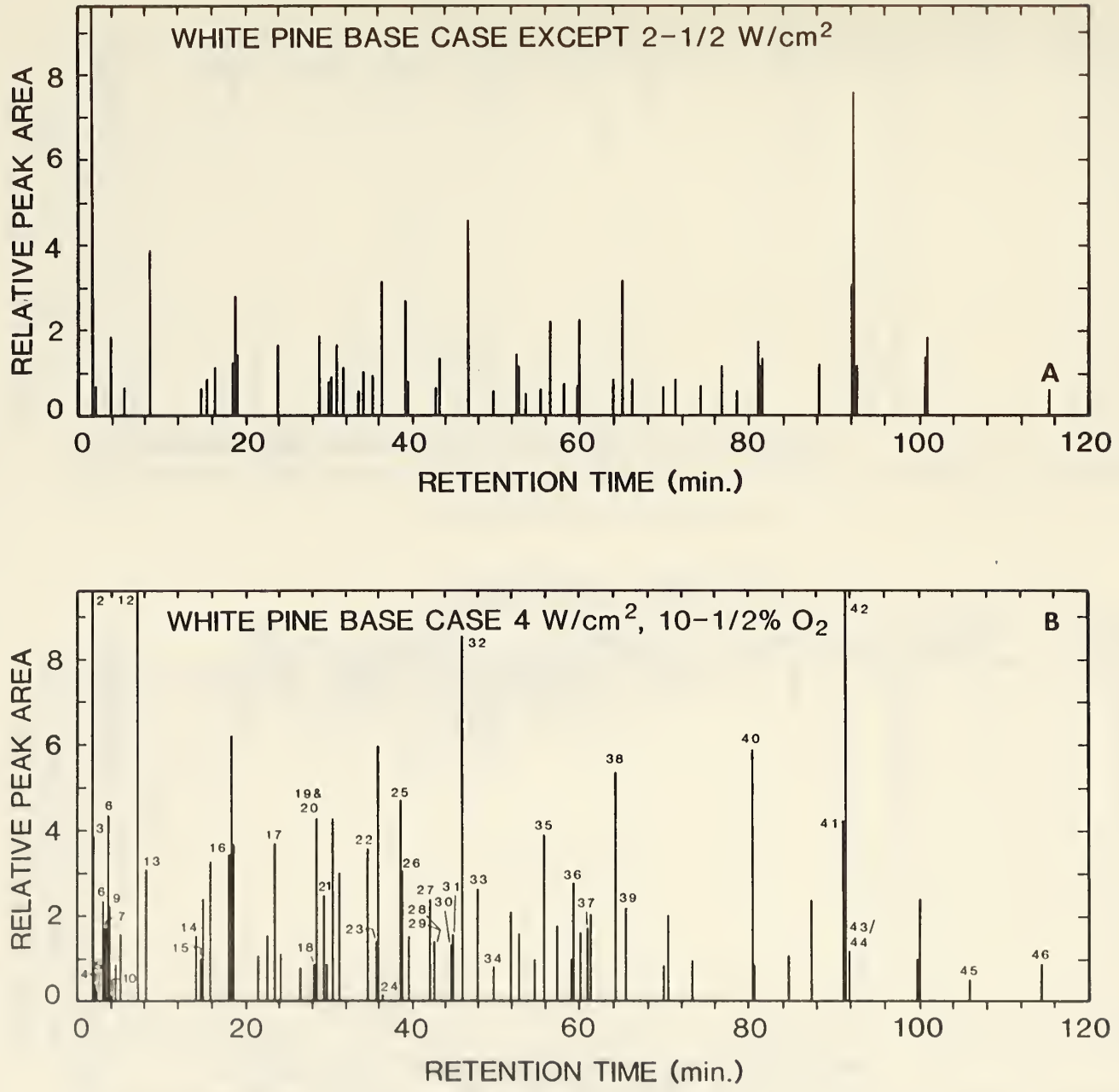

Figure 22. Capillary GC fingerprints of tar as a function of incident radiant flux: white pine base case conditions except: (a) 2-1/2 W/cm²; (b) 4 W/cm²; (c) 6.9 W/cm²; (d) 7.85 W/cm²

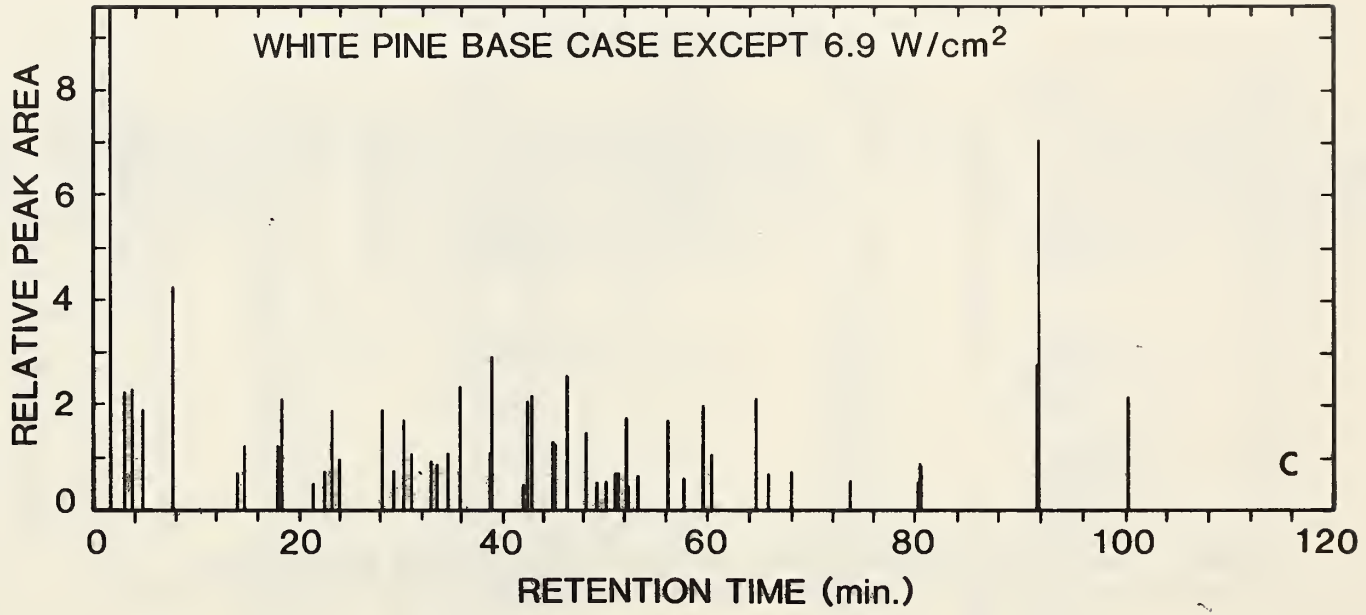
WHITE PINE BASE CASE EXCEPT 6.9 W/cm²
RELATIVE PEAK AREA
0
2
4
6
8
0
20
40
60
80
100
120
RETENTION TIME (min.)
C

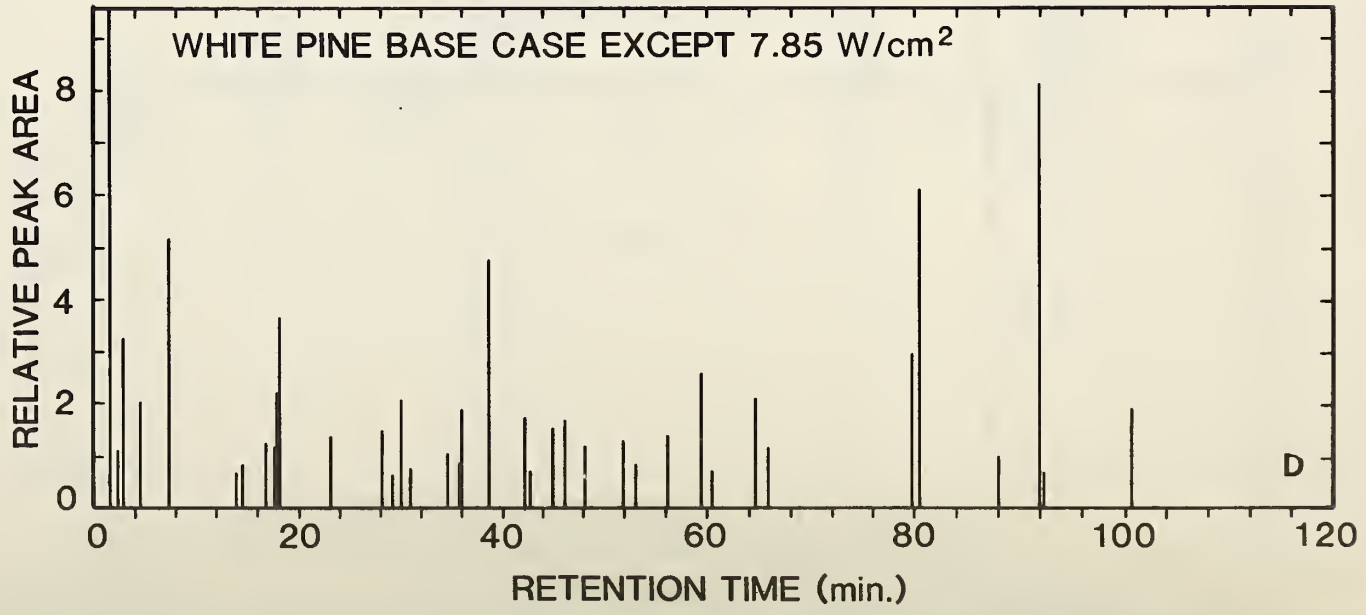
WHITE PINE BASE CASE EXCEPT 7.85 W/cm²
RELATIVE PEAK AREA
0
2
4
6
8
0
20
40
60
80
100
120
RETENTION TIME (min.)
D

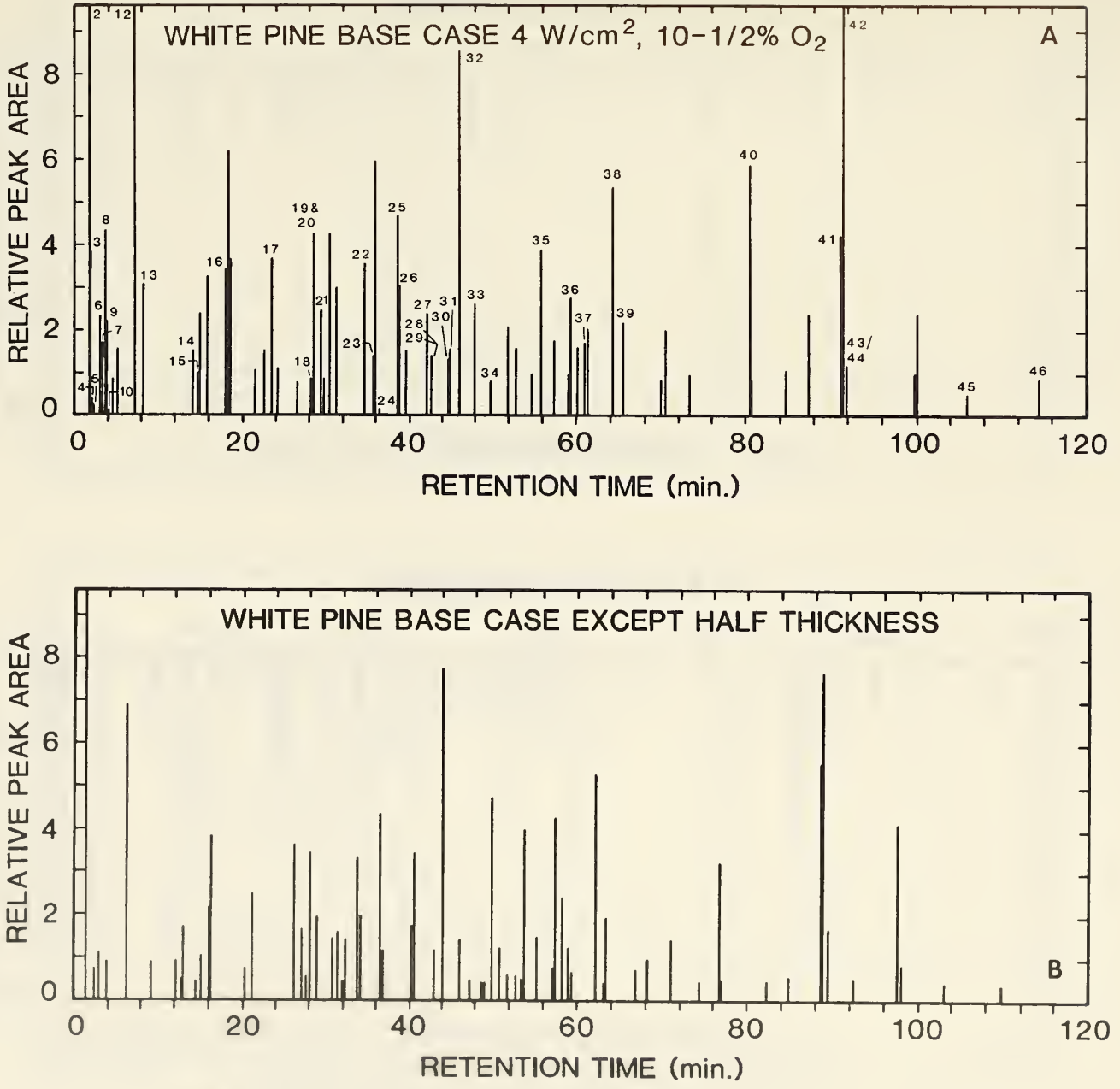

Figure 23. Capillary GC fingerprints of tar as a function of sample thickness: white pine at base case conditions (a) and half thickness (b)

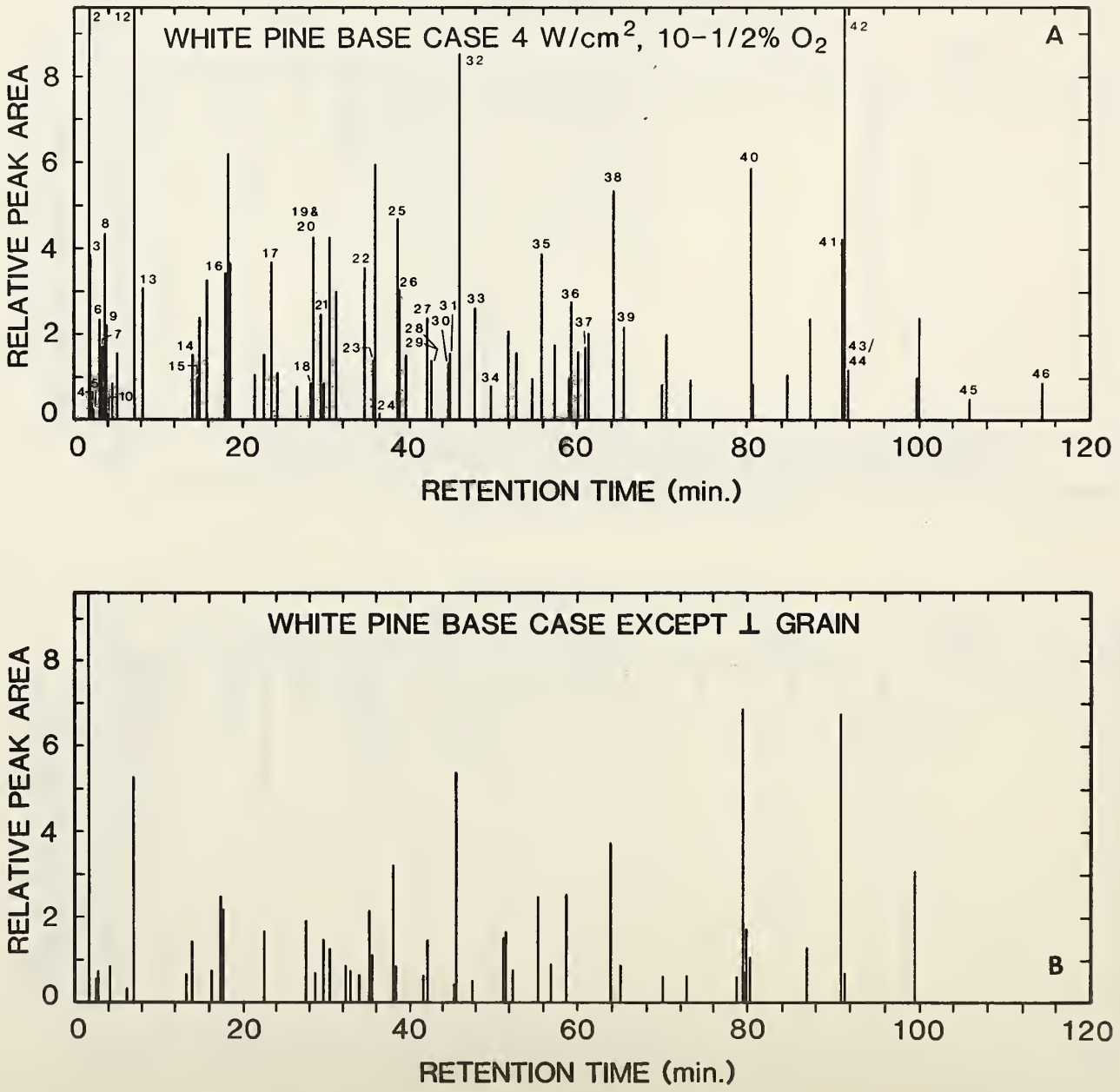

Figure 24. Capillary GC fingerprints of tar as a function of sample grain orientation; white pine at base case conditions (a) and with perpendicular grain (b)

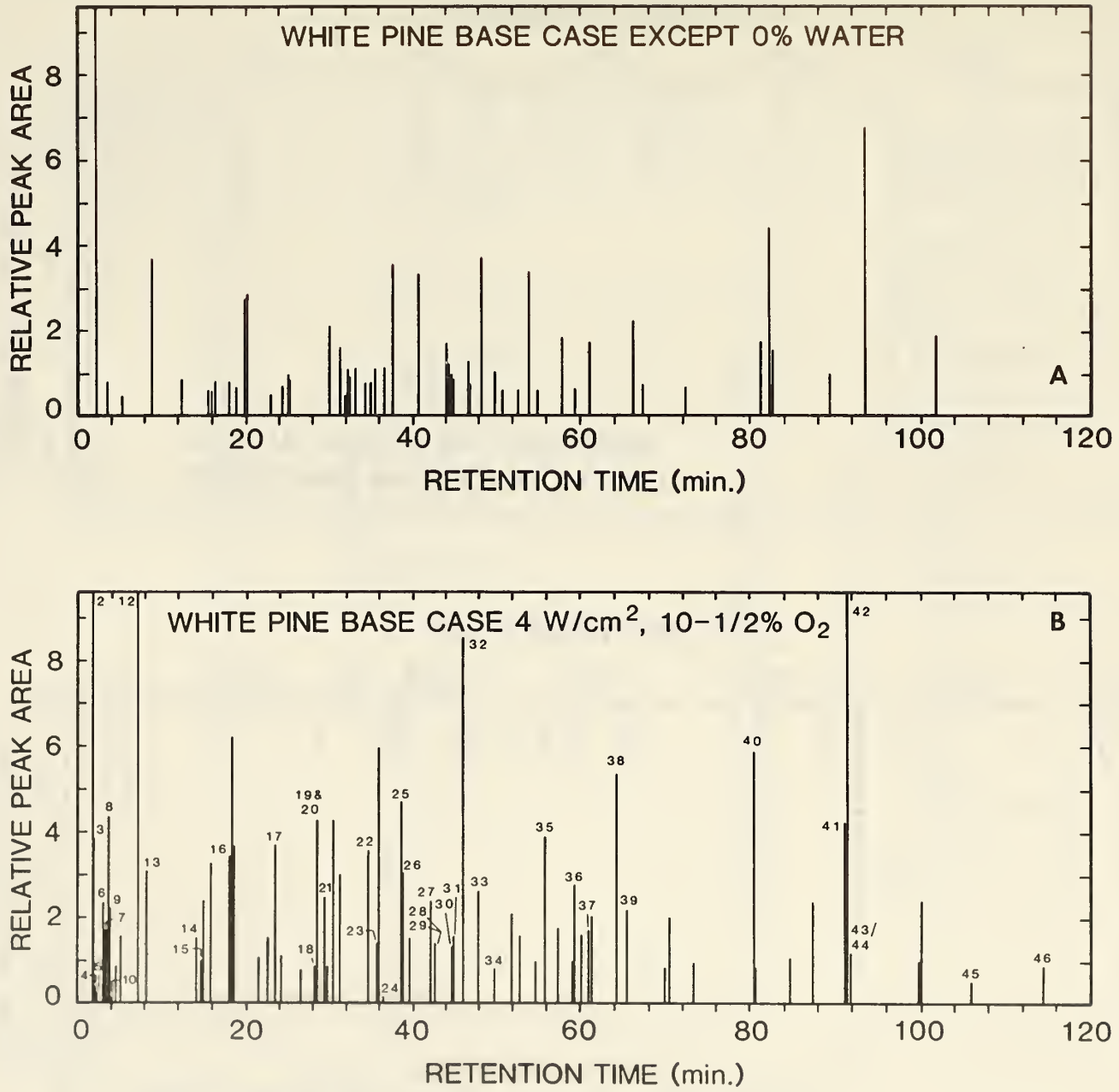

Figure 25. Capillary GC fingerprints of tar as a function of sample moisture content: white pine at base case conditions except: (a) 0%; (b) 5%; (c) 33%; (d) 33% water and 24 min exposure

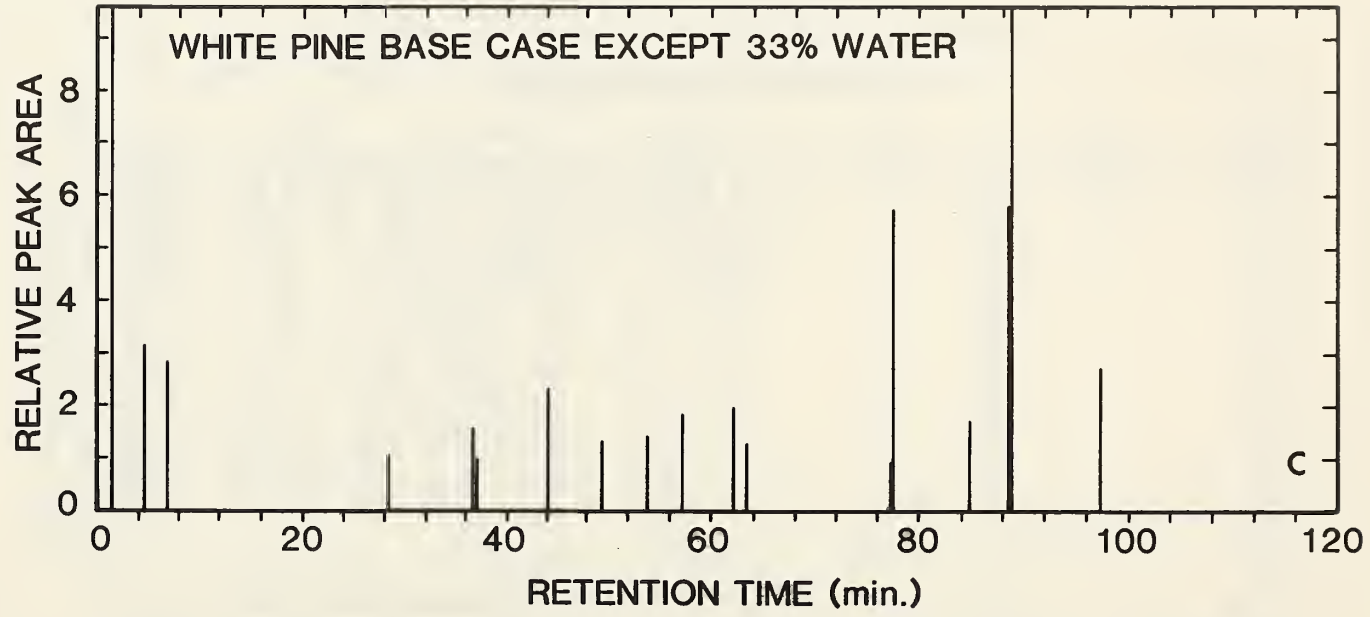
WHITE PINE BASE CASE EXCEPT 33% WATER
RELATIVE PEAK AREA
0
2
4
6
8
0
20
40
60
80
100
120
RETENTION TIME (min.)
C

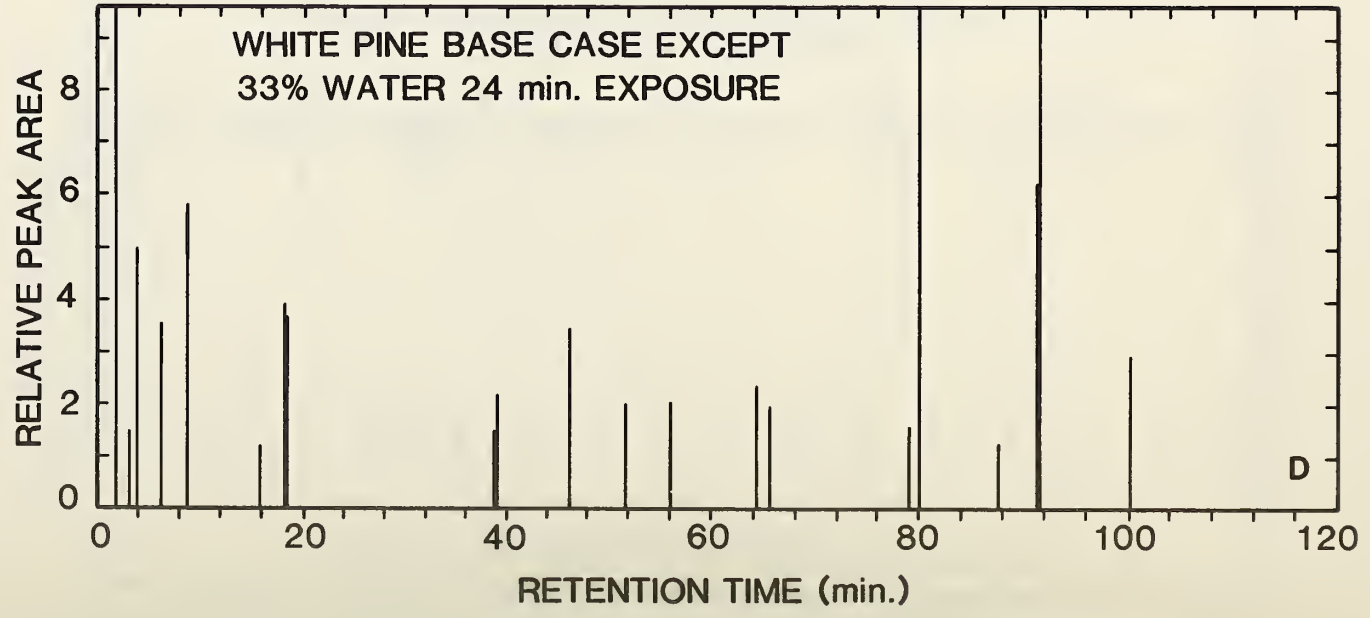
WHITE PINE BASE CASE EXCEPT
33% WATER 24 min. EXPOSURE
RELATIVE PEAK AREA
0
2
4
6
8
0
20
40
60
80
100
120
RETENTION TIME (min.)
D

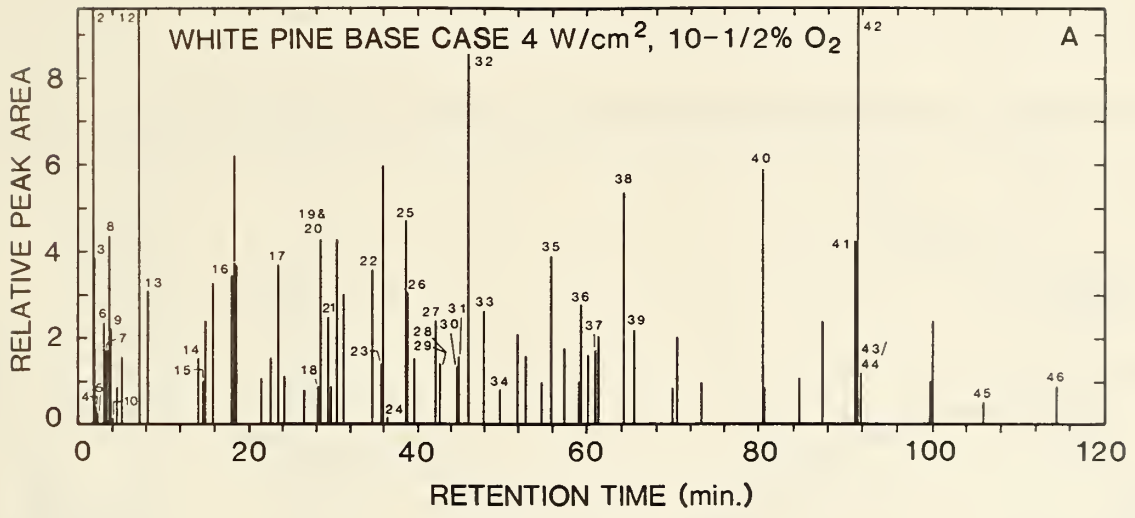

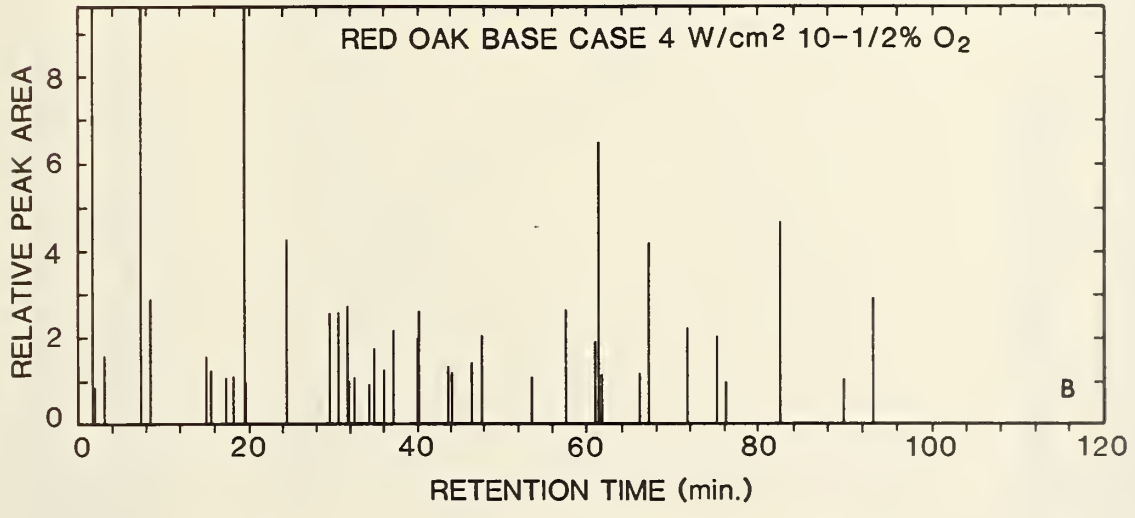

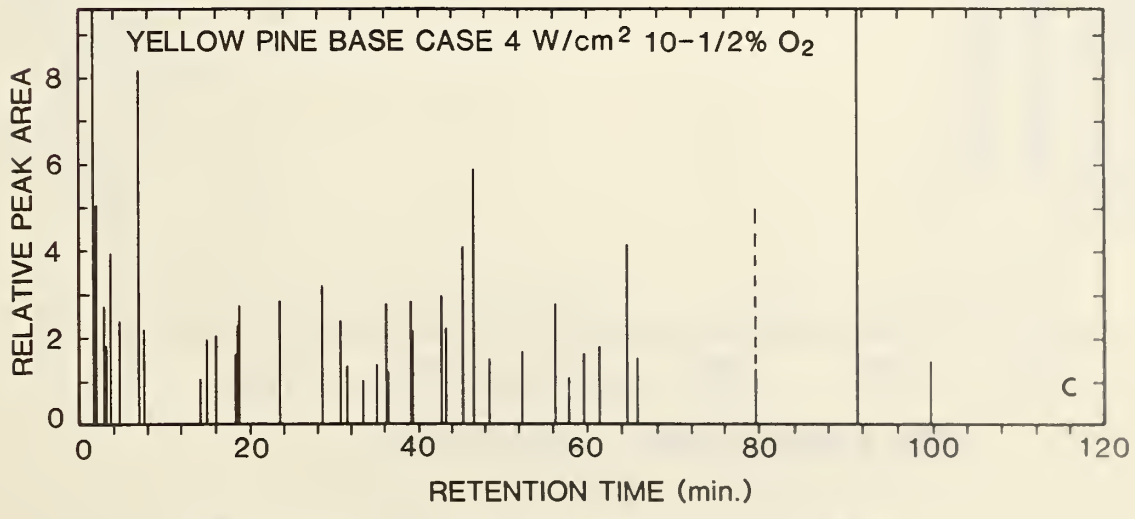

Figure 26. Capillary GC fingerprints of tar as a function of wood type: base case conditions: (a) white pine; (b) red oak; (c) yellow pine

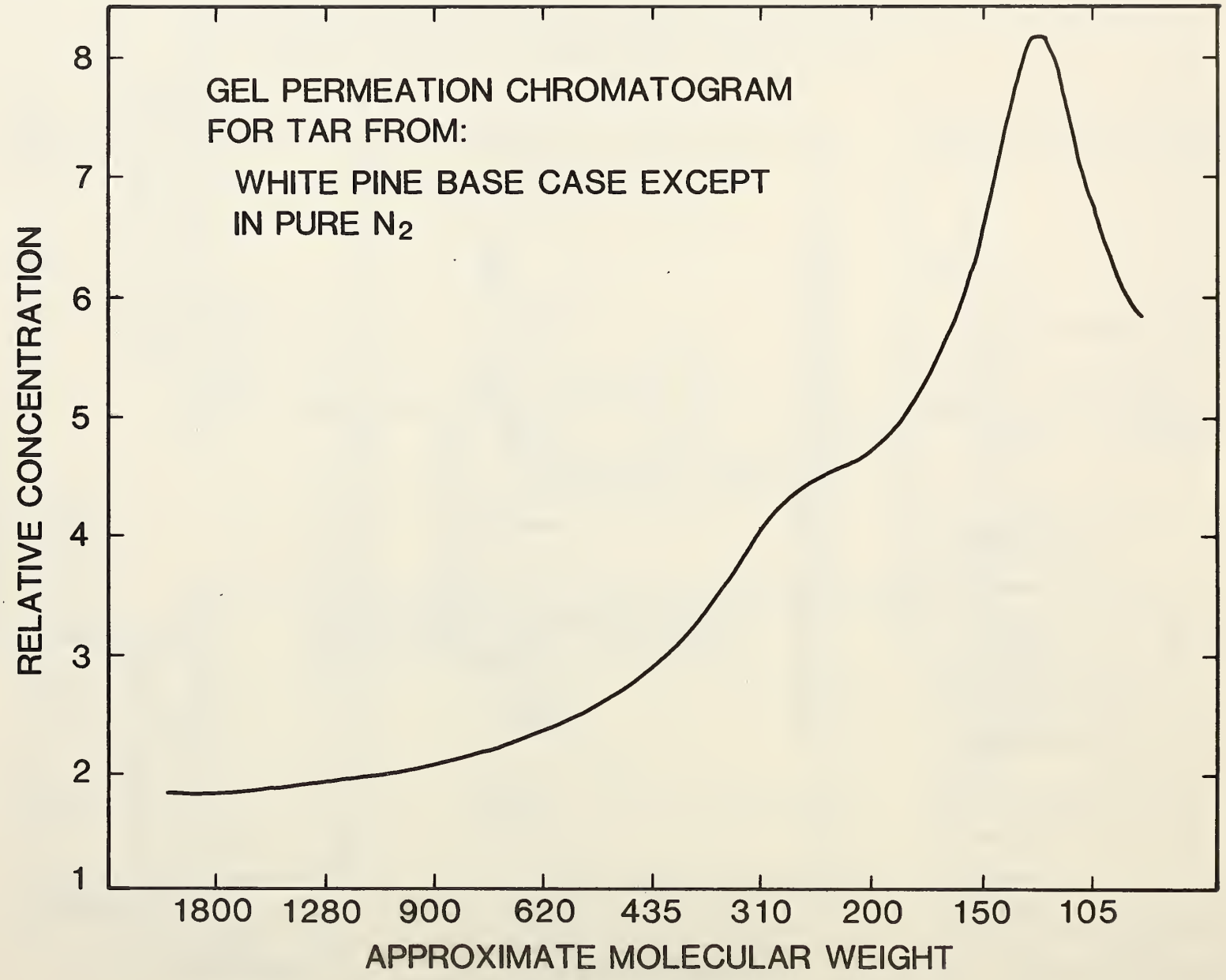

Figure 27(a). Gel permeation chromatogram of tar from white pine at base case conditions except in N_2 atmosphere

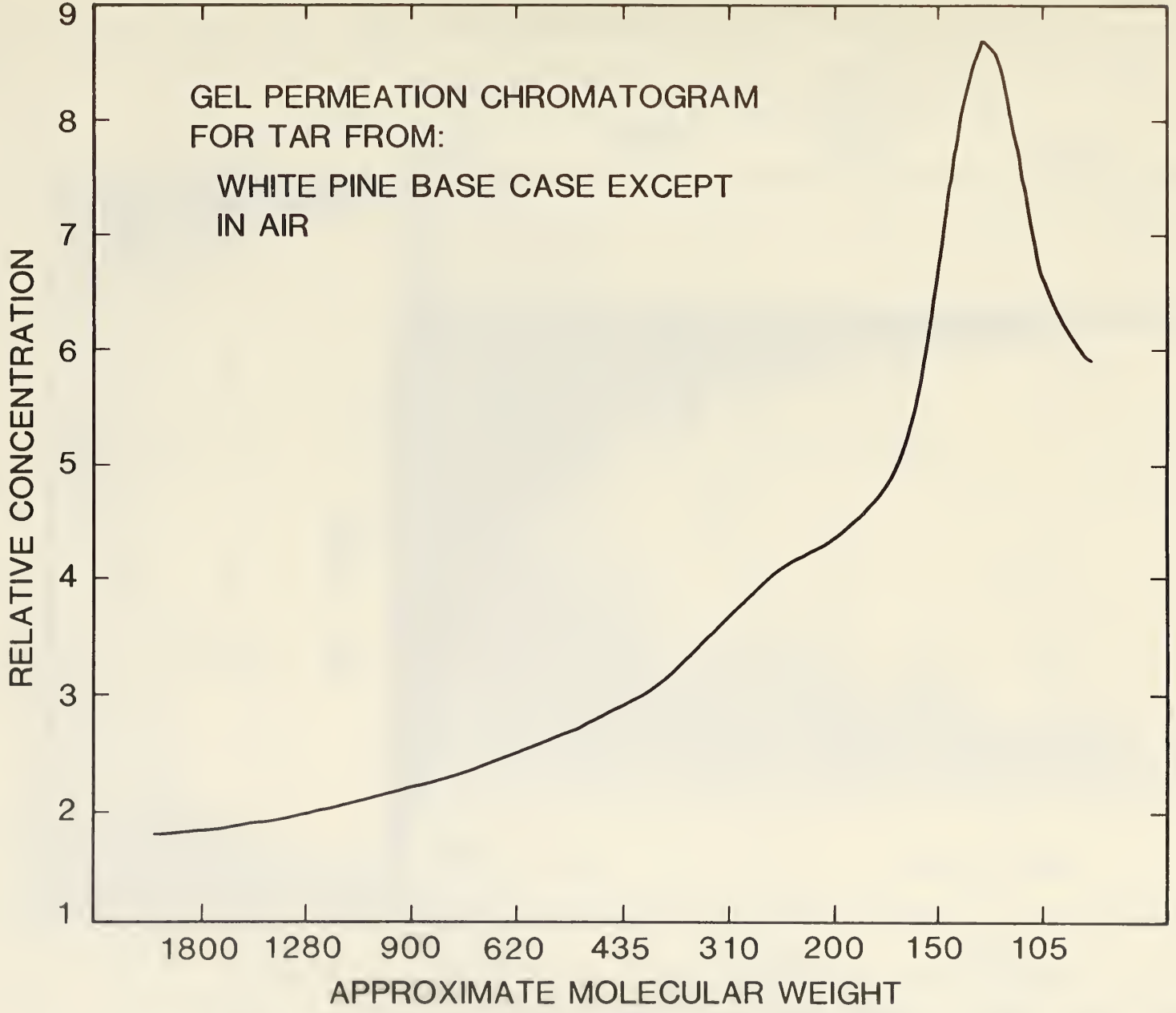

Figure 27(b). Gel permeation chromatogram of tar from white pine at base case conditions except in air atmosphere

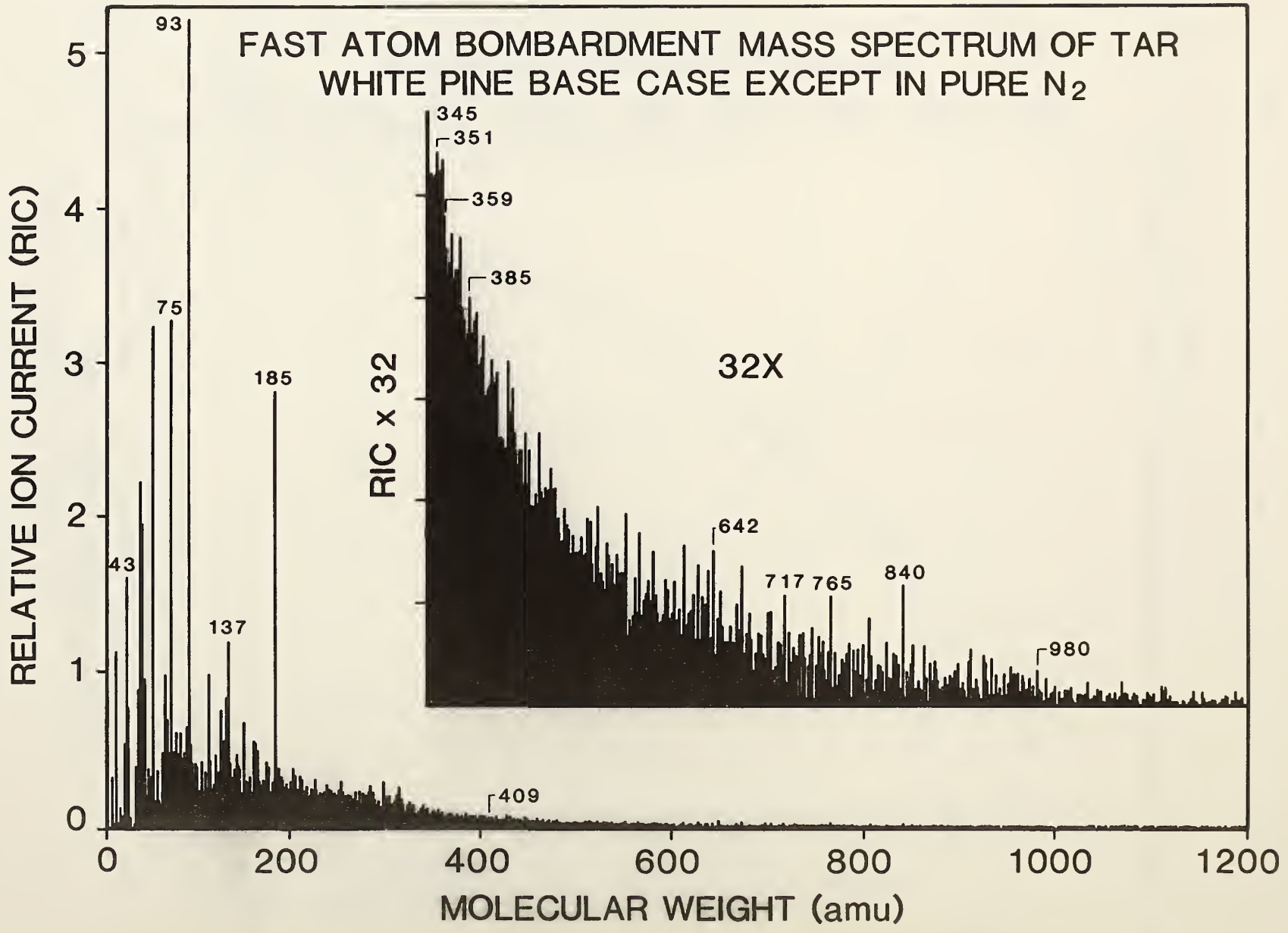

Figure 28(a). Fast atom bombardment mass spectrum of tar from white pine at base case conditions except in N_2 atmosphere

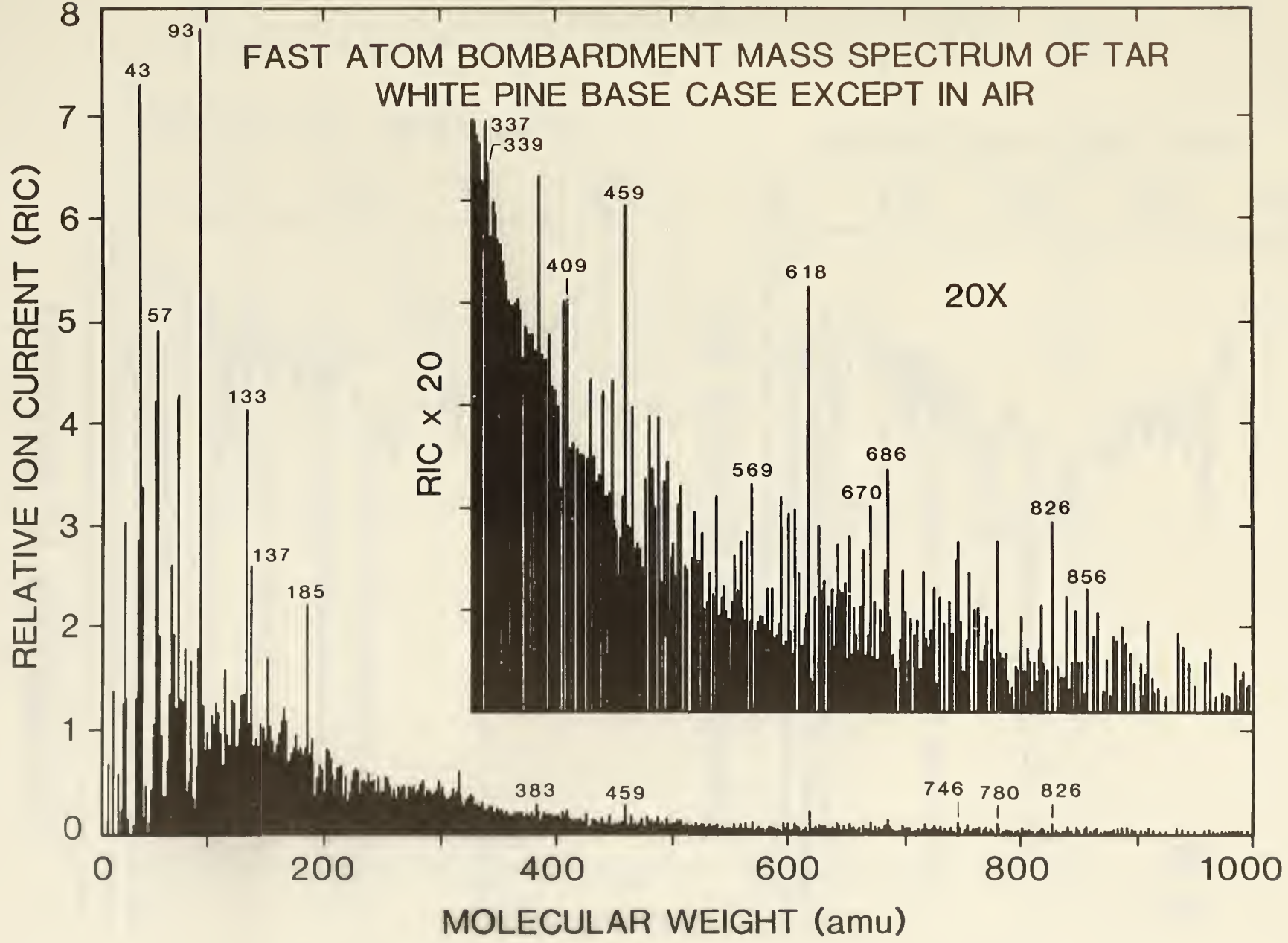

Figure 28(b). Fast atom bombardment mass spectrum of tar from white pine at base case conditions except in air atmosphere

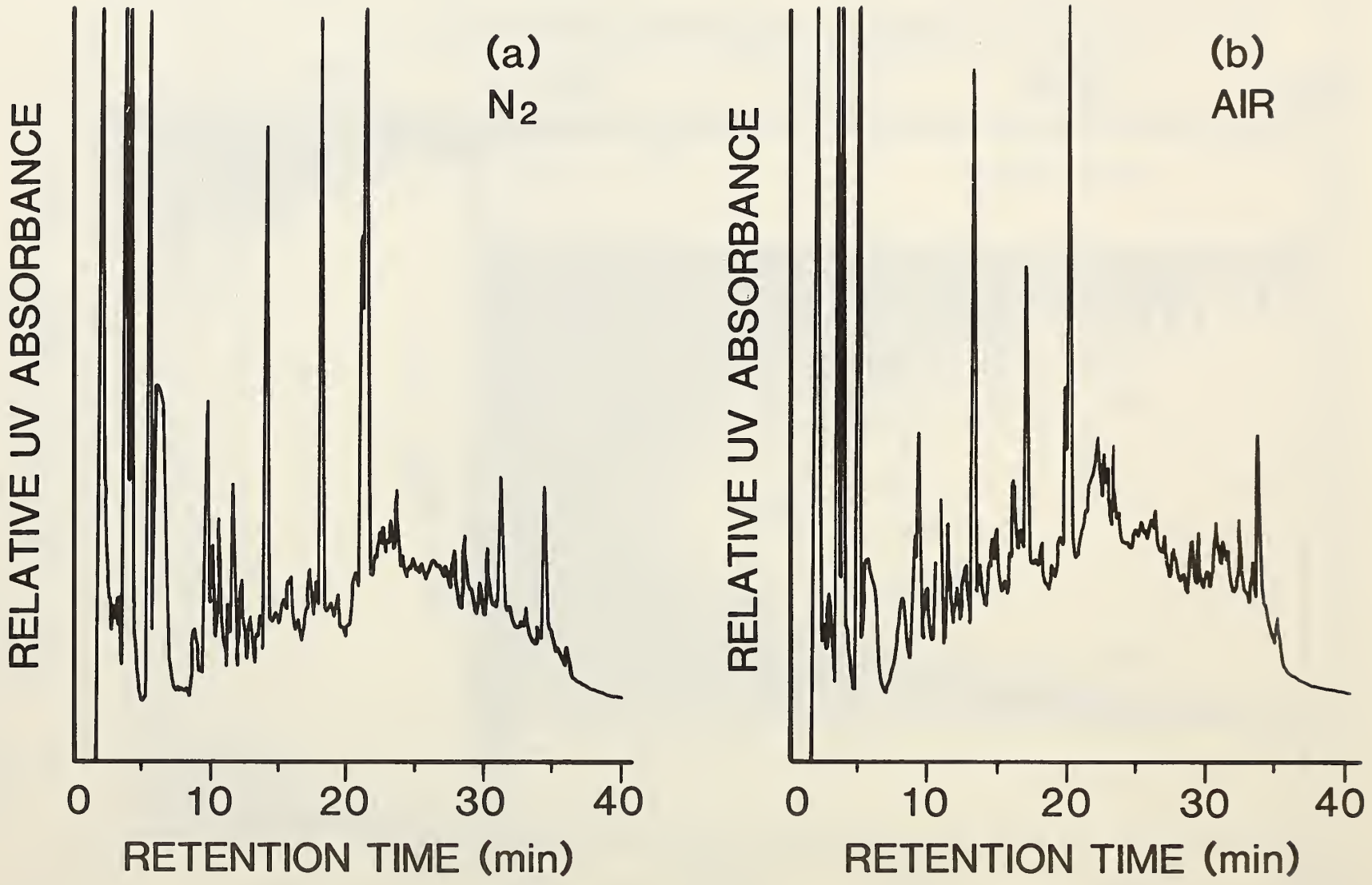

Figure 29. High pressure liquid chromatography results for tar from white pine at base case conditions except: (a) N_2 atmosphere; (b) air atmosphere

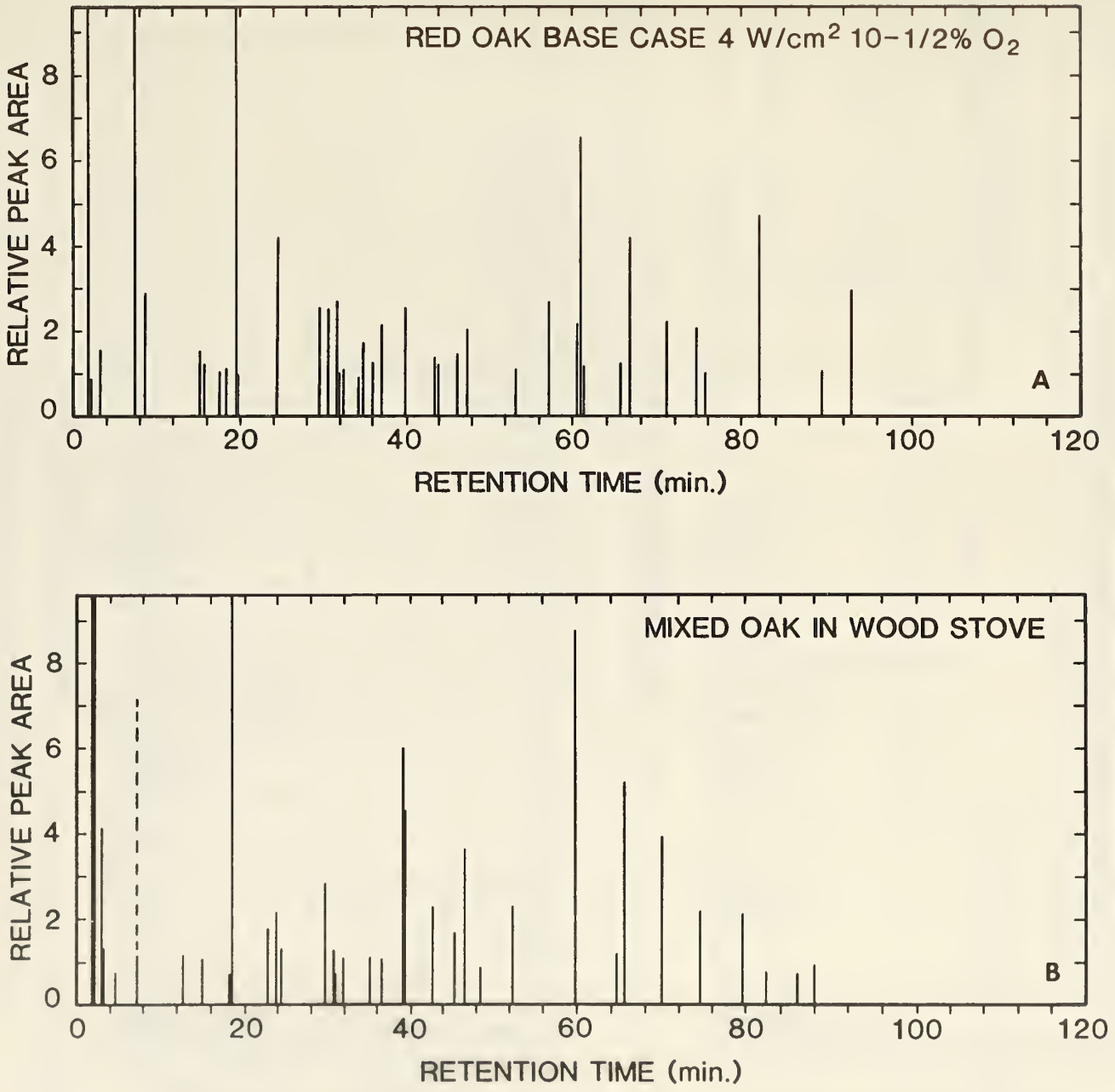

Figure 30. Capillary GC fingerprints of tar from: (a) red oak irradiated at base case conditions, (b) mixed oak burned in a wood stove at "overnight burn" conditions

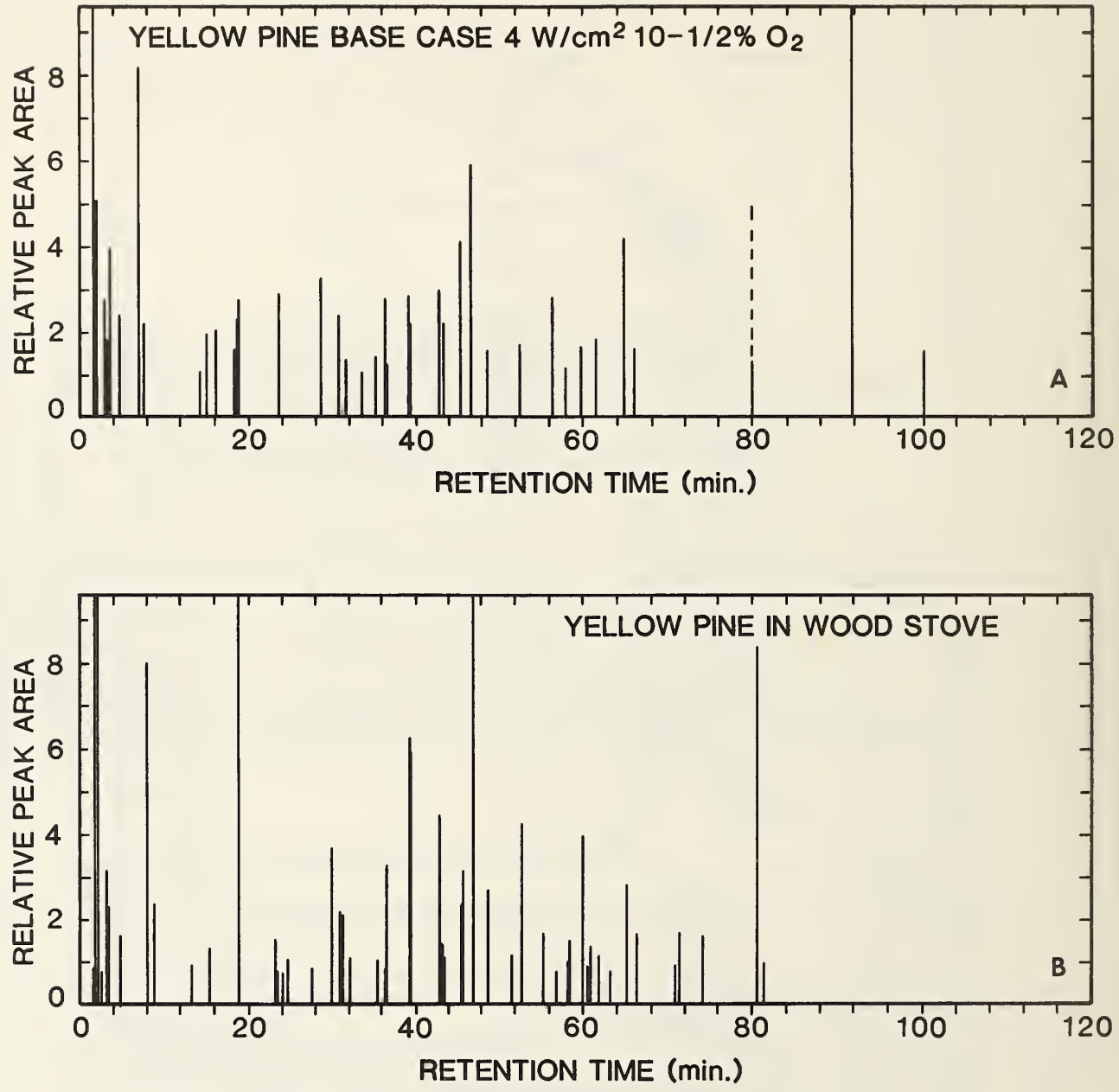

Figure 31. Capillary GC fingerprints of tar from: (a) yellow pine irradiated at base case conditions, (b) yellow pine burned in a wood stove at "overnight burn" conditions

NBS-114A (REV. 2-8C)

U.S. DEPT. OF COMM. BIBLIOGRAPHIC DATA SHEET (See instructions)	1. PUBLICATION OR REPORT NO. NBSIR-85-3127	2. Performing Organ. Report No.	3. Publication Date February 1985

4. TITLE AND SUBTITLE

Products of Wood Gasification

5. AUTHOR(S)

Thomas J. Ohlemiller, Takashi Kashiwagi, Kathleen E. Werner

6. PERFORMING ORGANIZATION (If joint or other than NBS, see instructions)

NATIONAL BUREAU OF STANDARDS
DEPARTMENT OF COMMERCE
Gaithersburg, MD 20899

7. Contract/Grant No.

8. Type of Report & Period Covered

9. SPONSORING ORGANIZATION NAME AND COMPLETE ADDRESS (Street, City, State, ZIP)

U. S. Dept. of Energy
Washington, D.C. 20585

10. SUPPLEMENTARY NOTES

☐ Document describes a computer program; SF-185, FIPS Software Summary, is attached.

11. ABSTRACT (A 200-word or less factual summary of most significant information. If document includes a significant bibliography or literature survey, mention it here)

The increasing problem of pollution from wood-burning stoves has prompted this examination of the basic gasification process of wood under conditions encompassing those in stoves. The emphasis is on the products generated when wood is heated, without flaming, in atmospheres of varying oxygen concentration (0 to 21% O_2 in N_2). Small wood samples (typically 4 x 4 cm face, 2-4 cm thick; white pine, red oak, plus two tests with yellow pine) were subjected to uniform radiative heat fluxes (2 to 7.8 W/cm^2) on one face. Other variables were sample grain orientation, thickness, exposure time and moisture content. Sample weight was followed in some tests; sample temperature (5 thermocouples) was followed in others. In all tests, all evolved products were either monitored (H_2O, CO, CO_2, total hydrocarbons not condensible at -40°C) or trapped and analyzed (condensible organic species) by gas chromatography and mass spectroscopy. The extent of change in these major products is rather limited (factor of two to four) over the range of variables explored here. The organic condensate was difficult to analyze; it is estimated that only 20% of it was chromatographable. More than forty species in this chromatographable portion were positively or tentatively identified and quantified. Chromatographic fingerprints of the organic condensate indicated that its composition does not vary a great deal for the conditions examined here. The fingerprints from the radiative heating tests bear a strong resemblance to those of the smoke condensate from a wood stove.

12. KEY WORDS (Six to twelve entries; alphabetical order; capitalize only proper names; and separate key words by semicolons)

air pollution; gasification; radiative heat; stoves; smoldering combustion; thermal degradation

13. AVAILABILITY

☒ Unlimited

☐ For Official Distribution. Do Not Release to NTIS

☐ Order From Superintendent of Documents, U.S. Government Printing Office, Washington, D.C. 20402.

☒ Order From National Technical Information Service (NTIS), Springfield, VA. 22161

14. NO. OF PRINTED PAGES

114

15. Price

$13.00

USCOMM-DC 6043-P80